EVALUATION OF PENDIMETHALIN BINDING TO HUMAN SERUM ALBUMIN: INSIGHTS FROM SPECTROSCOPIC AND MOLECULAR MODELING APPROACHES

LEE WEI QI

FACULTY OF SCIENCE
UNIVERSITY OF MALAYA
KUALA LUMPUR

2017

EVALUATION OF PENDIMETHALIN BINDING TO HUMAN SERUM ALBUMIN: INSIGHTS FROM SPECTROSCOPIC AND MOLECULAR MODELING APPROACHES

LEE WEI QI

DISSERTATION SUBMITTED IN FULFILMENT OF THE REQUIREMENTS FOR THE DEGREE OF MASTER OF SCIENCE

INSTITUTE OF BIOLOGICAL SCIENCES
FACULTY OF SCIENCE
UNIVERSITY OF MALAYA
KUALA LUMPUR

2017

UNIVERSITY OF MALAYA
ORIGINAL LITERARY WORK DECLARATION

Name of Candidate: Lee Wei Qi
Matric No: SGR 150040
Name of Degree: Master of Science

Title of Project Paper/Research Report/Dissertation/Thesis ("this Work"): "Evaluation of Pendimethalin Binding to Human Serum Albumin: Insights from Spectroscopic and Molecular Modeling Approaches

Field of Study: Biochemistry

I do solemnly and sincerely declare that:

(1) I am the sole author/writer of this Work;
(2) This Work is original;
(3) Any use of any work in which copyright exists was done by way of fair dealing and for permitted purposes and any excerpt or extract from, or reference to or reproduction of any copyright work has been disclosed expressly and sufficiently and the title of the Work and its authorship have been acknowledged in this Work;
(4) I do not have any actual knowledge nor do I ought reasonably to know that the making of this work constitutes an infringement of any copyright work;
(5) I hereby assign all and every rights in the copyright to this Work to the University of Malaya ("UM"), who henceforth shall be owner of the copyright in this Work and that any reproduction or use in any form or by any means whatsoever is prohibited without the written consent of UM having been first had and obtained;
(6) I am fully aware that if in the course of making this Work I have infringed any copyright whether intentionally or otherwise, I may be subject to legal action or any other action as may be determined by UM.

Candidate's Signature Date:

Subscribed and solemnly declared before,

Witness's Signature Date:
Name: Prof. Saad Tayyab
Designation: Supervisor

Witness's Signature Date:
Name: Dr. Saharuddin bin Mohamad
Designation: Supervisor

ABSTRACT

Interaction of pendimethalin (PM) herbicide with human serum albumin (HSA) was studied using fluorescence, circular dichroism (CD) and molecular modeling methods. The attenuation of the fluorescence intensity of HSA in the presence of PM revealed formation of the PM-HSA complex. Analysis of the fluorescence quenching data showed moderately strong binding affinity between PM and HSA. Both hydrophobic interactions and hydrogen bonds were suggested to stabilize the PM-HSA complex, based on thermodynamic data. Binding of PM to HSA induced perturbation in the microenvironment around the aromatic fluorophores as well as secondary and tertiary structural changes in the protein. Complex formation between PM and HSA led to an increase in its thermal stability. Both site marker displacement and molecular modeling results suggested site I, located in subdomain IIA, as the preferred binding site of PM on HSA. A comparative study on the interaction between PM and serum albumins of bovine (BSA), sheep (SSA), porcine (PSA), human (HSA) and rabbit (RbSA) was also made using fluorescence quenching titration and site marker displacement experiments. Similar magnitude of PM-induced fluorescence quenching was observed with BSA and HSA, compared to other albumins. The binding affinity of PM to these albumins was found to follow the order: SSA > HSA > BSA > RbSA > PSA. Warfarin (WFN) displacement results also suggested similar displacing action of PM on WFN-BSA and WFN-HSA complexes. All these results suggested close similarity between BSA and HSA in terms of PM binding characteristics.

ABSTRAK

Interaksi pendimethalin (PM) racun herba dengan pengangkut utama dalam edaran manusia, albumin serum manusia (HSA) dikaji menggunakan pendarfluor, dichroism bulat (CD) dan kaedah pemodelan molekul. Pengecilan keamatan pendarfluor di HSA di hadapan PM mendedahkan pembentukan kompleks PM-HSA. Analisis data pendarfluor pelindapkejutan menunjukkan pertalian mengikat sederhana kuat antara PM dan HSA. Kedua-dua interaksi hidrofobik dan ikatan hidrogen telah dicadangkan untuk menstabilkan kompleks PM-HSA, berdasarkan data termodinamik. Mengikat PM ke HSA pengusikan disebabkan dalam mikro di sekitar fluorophores aromatik serta perubahan struktur menengah dan pengajian tinggi dalam protein. Complexation PM dengan HSA membawa kepada peningkatan dalam kestabilan haba. Kedua-dua penanda tapak anjakan dan keputusan pemodelan molekul mencadangkan laman web saya, bertempat di subdomain IIA sebagai tapak mengikat yang digemari PM di HSA. Satu kajian perbandingan pada interaksi antara PM dan albumins serum lembu (BSA), biri-biri (SSA), babi (PSA), manusia (HSA) dan arnab (RbSA) juga dibuat menggunakan pendarfluor pelindapkejutan titratan dan tapak eksperimen penanda anjakan. Magnitud yang sama pelindapkejutan pendarfluor PM yang disebabkan diperhatikan dengan BSA dan HSA, berbanding albumins lain. Pertalian mengikat PM untuk albumins ini didapati untuk mengikuti susunan: SSA> HSA> BSA> RbSA> PSA. Keputusan Warfarin (WFN) anjakan juga mencadangkan tindakan penyisihan sama PM pada WFN-BSA dan kompleks WFN-HSA. Semua keputusan mencadangkan persamaan rapat antara BSA dan HSA, dari segi ciri-ciri pengikatan PM.

ACKNOWLEDGEMENTS

First of all, I would like to express my deepest gratitude to my supervisors, Professor Saad Tayyab and Dr. Saharuddin Mohamad for their encouragement, guidance and support throughout the entire project. I offer my sincere gratitude to Professor Saad Tayyab, who has guided me with a lot of patience along the dissertation writing to its completion. It is my honor to work under them and the experience is one that I am ever grateful for.

I am grateful to Dr. Zazali Alias, Coordinator of the Biochemistry Programme, Associate Professor Dr. Nurhayati binti Zainal Abidin, Head, Institute of Biological Sciences and Professor Zanariah Abdullah, Dean, Faculty of Science, University of Malaya for providing necessary facilities and a favorable environment for research.

My special thanks go to Malaysia Genome Institute (MGI) for allowing me to use the CD machine in their laboratory with reasonable charge. I also wish to thank Ms. Azyyati Mohd. Padzil for her patience in guiding me the way to handle the machine.

I am blessed that I have a good companion, Ida Syazwani Mohd. Affandi who went through up and down with me and always supported me throughout the project. My sincere thanks and appreciations are due to my cheerful group of colleagues, seniors and friends for their kind help and support. The journey would have not been colorful without them.

I would also like to acknowledge the Ministry of Higher Education, Government of Malaysia and the University of Malaya, for the financial support, in the form of High Impact Research Grant UM.C/625/1/HIR/MOHE/SC/02.

Nevertheless, I am extremely thankful to my parents and Goh Kok Keong for their inspiration, understanding and constant support.

Lee Wei Qi

October, 2016

TABLE OF CONTENTS

LIST OF FIGURES

LIST OF TABLES

LIST OF ABBREVIATIONS / SYMBOLS

Ala	Alanine
Arg	Arginine
BSA	Bovine serum albumin
℃	Degree Celcius
CD	Circular dichroism
cm	Centimeter
3-D	Three-dimensional
Da	Dalton
e.g.	Latin phrase *exempli gratia* (for example)
EU	European Union
Eq.	Equation
g	Gram
Gln	Glutamine
Glu	Glutamic acid
h	Hour
HSA	Human serum albumin
His	Histidine
IBN	Ibuprofen
IDM	Indomethacin
i.e.	Latin phrase *id est* (that is)
Ile	Isoleucine
J	Joules
K_a	Association / binding constant
K_{oc}	Soil organic carbon-water partitioning coefficient
K_{sv}	Stern-Volmer constant
k_q	Bimolecular quenching constant
kJ	Kilojoules
L	Liter
Leu	Leucine
Lys	Lysine
M	Molar
mg	Milligram
min	Minute

ml	Milliliter
mM	Millimolar
mPa	Millipascal
µM	Micromolar
µm	Micrometer
No.	Number
nm	Nanometer
PM	Pendimethalin
Phe	Phenylalanine
ppm	Parts per million
PSA	Porcine serum albumin
R	Gas constant
r	Correlation coefficient
RbSA	Rabbit serum albumin
Ser	Serine
SSA	Sheep serum albumin
T	Temperature
Trp	Tryptophan
Tyr	Tyrosine
UV	Ultraviolet
V	Voltage
Val	Valine
viz.	Latin phrase *videlicet* (that is to say)
WFN	Warfarin
Å	Angstrom
ΔG	Gibbs free energy change
ΔH	Enthalpy change
ΔS	Entropy change
λ_{em}	Emission wavelength
λ_{ex}	Excitation wavelength
~	Approximate
≥	Greater than or equal to
%	Percentage
±	Plus-minus

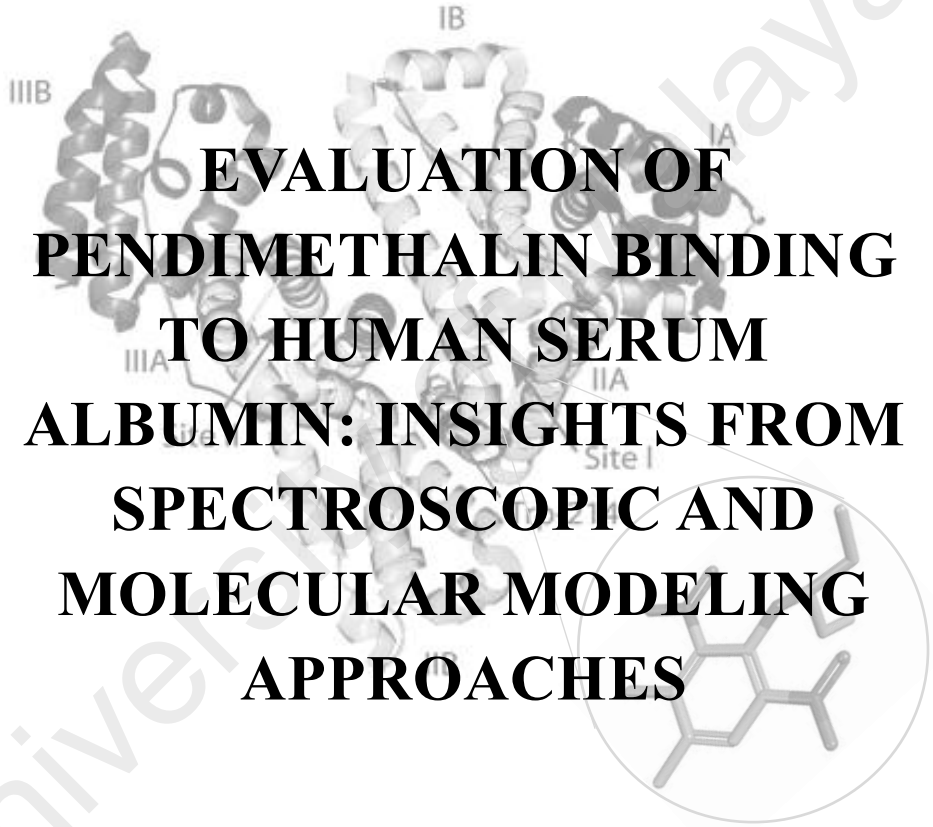

EVALUATION OF PENDIMETHALIN BINDING TO HUMAN SERUM ALBUMIN: INSIGHTS FROM SPECTROSCOPIC AND MOLECULAR MODELING APPROACHES

CHAPTER 1

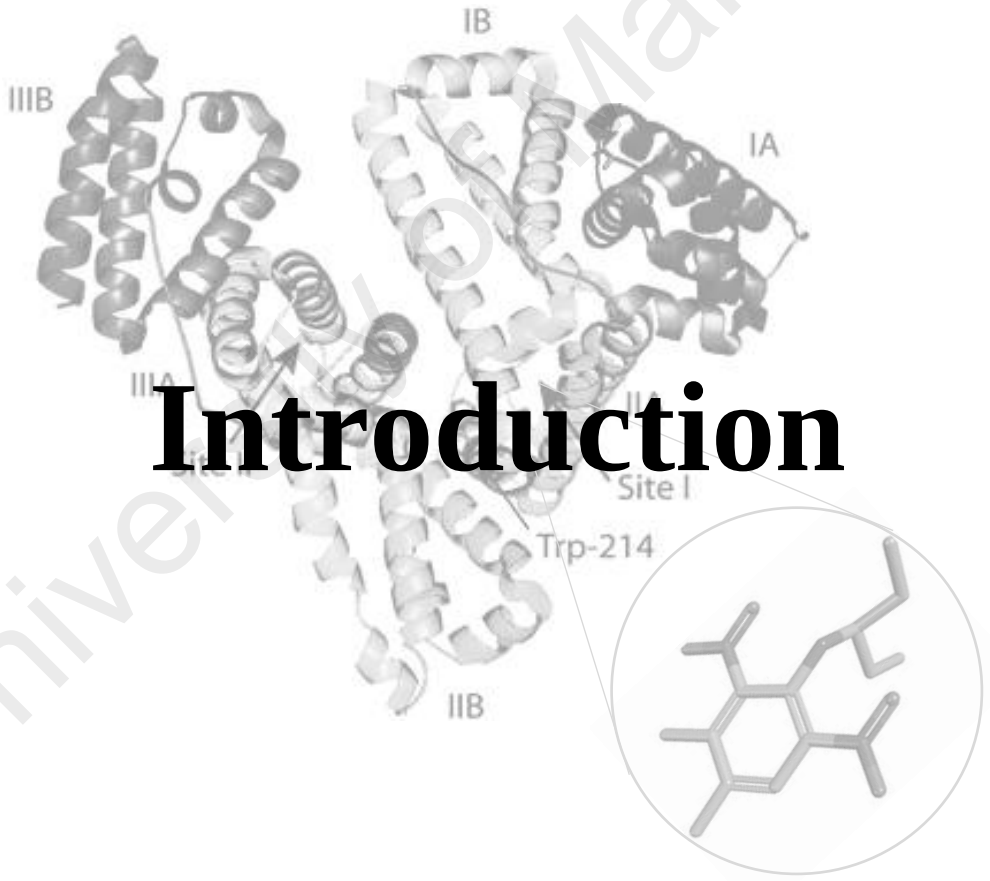

Introduction

CHAPTER 1

INTRODUCTION

Herbicides have been found useful in improving crop production in agricultural fields. However, their extensive use has provoked environmental and toxicological threats due to their persistency in the environment (Edwards and Adams, 1970). Pendimethalin (PM), a member of dinitroaniline group of herbicides is a soil residual pre-emergence herbicide, which is used primarily for the control of most annual grasses and certain broad-leaved weeds in various crops such as corn, wheat, soybeans and grapes. PM represses both root and shoot development via inhibition of chromosome separation and cell wall formation during cell mitosis (Appleby and Valverde, 1989; Gilliam et al., 1993). PM is a widely used herbicide in the world, particularly in the developed countries.

Due to its vast usage, PM has been detected as a contaminant in the water sources in USA (Larson et al., 1999), Denmark (Asman et al., 2005), Spain (Barba-Brioso et al., 2010) and France (CORPEP, 2010). The harmful chemicals of herbicides in the soil may leach into the water sources and cycle in the food web from aquatic organisms to human beings (Edwards and Adams, 1970). Several studies have reported the toxicological effects of PM on the aquatic organisms and other mammalian species (Danion et al., 2012; Dimitrov et al., 2006; Poleksic et al., 1995). Nevertheless, it is of much concern about the effects of PM on humans as the harmful compounds in the herbicides may reach humans directly through air after aerosol application or indirectly via food and drinking water.

Interaction of exogeneous compounds with the plasma proteins in human circulation decides the fate of their availability, metabolism and distribution in the body. Thus, interaction studies with the transport proteins become important to decipher their action in the human body. Human serum albumin (HSA) is the major transporter of many exogeneous and endogeneous compounds in human circulation. It is a single polypeptide

chain of 585 amino acid residues with a sole tryptophan residue (Trp-214) and is comprised of three homologous domains, namely, I, II and III. Most of the compounds have been found to bind with high affinity to Sudlow's sites I or II, which are located in subdomains IIA and IIIA, respectively (Carter et al., 1989; Sudlow et al., 1975). The toxicity of a herbicide depends on the level of its free concentration in the blood stream. Therefore, binding of a herbicide to HSA is toxicologically important as it can reduce the concentration of free herbicide. However, interaction of other endogeneous substances or drugs with HSA at the same binding site of the herbicide might strongly affect its distribution, elimination as well as its toxic properties (Bertucci and Domenici, 2002). Furthermore, unusually high affinity of the herbicide to HSA may influence its transportation and thus prevent its release at the target site for elimination purposes (Carter and Ho, 1994). Thus, a detailed study on the interaction between PM and HSA is required to understand its transport in human circulation.

The toxicological effects of PM on the human system can be predicted from the animal model study, which may provide useful information on the compound toxicity (Cicchetti et al., 2009). This makes the selection of an animal model an important subject. In principle, this selection is based on the similarity of the toxicokinetics / toxicodynamics of PM, including its transport in the blood circulation, between animal and human systems (Davidson et al., 1987). Most of the exogenous compounds including toxins are being transported in the circulation through serum albumin, which carries them to different target organs for further metabolism (Peters, 1996). Therefore, it is imperative to study the similarity in the transport of any ligand in the blood circulation of human and animal systems (Poór et al., 2014). In view of this, a comparative study on the binding characteristics of PM towards serum albumins of human (HSA), bovine (BSA), porcine (PSA), sheep (SSA) and rabbit (RbSA) is essential.

Problem statement

Does PM bind to HSA? If yes, what are the binding characteristics of PM-HSA interaction and which mammalian albumin shows close similarity to HSA in terms of PM binding characteristics?

In order to answer the above questions, the following objectives were set:

1. To study the interaction of PM with HSA in terms of binding affinity, binding forces and location of the binding site.
2. To study the effect of ligand binding on the conformation and thermal stability of HSA.
3. To compare PM binding characteristics in different mammalian serum albumins.

CHAPTER 2

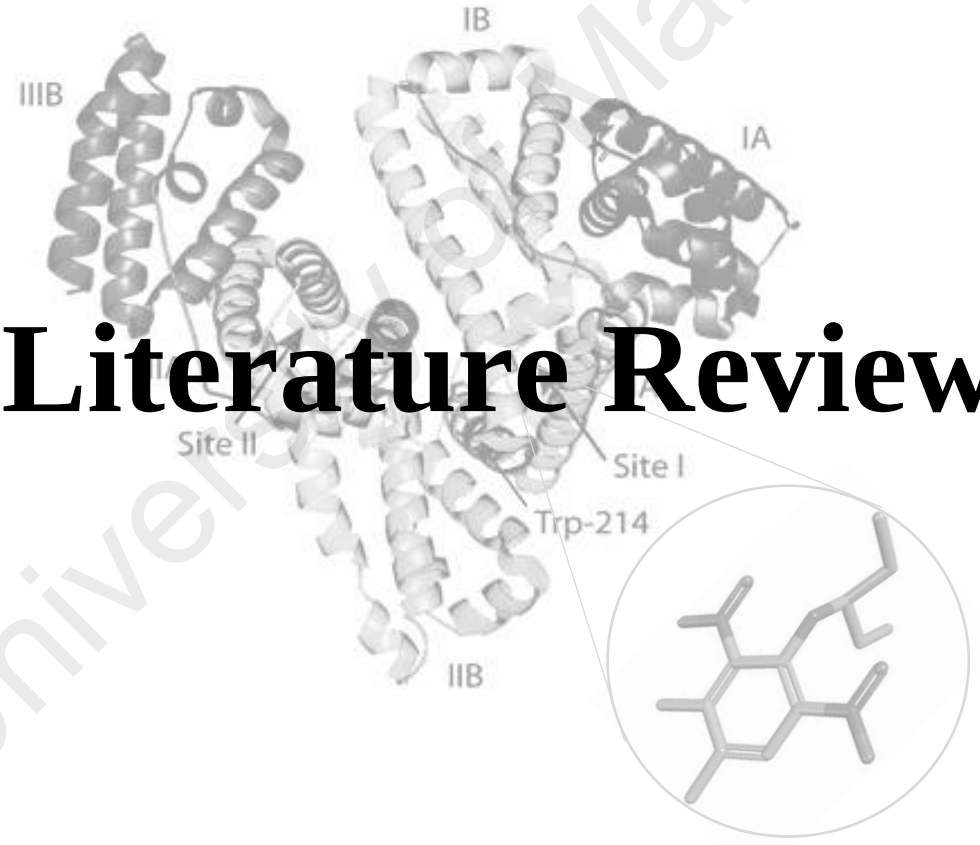

Literature Review

CHAPTER 2

LITERATURE REVIEW

2.1 Herbicides

Herbicides are chemicals used to kill or interrupt the normal growth of weeds, *i.e.* plants with more undesirable characteristics compared to its goodness (Hartwig, 1996). Herbicides were first introduced in 1940s and rapid development in the use of herbicides occurred after World War II (Zimdahl, 1993). The dominance of herbicides for weed control occurred during the revolution in the agriculture field, where herbicides save human energy and farmers achieved better crop quality and increased crop production at lower cost. According to one approximation, herbicides were used to reduce weed population on approximately 220 million acres of U.S. cropland (Gianessi and Reigner, 2007).

2.1.1 Classification of herbicides

Herbicides can be classified on the basis of selectivity, time of application, chemical structure and mechanism of action (Zimdahl, 1993).

On the selectivity ground, herbicides are grouped as 'selective' and 'non-selective' herbicides. 'Selective' herbicides are those that kill or suppress the targeted weeds without harming the desirable plant species, whereas 'non-selective' herbicides kill all plants when applied at right rate. Selectivity is not a precise system of classification as it is also affected by many other factors such as plant age and stage of growth, plant morphology, absorption, translocation, time and method of application, herbicide formulation and environmental conditions (Zimdahl, 1993).

Time of herbicide application is referred to 'pre-plant', 'pre-emergence' and 'post-emergence' applications. 'Pre-plant' applications are usually performed by introducing

the herbicides into the soil before planting. Application of herbicides after planting but prior to emergence of the crops or weeds is known as 'pre-emergence' application. If the herbicides are applied after the crop and/or weed have emerged, it is known as 'post-emergence' application (Zimdahl, 1993).

Based on the similarities in their chemical structures, herbicides of the same chemical group generally show common physiological characteristics. However, slight modification of a functional group may lead to significant change in the activity, selectivity, persistence and mode of action of a herbicide (Sherwani et al., 2015; Varshney and Sondhia, 2008).

Mechanism of action is referred to the biochemical and biophysical responses of the plants upon herbicidal treatment (Zimdahl, 1993). Herbicides of the same chemical family usually have the same mechanism of action. On the other hand, it is also possible for the herbicides with different chemical structures to possess the same action mechanism. Table 2.1 shows examples of the chemical family of several herbicides and their mechanism of action. The detailed information about the classification of herbicides is available in the *Herbicide Handbook* of the Weed Science Society of America (Vencill, 2002).

2.2 Pendimethalin

Pendimethalin (PM) [N-(1-ethylpropyl)-2,6-dinitro-3,4-xylidine], whose chemical structure is given in Figure 2.1, is a member of dinitroaniline group of herbicides and is registered in all European Union countries. It is commonly used in controlling most annual grasses and certain broadleaf weeds in various crops such as corn, potatoes, wheat, soybeans, cotton, tobacco, peanuts, grapes and onions (Tsiropoulos and Lolas, 2004). Approximately 9000 tons of PM were used for agricultural purposes in the USA in 1992 where around 60 % of it was applied in soybean fields (USGS, 1998). PM was found to

Table 2.1: Classification of several herbicides based on chemical structure and mode of action.

Mode of action	Chemical family	Common name
Inhibition of acetyl CoA carboxylase	Aryloxyphenoxy propionate	- Dichlofop - Haloxyfop
	Cyclohexanedione	- Alloxydim - Butroxydim
Inhibition of acetolactate synthase	Imidazolinone	- Imazamethabenz - Imazaqum
	Pyrimidinylthio-benzoate	- Bispyribac-sodium - Pyrithiobac
	Sulfonylurea	- Ethoxysulfuron - Iodosulfuron
	Triazolopyrimidine	- Cloransulam-methyl - Diclosulam
Inhibition of microtubule assembly	**Dinitroaniline**	- **Pendimethalin** - Trifuralin
	Pyridine	- Dithiopyr - Thiazopyr
Synthetic auxins	Phenoxy	- 2,4-D - Dichlorprop, 2,4-DP
	Benzoic acid	- Dicamba
	Carboxylic acid	- Clopyralid - Picloram
Inhibition of photosynthesis at photosystem II site A	Pyridazinone	- Pyrazon
	Triazine	- Atrazine - Prometryn
	Uracil	- Bromacil
Inhibition of photosynthesis at photosystem II site B	Benzothiadiazole	- Bentazon
	Nitrile	- Bromoxynil

Table 2.1: continued

Inhibition of lipid synthesis; not ACCase inhibition	Thiocarbamate	- Prosulfocarb - Vernolate
Inhibition of carotenoid biosynthesis	Triazole	- Amitrole - Aclonifen
Inhibition of the phytoene desaturase	Pyridazinone	- Norflurazon
	Pyridinecarboxamide	- Picolinafen
Photosystem I electron diverters	Bipyridylium	- Diquat - Paraquat
Inhibition of synthesis of very long-chain fatty acids	Acetamide	- Napropamide
	Chloroacetamide	- Acetochlor - Metalochlor
Inhibitiom of mitosis	Carbanilate	- Carbetamide
Membrane disruption	Dinitrophenol	- Dinoterb

Taken from Mallory-Smith and Retzinger (2003)

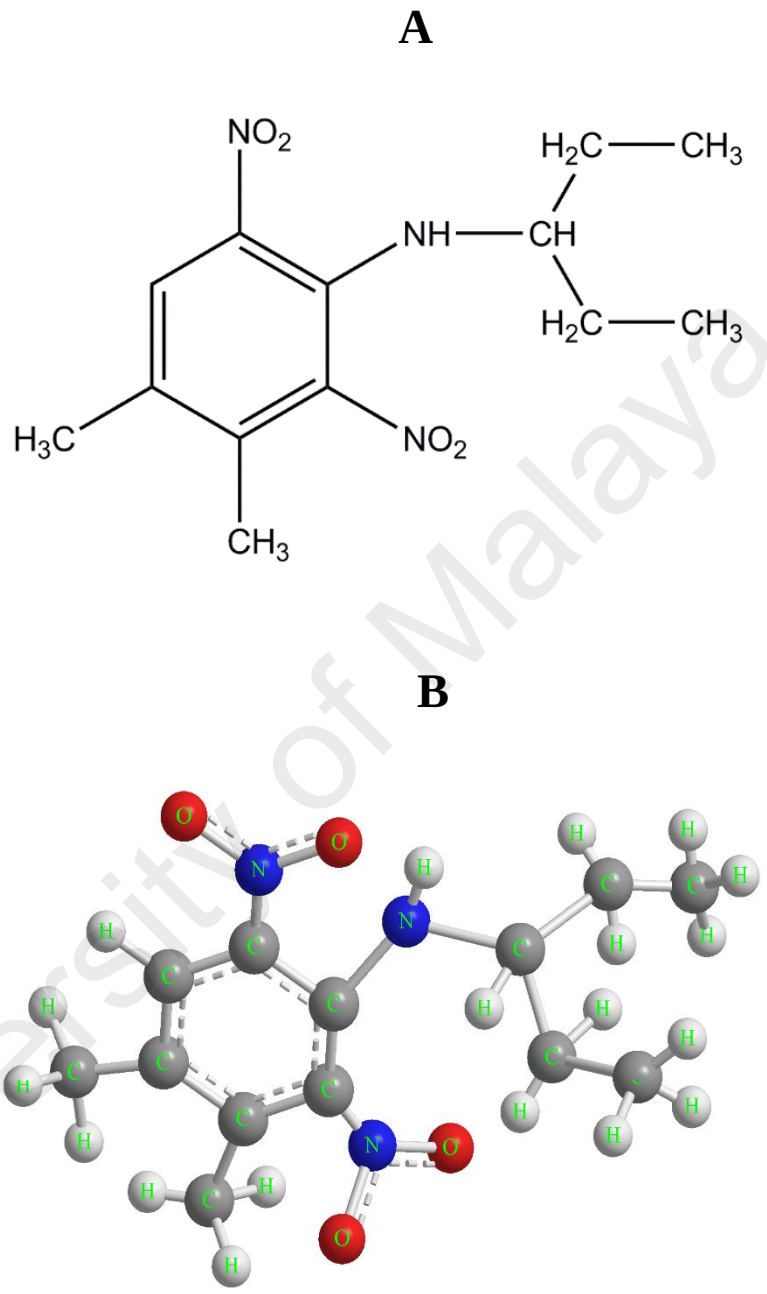

Figure 2.1: Chemical structure (A) and ball-and-stick model (B) of pendimethalin.

be one of the most effective pre-emergence herbicides used in dry-seeded rice among the available herbicides in Bangladesh (Ahmed and Chauhan, 2014). Being classified as a selective herbicide, it kills the targeted weeds by inhibiting microtubule synthesis, which are needed in cell wall formation and chromosomal separation during cell mitosis (Parka and Soper, 1977). PM (trade name: Prowl) is available in the market in the form of emulsifiable concentrate, wettable powder or dispersible granule formulations.

2.2.1 The fate of PM in soil

The rate of degradation of PM in soil depends on the method of application as well as the soil properties such as soil type, soil temperature and soil moisture content. PM is found to be more persistent when it is applied by incorporation than its application on the soil surface. The half-life of PM varies from 72 to 172 days at 25 ℃ and depends on soil types, thus reflecting its different persistency levels in the soil. At the same temperature, the half-life increases with decreasing soil moisture content, whereas it shows slower rate of degradation at lower temperatures (Walker and Bond, 1977). A certain persistence level of herbicides in soil might be useful for efficient control of weeds (Tsiropoulos and Lolas, 2004).

PM has low water solubility (0.3 mg L^{-1} at 20 ℃), moderate to high vapor pressure (4.0 mPa at 25 ℃) and strong adsorption to soil (K_{oc} = 7 011 ml g^{-1} in loamy sandy soil of 0.87 % organic carbon) (Tomlin 1997). Therefore, movement of this herbicide in surface runoff and leaching under normal usage is expected to be low except through sediment transport of adsorbed herbicide during soil erosion (Starett et al., 1996; Suzuki, 2000).

2.2.2 Environmental impact of PM

The extensive use of PM in agriculture may lead to environmental contamination. Figure 2.2 shows the possible routes through which herbicides can reach different

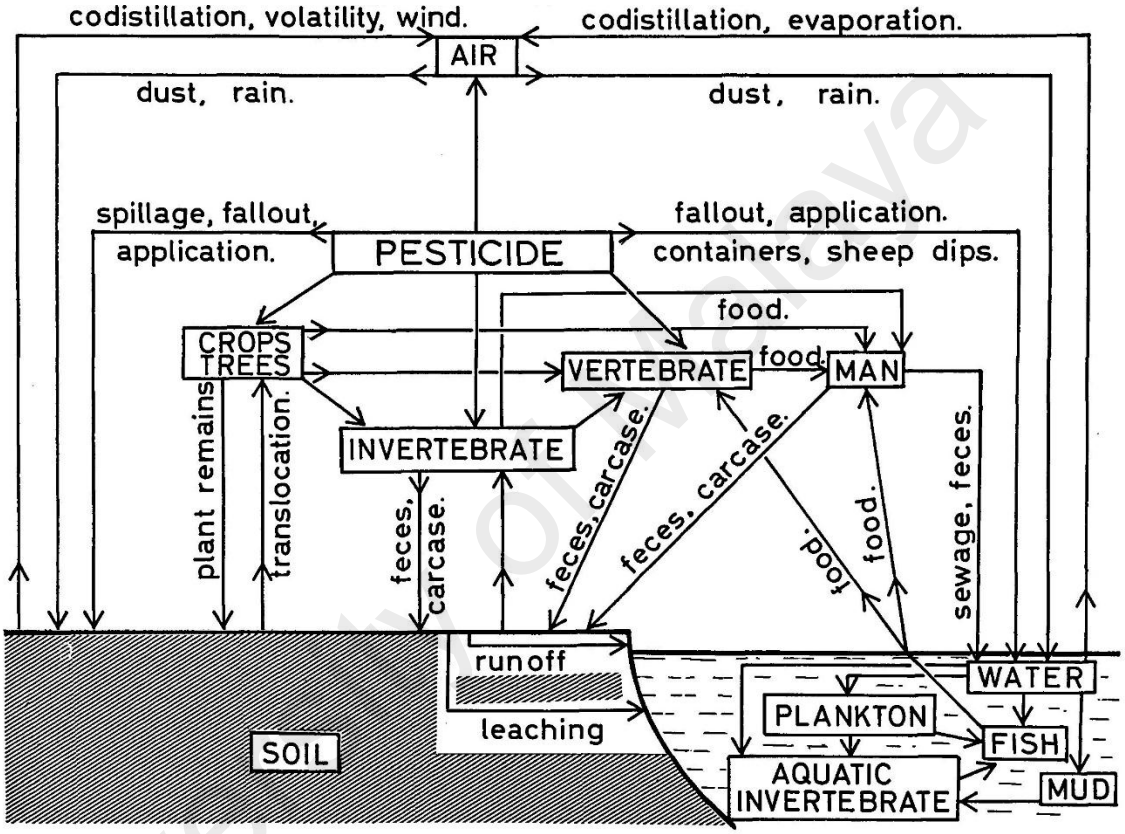

Figure 2.2: Schematic diagram showing the cycling of pesticides in the environment. (Acquired from Edwards and Adams, 1970)

environments and its cycle in the environment. The soil may serve as a reservoir of PM residues due to its strong adsorption to the soil. However, these PM residues may reach other parts of the environment, *i.e.* the aquatic environment and the air through agricultural runoff, leaching, drift, evaporation and aerosol application and thus causes water and air pollutions (Edwards and Adams, 1970; Strandberg and Scott-fordsmand, 2004). As an evidence to it, presence of PM was detected in the pond water and sediment originating from runoff from a commercial nursery in South Carolina (Riley et al., 1994) as well as in streams draining soils in agricultural areas at concentration up to 0.1 µg/L in Denmark (Lokke, 1999). PM was also detected as a contaminant in surface water, air and precipitation in USA in the years 1998 and 1999 (Capel et al., 1998; Larson et al., 1999). PM has been reported as one of the most frequently detected contaminants of groundwater in Portugal, which exceeded the EU regulatory limit (Goncalves et al. 2007). A recent study has reported that White Nile River, recycle and drainage water in Kenana, Sudan were contaminated by PM due to its heavy use for weed control in White Nile State (Abd-Algadir et al., 2011).

2.2.3 Adverse effects of PM to the biota

Soil and sediment provide habitat for wide variety of soil biota. Sediment contamination directly affects the ecology of these sediment-inhabiting organisms. A study on the effect of PM on the soil populations reported significant decrease in the number of bacteria, fungi and actinomycetes upon exposure to PM (Nayak et al., 1994). PM was found to inhibit the formation of sporangia and reduce the motility of zoospore of certain population of fungi (Wilcox, 1996). Besides, PM was also found to cause genotoxic effect on maize and onion by inducing chromosomal aberration in the root meristematic cells of the exposed plants (Promkaew et al., 2010).

The US Environmental Protection Agency (EPA) has classified PM as a persistent bioaccumulative toxic (PBT) agent and a possible 'Group C' human carcinogen (Megadi et al., 2010). The adverse effects of PM on the fresh-water population including phytoplankton, zooplankton and bottom fauna have also been reported (Poleksic et al., 1995). A study on Nile tilapia (*Oreochromis niloticus*), a common freshwater fish has shown significant decrease in body weight and increased levels of serum glucose, alkaline phosphatase, aspartate amino transferase, total protein and cholesterol in the fish upon exposure to PM. In addition, PM was also found to induce genotoxic effects on the PM-exposed fish (El-Sharkawy et al., 2011). Danion et al. (2014) have also shown deactivation of ethoxyresorufin-O-deethylase in the liver of PM-treated fish. Numerous *in vitro* studies conducted on the other terrestrial animals have shown induction of chromosomal aberration and formation of micronuclei in bone marrow cells of PM-treated mice (Dimitrov et al., 2006) as well as DNA strand breaks in Chinese hamster ovary cells upon exposure to PM (Patel et al., 2007).

2.2.4 The fate of PM in the mammalian system

An *in vivo* study using rat as a model (Zulalian, 1990) showed that rats treated with a single oral dose (37 mg kg^{-1} body weight) of [^{14}C]-4-methyl-labeled PM excreted major portion of the dose within 24 h both in urine and feces. However, less than 0.3 ppm PM residues were found in all tissues after 96 h except the fat which retained 0.9 ppm residues due to the lipophilic natue of PM or its metabolites. In view of the effectiveness of liver and kidney to remove PM and its metabolites from the blood, highest level of PM residues were detected at 6 h in these tissues. The major metabolic reactions of PM include hydroxylation of the 4-methyl and the N-1-ethyl group, oxidation of these alkyl groups to carboxylic acids, nitro reduction, cyclization and conjugation. Whereas the oxidation products were predominant in urine, methylbenzimidazolecarboxylic acids (products of

cyclization reactions) were found as unique metabolites in liver and kidney (Zulalian, 1990).

2.2.5 The importance of the interaction between PM and serum albumin

The toxicity of a compound is closely related to its toxicokinetics (change in concentration of a toxicant over time during absorption, distribution, biotransformation and elimination process) and toxicodynamics (interaction of a toxicant with biological target and its molecular, biochemical and physiological effects) in biological systems (Ringot et al., 2006). In order to exert its toxic effect, a toxicant should exist in its free state. Therefore, binding of the potential toxic compounds to the transport proteins in blood circulation is extremely important as it may reduce the bioavailability of the free toxicant. As evident from a previous study (Lie and Bratlid, 1970), binding of bilirubin to serum albumin led to its detoxification. Thus, transport proteins play crucial roles to carry toxic compounds especially those with low water solubility to the target site for elimination purposes (Vallner, 1977). Since PM exhibits low solubility in water, it is important to understand its interaction with the main transport protein in the human blood circulation, *i.e.* human serum albumin.

2.3 Human serum albumin

Human serum albumin (HSA) is coded by a single gene situated on the long arm of chromosome 4, near the centromere at position q11-22 (Harper and Dugaiczyk, 1983). The basic pathway of albumin synthesis follows the route: ribosome → rough endoplasmic reticulum → Golgi apparatus → exocytosis (Glaumann, 1970; Peters et al., 1971). It is synthesized in liver with the cleavage of the N-terminal peptide of the nascent chain before its release from the rough endoplasmic reticulum. The product, proalbumin is again cleaved at its N-terminal (Arg-Cly-Val-Phe-Arg-Arg) in the Golgi apparatus to produce secreted albumin (Peters and Davidson, 1982).

HSA is the predominant protein in the blood plasma at a concentration of about 40 mg mL^{-1} (Evans, 2002). However, this only constitutes 40 % of the total albumin content, the remaining albumin is distributed in the extracellular locations such as skin, muscle, fluids of the body (cerebrospinal, pleural, peritoneal, pericardial, amniotic fluids etc.) as well as secretions including milk, sweat, tears and saliva (Peters, 1996).

2.3.1 Physicochemical properties of HSA

The major physicochemical properties of HSA are shown in Table 2.2. It has a molecular mass of ~66 kDa as obtained from the calculation based on its amino acid composition (66 438 Da) as well as matrix-assisted laser desorption/ionization-time of flight (MALDI-TOF) mass spectrometry (66 479 Da) (Dockal et al., 1999; Minghetti et al., 1986). Oncley et al. (1947) have reported the values of the diffusion coefficient ($D_{20,W}$), the sedimentation coefficient ($S_{20,W}$) and the frictional ratio of HSA as 6.1×10^{-7} cm^2 s^{-1}, 4.5 S and 1.28:1, respectively. Based on the frequency dispersion of the dielectric constant study, the axial ratio of HSA has been predicted as 3:1 (Scheider et al., 1976). The radius of gyration has been found to be 26.7 Å (Carter and Ho, 1994). The shape of HSA is described as a 3-D equilateral triangle with sides of 80 Å and a depth of 30 Å (He and Carter, 1992). HSA has the intrinsic viscosity, $[\eta]$ and partial specific volume, $\bar{v}_2$ as 0.046 dL g^{-1} and 0.733 cm^3 g^{-1}, respectively (Hunter, 1996). Its isoelectric point varies from 4.7 (in the native form) to 5.8 (in the fatty acid free form) (Longsworth and Jacobsen, 1949). The isoionic point of HSA has been reported as 5.16 (Hughes, 1954), whereas the calculated net charge at pH 7.4 is –19 (Tanford, 1950). HSA exhibits a specific absorption coefficient, $\varepsilon_{1\,cm}^{1\,\%}$ of 5.3 at 280 nm (Wallevik, 1973). HSA mainly consists of α-helical structure (67 %), whereas the rest of the residues are folded in β-form (10 %) and flexible regions (23%) between subdomains (Carter and Ho, 1994).

Table 2.2: Physicochemical properties of HSA.

Property	Value	Reference
Molecular mass		
- Amino acid composition	66 438 Da	Minghetti et al. (1986)
- MALDI-TOF	66 479 Da	Dockal et al. (1999)
Diffusion coefficient, $D_{20,W}$	6.1×10^{-7} cm^2 s^{-1}	Oncley et al. (1947)
Sedimentation coefficient, $S_{20,W}$	4.5 S	Oncley et al. (1947)
Frictional ratio	1.28:1	Oncley et al. (1947)
Axial ratio	3:1	Scheider et al. (1976)
Radius of gyration	26.7 Å	Carter and Ho (1994)
Overall dimension	80 × 80 × 30 Å	He and Carter (1992)
Intrinsic viscosity, $[\eta]$	0.046 dL g^{-1}	Hunter (1996)
Partial specific volume, $\bar{v}_2$	0.733 cm^3 g^{-1}	Hunter (1996)
Isoelectric point		
- Native	4.7	Longsworth and Jacobsen (1949)
- Defatted	5.8	Gianazza et al. (1984)
Isoionic point	5.16	Hughes (1954)
Net charge (pH 7.4)	–19	Tanford (1950)
$\varepsilon_{1\ cm}^{1\ \%}$ at 280 nm	5.3	Wallevik (1973)
Secondary structures		
- α-helix	67 %	Carter and Ho (1994)
- β-form	10 %	Carter and Ho (1994)

2.3.2 Structural organization of HSA

The primary structure of HSA, *i.e.* its amino acid sequence and disulfide bonding pattern is shown in Figure 2.3. HSA consists of 585 amino acid residues, which form nine loops and are linked together by 17 disulfide bridges. These are further grouped into three homologous domains, consisting triplets of long-short-long loops. The different domains of HSA are named as domain I (residues 1-195), domain II (residues 196-383) and domain III (residues 384-585), as indicated by arrows in Figure 2.3. These domains are further divided into several subdomains. The first two loops of each domain, *viz.* loops 1-2, 4-5 and 7-8 are grouped into subdomains IA, IIA and IIIA, respectively; whereas loops 3, 6 and 9 form subdomains IB, IIB and IIIB, respectively (Peters, 1996). As illustrated in Figure 2.4, subdomains A consist of six α-helices, whereas subdomains B are made up of four α-helices. The helices, h1-h4 share the similar pattern between subdomains A and B. However, there are extra two short helices (h5 and h6) in subdomains A. A total of 35 cysteine residues are present in HSA, where 34 of them form 17 disulfide bridges that connect these helices (Sugio et al., 1999). The arrangement of different subdomains of HSA in its three-dimensional structure is shown in Figure 2.5.

2.3.3 Functions of HSA

One of the major functions of HSA is to act as a transport protein in the blood circulation for the distribution of a wide variety of compounds such as steroid hormones, vitamin D, bile salts, fatty acids, amino acids, etc., which possess low water solubility. It also carries metal ions, *i.e.* zinc, iron, calcium, copper and chloride in the blood stream (Peters, 1996). HSA has also been reported to transport various exogeneous ligands such as pharmaceutical drugs (Kragh-Hansen et al., 2002; Otagiri, 2005; Peters, 1996) and potential toxic compounds (Tunç et al., 2014; Zhang et al., 2013). Besides, it also transports toxic metabolites (e.g. bilirubin) to the liver for detoxification (Knudsen et al.,

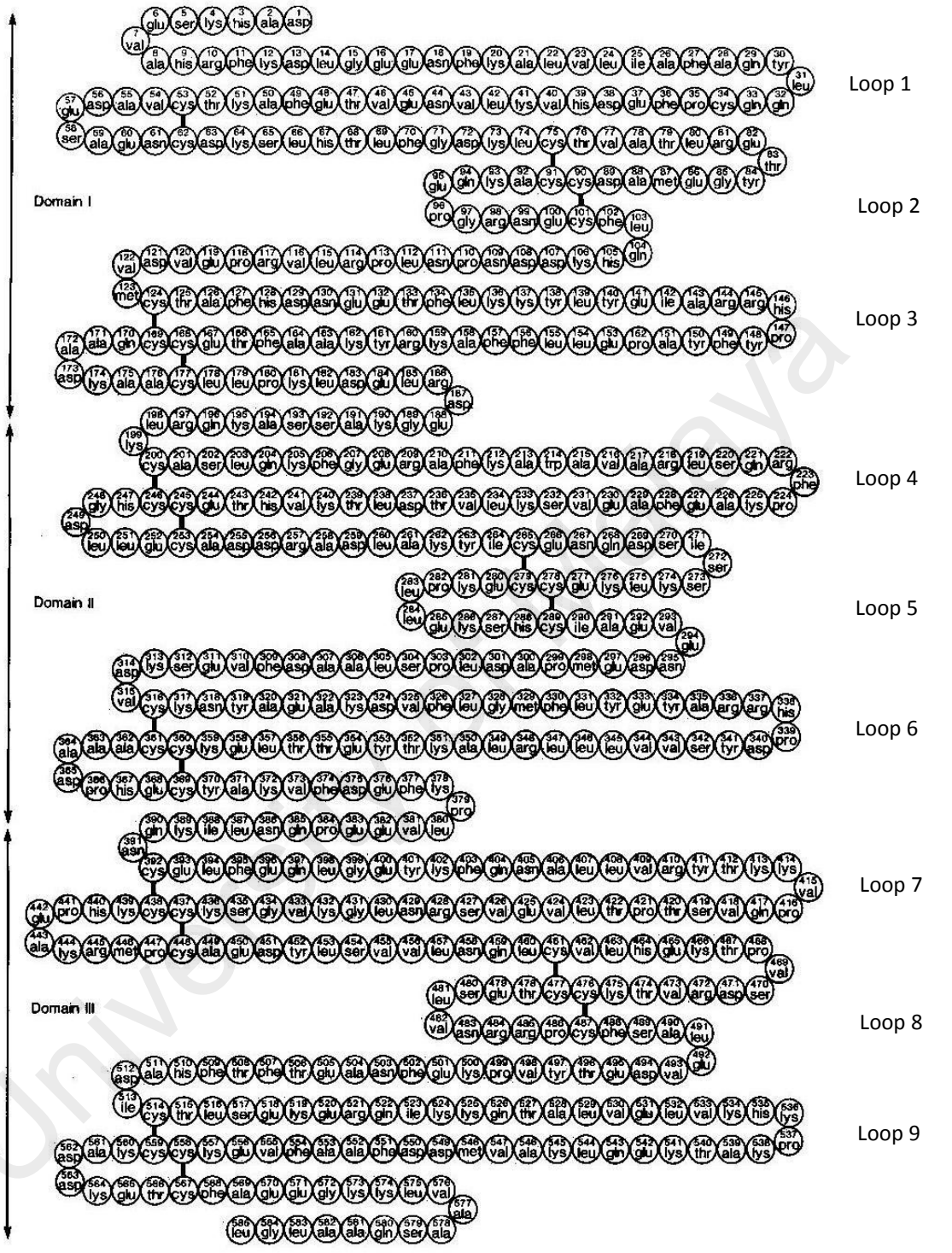

Figure 2.3: Amino acid sequence and disulfide bonding pattern of human serum albumin. A triple-domain structure of internal homology is indicated by arrows. (Acquired from Dugaiczyk et al., 1982)

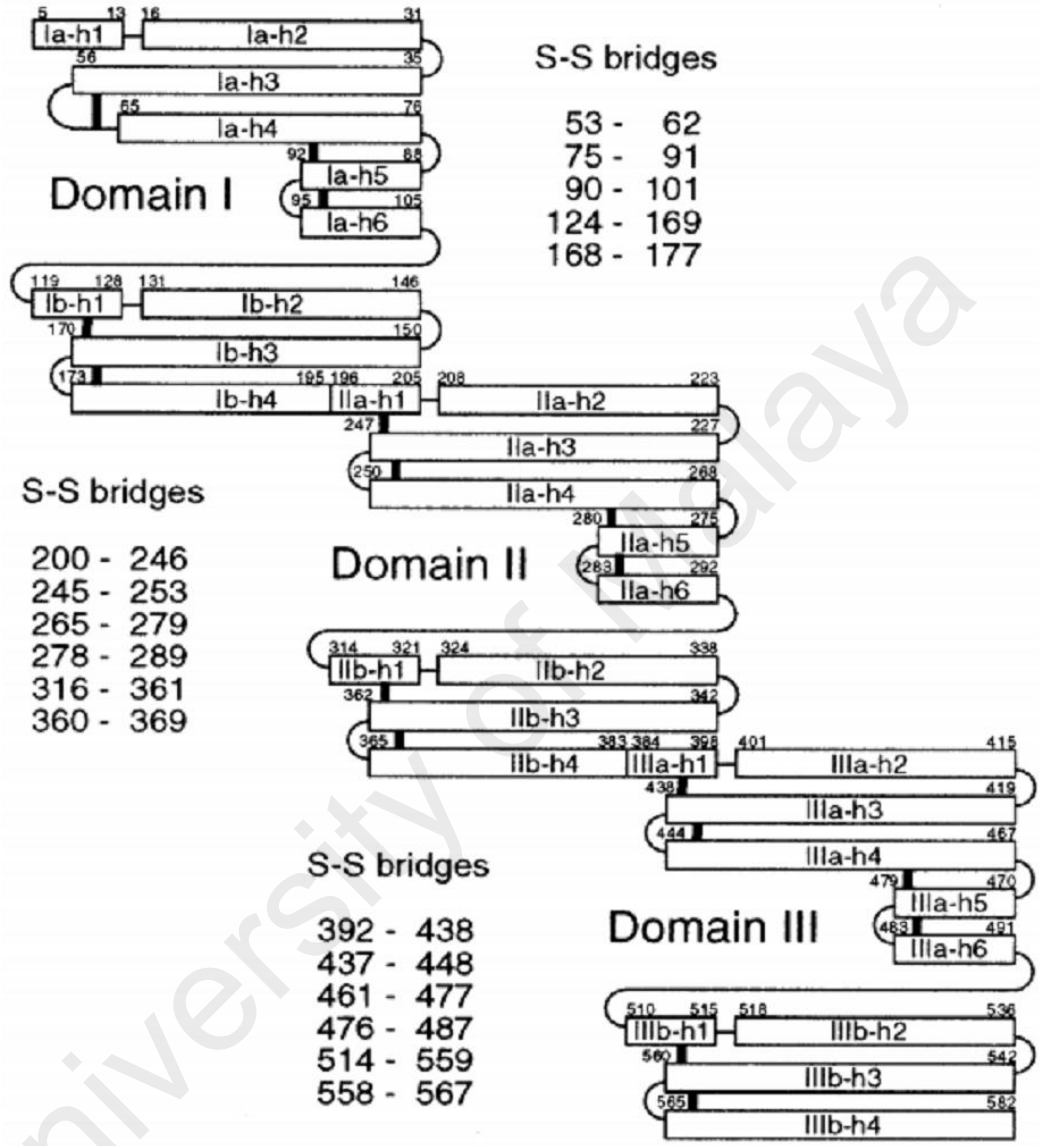

Figure 2.4: Schematic diagram showing the helices and disulfide bridges of HSA. Helices are shown in rectangles; loops and turns are indicated by thin lines; disulfide bridges are drawn with thick lines. The sequence nomenclature was derived from Minghetti et al., 1986. (Acquired from Sugio et al., 1999)

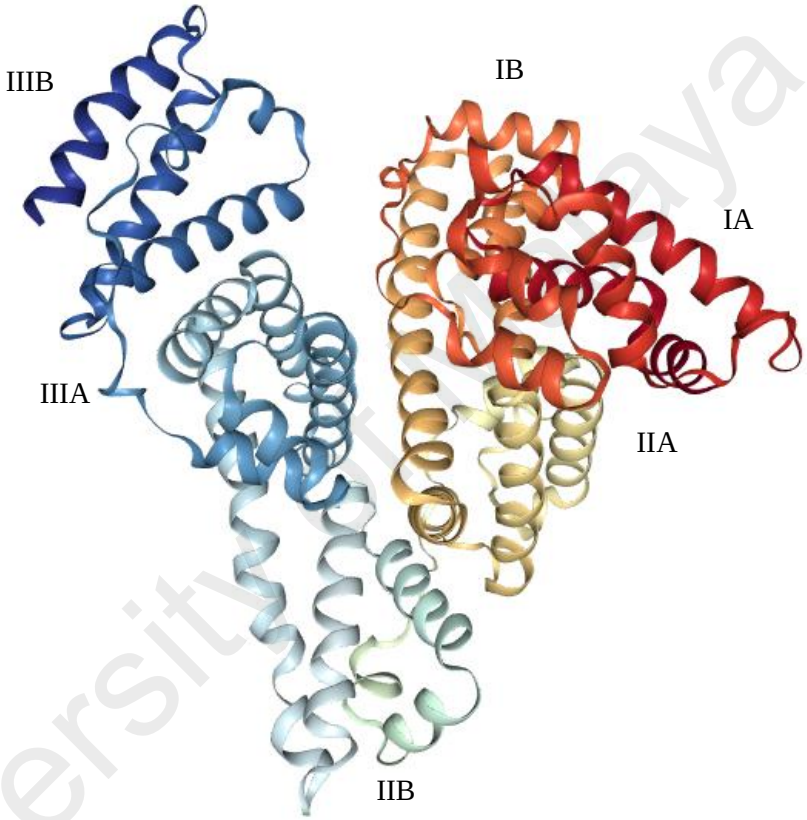

Figure 2.5: Three-dimensional structure of HSA, showing six subdomains in different colors. (Adapted from RCSB Protein Data Bank, PDB ID code 1BM0).

1986). In addition, HSA also acts as a depot protein for nitric oxide, a major signaling molecule (Stamler et al., 1992).

HSA plays important role in the regulation of colloid osmotic pressure (Quinlan et al., 2005) and the maintenance of blood pH (Figge et al., 1991). It also functions as an anti-oxidant by binding free copper (Cu^{2+}) ions, which are responsible for the production of reactive oxygen and nitrogen species (Evans, 2002). Besides, HSA is known to possess esterase activity (Dubois-Presle et al., 1995).

2.3.4 Ligand binding sites of HSA

HSA has been reported to bind large number of ligands at different ligand binding sites (Curry et al., 1998; Peters, 1996). Majority of the ligands bind reversibly to HSA with an association constant, falling in the range of 10^4 to 10^6 M^{-1} (Carter and Ho, 1994; Kragh-Hansen et al., 2002). Sudlow et al. (1975) identified two specific ligand binding sites on HSA, namely, site I and site II, based on fluorescent probe displacement study. Sites I and II were found to be located in domains II and III, respectively, on the basis of peptic and tryptic digestion results (Bos et al., 1988). Later on, crystallographic studies assigned the locations of sites I and II in subdomains IIA and IIIA, respectively (Carter and Ho, 1994; Curry et al., 1998; Sugio et al., 1999). Several ligands and their respective binding sites are shown in Figure 2.6. Names of the ligands, which share the same binding sites have also been included in the figure.

2.3.4.1 Site I

Site I is made up of a pair of nonpolar clusters with two centrally-located clusters of polar residues, formed by Lys-195, Lys-199, Arg-218 and Arg-222 at the entrance, and Tyr-150, His-242 and Arg-257 at the bottom of the pocket (Ghuman et al., 2005). Site I seems to be a large and flexible binding region as it can fit wide variety of ligands including those with large molecular structure (*e.g.* bilirubin). Ligands that bind to site I

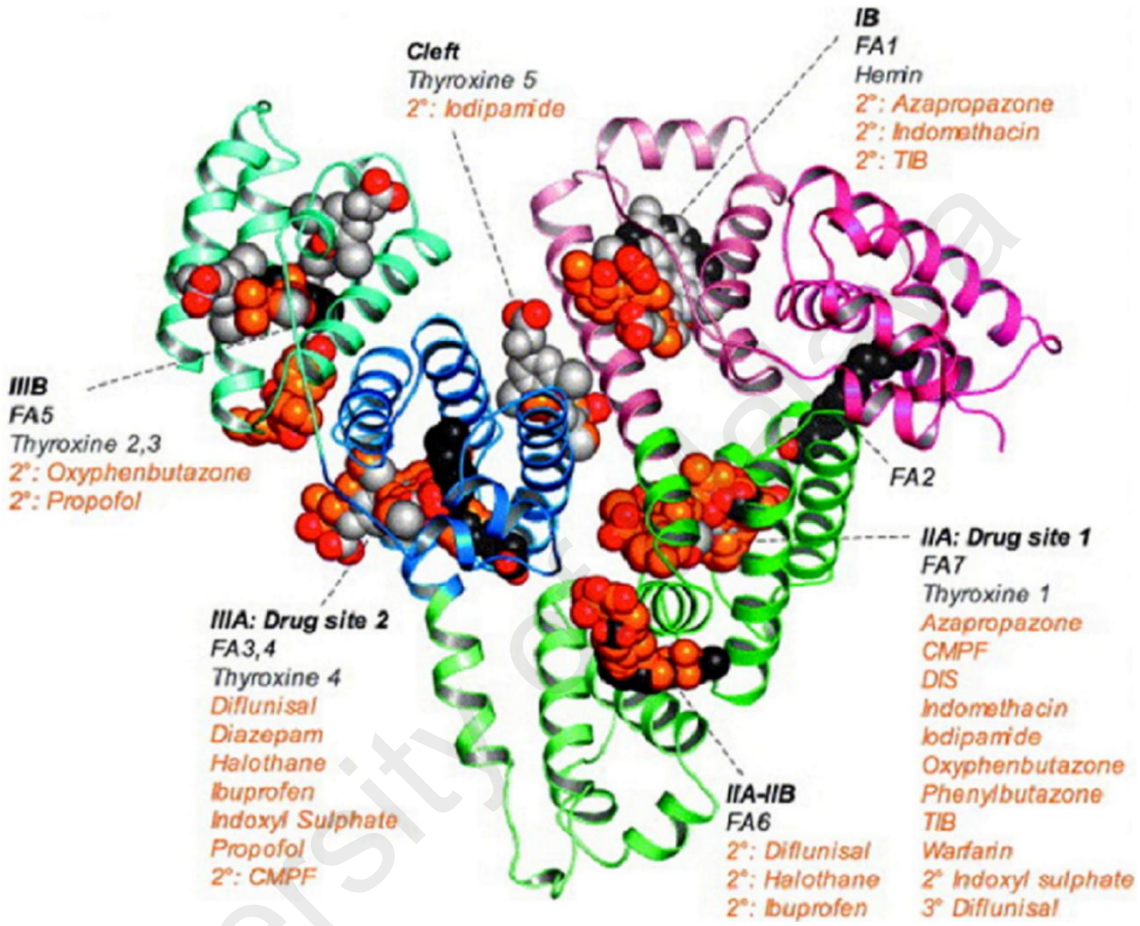

Figure 2.6: Three-dimensional structure of HSA showing various ligand binding sites. Ligands are depicted in space-filling models; oxygen atoms are colored red; all other atoms in fatty acids, other endogeneous ligands (hemin and thyroxine) and drugs are colored black, grey and orange, respectively. (Acquired from Ghuman et al., 2005)

with high affinity are usually bulky heterocyclic compounds with a negative charge or dicarboxylic acids (Kragh-Hansen et al., 2002). Several studies have shown the complexity of site I. Fehske et al., (1982) reported mutual interactions between warfarin and azapropazone at site I due to overlapping binding regions, whereas Kragh-Hansen (1985 and 1988) suggested presence of two independent binding regions within site I. On the other hand, Yamasaki et al. (1996) proposed the existence of three binding regions within this site, *i.e.* subsites Ia, Ib and Ic, which are the binding regions for warfarin, azapropazone and butamben, respectively. The location of the single Trp residue (Trp-214) of HSA is in the non-overlapping region of warfarin site (Fehske et al., 1982).

2.3.4.2 Site II

The pocket of site II is lined by hydrophobic side chains and the double disulfide bridges of helix IIIa-h3. The side chain of Arg- 410 is located at the entrance of the pocket, whereas the hydroxyl of Tyr-411 faces toward the inside of the pocket (Sugio et al., 1999). According to Kragh-Hansen et al., (2002), aromatic carboxylic acids with a negatively charged group at one end of the molecule away from the hydrophobic center tend to bind to site II on HSA. Site II appears to be smaller and narrower compared to site I, as large molecules are rarely found to bind to this site. In addition, no overlapping subsites are seen in site II. It is also less flexible because ligand binding is often strongly influenced by stereoselectivity (Kragh-Hansen et al., 2002). This was supported by the evidence that the binding affinity of L-Trp to site II was ~100 times higher than its D-isomer (Kragh-Hansen et al., 2002). Furthermore, substitution of site II ligands with a small group may influence its binding as evident from the inhibition of binding of fluorinated diazepam to this site, which is known as the preferred binding site of diazepam (Chuang and Otagiri, 2001).

2.4 Serum albumins of different mammalian species

The amino acid compositions of five mammalian serum albumins, *i.e.* HSA, BSA, SSA, PSA and RbSA are shown in Table 2.3. The total number of amino acid residues of HSA and RbSA are 585 and 584, respectively, whereas BSA, SSA and PSA possess similar number (583) of amino acid residues. Albumins are rich in cysteine and charged amino acids but have low content of tryptophan, glycine and methionine (Brown and Shockley, 1982; Peters, 1985). The high percentage of total charged residues in albumin contributes to its solubility and the 17 disulfide bridges give its stability. All of these albumins have a Trp residue, invariably located in the long loop 4, whereas BSA, PSA and SSA possess an additional Trp residue in a homologous site in long loop 3 (Peters, 1996).

The complete amino acid sequences of different mammalian serum albumins are shown in Figure 2.7. The sequence homology among these albumins is indicated in blue color (Figure 2.7) and is expressed as the protein sequence similarity score in Table 2.4. All these albumins show high degree of similarity (72-92 %) among each other. Similarity in the molecular weight is also noticed among these albumins, which varies from 66 015 Da (rabbit) to 66 798 Da (porcine) (Michaud et al., 2009).

The use of animal models in modern biomedical research increased dramatically in the early 20th century (Ericsson et al., 2013). In order to select a suitable animal model, a few criteria such as close phylogenetic relationship or anatomical similarity between the animal and human as well as similar biochemical or physiological response to the process under investigation should be considered (Simon and Maibach, 2000). By using an animal model, the toxicological effect of PM can be extrapolated from animals to human. However, the validity of the extrapolation depends strictly on the interspecies similarities in ligand metabolism, physiology, absorption and distribution (Martinez, 2011). In order to identify the suitable animal model for further investigation in toxicological studies of

Table 2.3: Amino acid compositions of different mammalian albumins.

Amino acid	No. of residues				
	Human[a]	Bovine[a]	Sheep[b]	Porcine[c]	Rabbit[d]
Alanine	62	46	50	50	54
Arginine	24	23	22	26	22
Asparagine	17	14	14	13	12
Aspartic acid	36	40	44	37	43
Cysteine	35	35	35	35	35
Glutamic acid	62	59	56	61	56
Glutamine	20	20	19	20	14
Glycine	12	16	17	16	20
Histidine	16	17	18	18	23
Isoleucine	8	14	13	23	16
Leucine	61	61	61	62	62
Lysine	59	59	60	57	57
Methionine	6	4	4	-	1
Phenylalanine	31	27	28	29	24
Proline	24	28	28	30	29
Serine	24	28	25	23	26
Threonine	28	34	31	26	27
Tryptophan	1	2	2	2	1
Tyrosine	18	20	20	22	24
Valine	41	36	36	33	38
Total	**585**	**583**	**583**	**583**	**584**

[a] Peters (1995); [b] Brown et al. (1989); [c] Weinstock and Badwin (1988); [d] NCBI PDB accession no. NP_001075813

	1 10	20	30	40	50
Human	DAHKSEVAHR	FKDLGEENFK	ALVLIAFAQY	LQQCPFEDHV	KLVNEVTEFA
Bovine	DTHKSEIAHR	FKDLGEEHFK	GLVLIAFSQY	LQQCPFDEHV	KLVNELTEFA
Sheep	DTHKSEIAHR	FNDLGEENFQ	GLVLIAFSQY	LQQCPFDEHV	KLVKELTEFA
Porcine	DTYKSEIAHR	FKDLGEQYFK	GLVLIAFSQH	LQQCPYEEHV	KLVREVTEFA
Rabbit	EAHKSEIAHR	FNDVGEEHFI	GLVLITFSQY	LQKCPYEEHA	KLVKEVTDLA

	60	70	80	90	100
Human	KTCVADESAE	NCDKSLHTLF	GDKLCTVATL	RETYGEMADC	CAKQEPERNE
Bovine	KTCVADESHA	GCEKSLHTLF	GDELCKVASL	RETYGDMADC	CEKQEPERNE
Sheep	KTCVADESHA	GCDKSLHTLF	GDELCKVATL	RETYGDMADC	CEKQEPERNE
Porcine	KTCVADESAE	NCDKSIHTLF	GDKLCAIPSL	REHYGDLADC	CEKEEPERNE
Rabbit	KACVADESAA	NCDKSLHDIF	GDKICALPSL	RDTYGDVADC	CEKKEPERNE

	110	120	130	140	150
Human	CFLQHKDDNP	NLPRLVRPEV	DVMCTAFHDN	EETFLKKYLY	EIARRHPYFY
Bovine	CFLSHKDDSP	DLPKL-KPDP	NTLCDEFKAD	EKKFWGKYLY	EIARRHPYFY
Sheep	CFLNHKDDSP	DLPKL-KPEP	DTLCAEFKAD	EKKFWGKYLY	EVARRHPYFY
Porcine	CFLQHKNDNP	DIPKL-KPDP	VALCADFQED	EQKFWGKYLY	EIARRHPYFY
Rabbit	CFLHHKDDKP	DLPPFARPEA	DVLCKAFHDD	EKAFFGHYLY	EVARRHPYFY

	160	170	180	190	200
Human	APELLFFAKR	YKAAFTECCQ	AADKAACLLP	KLDELRDEGK	ASSAKQRLKC
Bovine	APELLYYANK	YNGVFQECCQ	AEDKGACLLP	KIETMREKVL	ASSARQRLRC
Sheep	APELLYYANK	YNGVFQECCQ	AEDKGACLLP	KIDAMREKVL	ASSARQRLRC
Porcine	APELLYYAII	YKDVFSECCQ	AADKAACLLP	KIEHLREKVL	TSAAKQRLKC
Rabbit	APELLYYAQK	YKAILTECCE	AADKGACLTP	KLDALEGKSL	ISAAQERLRC

	210	220	230	240	250
Human	ASLQKFGERA	FKAWAVARLS	QRFPKAEFAE	VSKLVTDLTK	VHTECCHGDL
Bovine	ASIQKFGERA	LKAWSVARLS	QKFPKAEFVE	VTKLVTDLTK	VHKECCHGDL
Sheep	ASIQKFGERA	LKAWSVARLS	QKFPKADFTD	VTKIVTDLTK	VHKECCHGDL
Porcine	ASIQKFGERA	FKAWSLARLS	QRFPKADFTE	ISKIVTDLAK	VHKECCHGDL
Rabbit	ASIQKFGDRA	YKAWALVRLS	QRFPKADFTD	ISKIVTDLTK	VHKECCHGDL

	260	270	280	290	300
Human	LECADDRADL	AKYICENQDS	ISSKLKECCE	KPLLEKSHCI	AEVENDEMPA
Bovine	LECADDRADL	AKYICDNQDT	ISSKLKECCD	KPLLEKSHCI	AEVEKDAIPE
Sheep	LECADDRADL	AKYICDHQDA	LSSKLKECCD	KPVLEKSHCI	AEVDKDAVPE
Porcine	LECADDRADL	AKYICENQDT	ISTKLKECCD	KPLLEKSHCI	AEAKRDELPA
Rabbit	LECADDRADL	AKYMCEHQET	ISSHLKECCD	KPILEKAHCI	YGLHNDETPA

Contd.....

	310	320	330	340	350
Human	DLPSLAADFV	ESKDVCKNYA	EAKDVFLGMF	LYEYARRHPD	YSVVLLLRLA
Bovine	NLPPLTADFA	EDKDVCKNYQ	EAKDAFLGSF	LYEYSRRHPE	YAVSVLLRLA
Sheep	NLPPLTADFA	EDKEVCKNYQ	EAKDVFLGSF	LYEYSRRHPE	YAVSVLLRLA
Porcine	DLNPLEHDFV	EDKEVCKNYK	EAKDVFLGTF	LYEYSRRHPD	YSVSLLLRIA
Rabbit	GLPAVAEEFV	EDKDVCKNYE	EAKDLFLGKF	LYEYSRRHPD	YSVVLLLRLG

	360	370	380	390	400
Human	KTYETTLEKC	CAAADPHECY	AKVFDEFKPL	VEEPQNLIKQ	NCELFKQLGE
Bovine	KEYEATLEEC	CAKDDPHACY	STVFDKLKHL	VDEPQNLIKQ	NCDQFEKLGE
Sheep	KEYEATLEDC	CAKEDPHACY	ATVFDKLKHL	VDEPQNLIKK	NCELFEKHGE
Porcine	KIYEATLEDC	CAKEDPPACY	ATVFDKFQPL	VDEPKNLIKQ	NCELFEKLGE
Rabbit	KAYEATLKKC	CATDDPHACY	AKVLDEFQPL	VDEPKNLVKQ	NCELYEQLGD

	410	420	430	440	450
Human	YKFQNALLVR	YTKKVPQVST	PTLVEVSRNL	GKVGSKCCKH	PEAKRMPCAE
Bovine	YGFQNALIVR	YTRKVPQVST	PTLVEVSRSL	GKVGTRCCTK	PESERMPCTE
Sheep	YGFQNALIVR	YTRKAPQVST	PTLVEISRSL	GKVGTKCCAK	PESERMPCTE
Porcine	YGFQNALIVR	YTKKVPQVST	PTLVEVARKL	GLVGSRCCKR	PEEERLSCAE
Rabbit	YNFQNALLVR	YTKKVPQVST	PTLVEISRSL	GKVGSKCCKH	PEAERLPCVE

	460	470	480	490	500
Human	DYLSVVLNQL	CVLHEKTPVS	DRVTKCCTES	LVNRRPCFSA	LEVDETYVPK
Bovine	DYLSLILNRL	CVLHEKTPVS	EKVTKCCTES	LVNRRPCFSA	LTPDETYVPK
Sheep	DYLSLILNRL	CVLHEKTPVS	EKVTKCCTES	LVNRRPCFSD	LTLDETYVPK
Porcine	DYLSLVLNRL	CVLHEKTPVS	EKVTKCCTES	LVNRRPCFSA	LTPDETYKPK
Rabbit	DYLSVVLNRL	CVLHEKTPVS	EKVTKCCSES	LVDRRPCFSA	LGPDETYVPK

	510	520	530	540	550
Human	EFNAETFTFH	ADICTLSEKE	RQIKKQTALV	ELVKHKPKAT	KEQLKAVMDD
Bovine	AFDEKLFTFH	ADICTLPDTE	KQIKKQTALV	ELLKHKPKAT	EEQLKTVMEN
Sheep	PFDEKFFTFH	ADICTLPDTE	KQIKKQTALV	ELLKHKPKAT	DEQLKTVMEN
Porcine	EFVEGTFTFH	ADLCTLPEDE	KQIKKQTALV	ELLKHKPHAT	EEQLRTVLGN
Rabbit	EFNAETFTFH	ADICTLPETE	RKIKKQTALV	ELVKHKPHAT	NDQLKTVVGE

	560	570	580	585
Human	FAAFVEKCCK	ADDKETCFAE	EGKKLVAASQ	AALGL
Bovine	FVAFVDKCCA	ADDKEACFAV	EGPKLVVSTQ	TALA
Sheep	FVAFVDKCCA	ADDKEGCFVL	EGPKLVASTQ	AALA
Porcine	FAAFVQKCCA	APDHEACFAV	EGPKFVIEIR	GILA
Rabbit	FTALLDKCCS	AEDKEACFAV	EGPKLVESSK	ATLG

Figure 2.7: Amino acid sequences of different mammalian albumins. Human (Minghetti et al., 1986); Bovine (Holowachuk, 1991); Sheep (Brown et al., 1989); Porcine (Weinstock and Baldwin, 1988); Rabbit (NCBI PDB accession no. NP_001075813)

Table 2.4: Molecular weight and sequence similarity score of different mammalian serum albumins.

Organism	MW (Da)	Protein sequence similarity score*				
		Human	Bovine	Porcine	Rabbit	Sheep
Human	66 472	1	0.77	0.77	0.75	0.76
Bovine	66 433		1	0.80	0.72	0.92
Porcine	66 798			1	0.75	0.78
Rabbit	66 015				1	0.73
Sheep	66 328					1

* Huang and Miller (1991)

Adapted from: Michaud, F.T., Garnier, A., Lemieux, L., and Duchesne, C. Multivariate analysis of single quadrupole LC-MS spectra for routine characterization and quantification of intact proteins. *Proteomics.* 2009. *9*(3), 512-520. Copyright Wiley-VCI. (Reproduced with permission)

PM, a comparative study on the binding characteristics of PM towards serum albumins of different mammalian species is necessary. On the other hand, differences in serum composition (*e.g.* α1-glycoprotein level, amount of total body water and extracellular body water) has been reported to result in species-specific differences in ligand binding and transportation of ligand across the blood circulation. Furthermore, presence of competitors for the ligand binding site has also contributed to the differences in ligand-protein interactions (Martinez, 2011). In spite of the close similarities among the five mammalian serum albumins used in this study, many other species-specific factors that may influence the *in vivo* performance should be taken into consideration.

CHAPTER 3

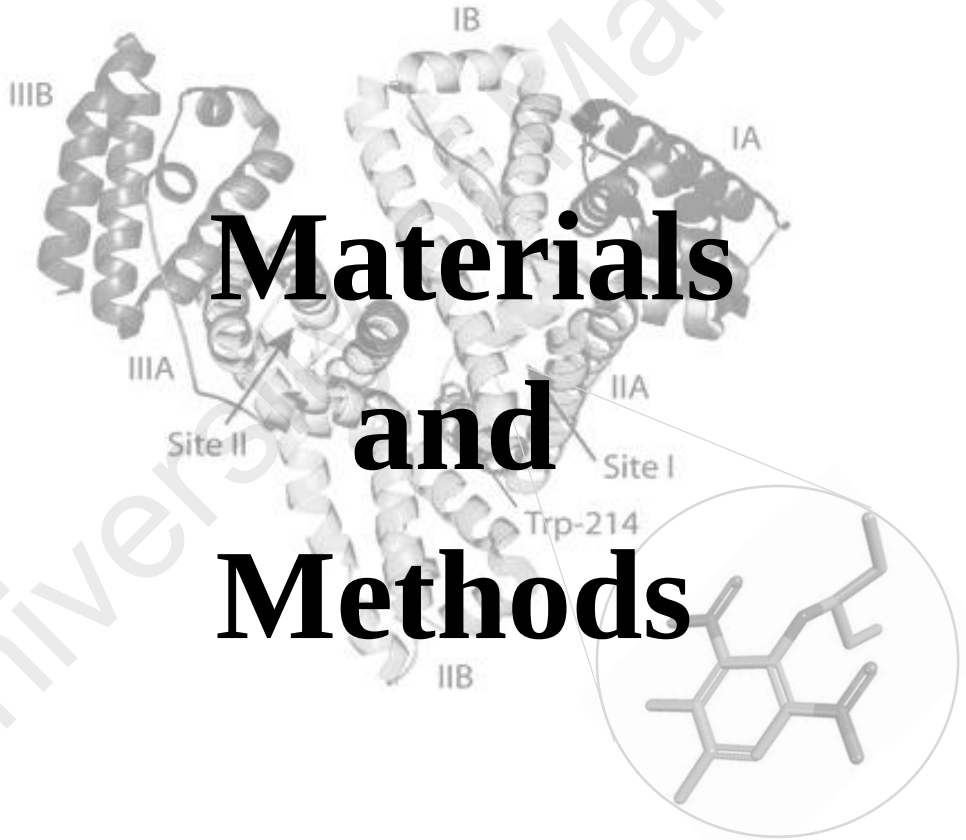

Materials and Methods

CHAPTER 3

MATERIALS AND METHODS

3.1 Materials

3.1.1 Proteins

Human serum albumin (HSA), essentially fatty acid free, ≥ 96 % (Lot # 068K7538V) was purchased from Sigma-Aldrich Co., USA. Other mammalian serum albumins, *viz.* bovine serum albumin (BSA), ≥ 96 % (Lot # 011M7406V), porcine serum albumin (PSA), ≥ 98 % (Lot # 084K7636), rabbit serum albumin (RbSA), ~ 99 % (Lot # 104K7560) and sheep serum albumin (SSA), ≥ 97 % (Lot # 117K7540) were also the products of Sigma-Aldrich Co., USA.

3.1.2 Herbicide

Pendimethalin (PM), Pestanal®, analytical standard (empirical formula: $C_{13}H_{19}N_3O_4$, molecular weight: 281.31) (Lot # SZBD302XV) was procured from Sigma-Aldrich Co., USA.

3.1.3 Ligands used in site marker displacement studies

Warfarin (WFN) (Lot # 104K1261), indomethacin (IDM) (Lot # 115K0689) and ibuprofen (IBN) (Lot # 122K0676V) were obtained from Sigma-Aldrich Co., USA.

3.1.4 Miscellaneous

Analytical grade quality of sodium dihydrogen phosphate and disodium hydrogen phosphate were purchased from SYSTERM®, Malaysia, whereas absolute ethanol was supplied by BDH Prolabo®, UK. Standard buffers of pH 7.0 and pH 10.0 were procured from Sigma-Aldrich Co., USA. Merck Millipore, Germany was the source of the PVDF

(0.45 µm) membrane filters, whereas cellulose nitrate (0.45 µm) membrane filters were supplied by Whatman®, England.

Ultrapure (Type 1) water produced by Mili-Q water purification system (Merck Milipore, Germany) was used throughout this study.

3.2 Methods

3.2.1 pH measurements

Delta 320 pH meter (Mettler-Toledo GmbH, Switzerland), attached with a HA405-K2/120 combination electrode was used in pH measurements. Calibration of the pH meter was made with standard buffers of pH 7.0 and pH 10.0 before pH measurements in the neutral and alkaline pH ranges, respectively. The least count of the pH meter was 0.01 pH unit.

3.2.2 Sample preparations

Serum albumin stock solutions were prepared by dissolving ~22 mg of lyophilized powder in 10 ml of 60 mM sodium phosphate buffer, pH 7.4. The samples were then filtered through PVDF filters. The protein concentrations of different stock solutions were determined spectrophotometrically, using molar absorption coefficients at 280 nm, *i.e.* 36 500 $M^{-1}cm^{-1}$ for HSA (Painter et al., 1998), 43 827 $M^{-1}cm^{-1}$ for BSA, 43 385 $M^{-1}cm^{-1}$ for both PSA and RbSA and 42 925 $M^{-1}cm^{-1}$ for SSA (Khan et al., 2013). The stock solutions were stored at 4 °C and were used within one week.

An appropriate amount of individual site marker ligands (WFN, IDM and IBN) as well as herbicide (PM) was dissolved in 10 ml of ethanol to prepare their stock solutions. Working solutions of these site marker ligands/herbicide were obtained by diluting the stock solution with 60 mM sodium phosphate buffer, pH 7.4 to the desired concentrations.

3.2.3 Absorption spectroscopy

Absorption measurements were made on a Perkin Elmer Lambda 25 UV/Vis spectrophotometer, using a pair of 1 cm path-length quartz cuvette. Scattering corrections, if required, were made by extrapolation of the absorbance values in the wavelength range, 360–340 nm to the desired wavelength (Tayyab and Qasim, 1986).

3.2.4 Fluorescence spectroscopy

Fluorescence measurements were carried out on a Jasco FP-6500 spectrofluorometer, equipped with a jacketed cell holder, connected to an external thermostated circulating water bath, using a 1 cm path-length quartz cuvette. Both excitation and emission slit widths were set at 10 nm while the scanning speed was fixed at 500 nm/min. The data pitch and the detector voltage used were 1 nm and 240 V, respectively. The fluorescence spectra were recorded in the wavelength range of 310–400 nm upon exciting the protein solution at 295 nm.

For three-dimensional (3-D) fluorescence measurements, emission scans were recorded in the wavelength range of 220–500 nm with a data pitch of 1 nm, while the excitation wavelength range was set at 220–350 nm with 5 nm intervals. The other scanning parameters were kept the same as mentioned above. The protein samples were prepared by incubating 3 μM HSA both in the absence and the presence of PM (3 μM and 6 μM) for 1 h at 25 °C.

3.2.5 Circular dichroism spectroscopy

Circular dichroism (CD) spectra were recorded on a Jasco J-815 spectropolarimeter, attached with a Jasco PTC-423S/15 Peltier-type thermostated cell holder, under constant nitrogen flow at 25 ℃. Far-UV (200–250 nm) CD spectral measurements were performed using a protein concentration of 3 μM in a 1 mm path-length quartz cuvette, whereas the

protein concentration and path-length of the cuvette used for near-UV (250–300 nm) CD spectral measurements were 10 μM and 10 mm, respectively. CD spectra were recorded both in the absence and the presence of PM using PM/HSA molar ratio of 2:1 and 1:1.

3.2.6 Interaction study of PM with HSA

The interaction between PM and HSA was investigated using fluorescence quenching titration method (Feroz et al., 2012).

3.2.6.1 Fluorescence quenching titration

The titration was performed at four different temperatures *viz.* 15, 25, 35 and 45 °C. A constant volume (300 μL) of the stock protein solution (30 μM), taken in different tubes, was titrated with increasing PM concentrations (0–7.2 μM) in 0.9 μM intervals. The total volume in each tube was made to 3.0 ml with 60 mM sodium phosphate buffer, pH 7.4. The mixture was incubated at constant temperature for 1 h before fluorescence measurements in the wavelength range, 310–400 nm upon excitation at 295 nm.

3.2.6.2 Data analysis

Inner filter effect correction

The observed fluorescence intensity values were corrected for the inner filter effect, using the following equation (Lakowicz, 2006):

$$F_{cor} = F_{obs} \times e^{(Aex + Aem)/2} \quad (1)$$

where F_{cor} is the corrected fluorescence intensity, F_{obs} is the observed fluorescence intensity, A_{ex} and A_{em} are the absorbance values at the excitation and the emission wavelengths, respectively.

Quenching and binding parameters

The decrease in the fluorescence intensity of HSA at λ_{max} was analyzed using Stern-Volmer equation (Lakowicz, 2006).

$$F_0 / F = K_{sv} [Q] + 1 = k_q \tau_0 [Q] + 1 \quad (2)$$

where F_0 and F are the fluorescence intensity values of HSA before and after the addition of the quencher (PM), respectively, K_{sv} is the Stern-Volmer constant, [Q] is the quencher concentration, k_q is the bimolecular quenching rate constant and τ_0 is the excited state lifetime of the biomolecule (HSA) in the absence of the quencher and its value was taken as 6.38×10^{-9} s (Abou-Zied & Al-Shihi, 2008).

Values of the association constant, K_a for PM-HSA interaction were obtained after treating the fluorescence quenching data according to the following equation (Bi et al., 2004):

$$\log (F_0 - F) / F = n \log K_a - n \log [1 / ([L_T] - (F_0 - F)[P_T] / F_0)] \quad (3)$$

where n is the Hill coefficient, $[L_T]$ is the total ligand (PM) concentration and $[P_T]$ refers to the total protein (HSA) concentration. K_a values at different temperatures were determined from the plot of $\log (F_0 - F) / F$ versus $\log [1 / ([L_T] - (F_0 - F)[P_T] / F_0)]$.

Thermodynamic parameters

Thermodynamic parameters such as the entropy change (ΔS) and the enthalpy change (ΔH) of the binding reaction were obtained from the plot of 1n K_a versus 1 / T, based on the van't Hoff equation (Raffa, 2003).

$$1n K_a = -\Delta H / RT + \Delta S / R \quad (4)$$

where T is the absolute temperature (273 + °C) and R is the gas constant (8.3145 J mol^{-1} K^{-1}).

The values of Gibbs free energy change (ΔG) were calculated by substituting the values of ΔH and ΔS in the following equation:

$$\Delta G = \Delta H - T\Delta S \quad (5)$$

3.2.7 Thermal stability study

Thermal stability of HSA (3 μM) was evaluated both in the absence and the presence of PM (6 μM) using fluorescence spectroscopy within the temperature range, 25–100 ℃ in equal increments of 5 ℃. The protein sample, taken in a 1 cm path-length quartz cell was capped and placed in a jacketed cell holder. The samples were allowed to equilibrate for 6 min at each temperature before recording the fluorescence intensity at 343 nm. The sample containing the PM-HSA mixture was incubated for 1 h at 25 ℃ prior to fluorescence measurements at different temperatures. The other parameters were the same as those used in fluorescence spectroscopy.

3.2.8 Site marker displacement study

The competitive experiments were carried out at 25 ℃ using WFN and IDM as site I markers, whereas IBN was selected as site II marker. Increasing concentrations (0–6.3 μM with 0.9 μM intervals) of PM were added to either HSA (3 μM) or an equimolar (3 μM) mixture of site marker and HSA, preincubated for 1 h at 25 ℃ and the final mixture (3 ml) was further incubated for 1 h at 25 ℃ before fluorescence measurements. The fluorescence spectra of WFN-HSA complex were recorded in the wavelength range, 360–480 nm upon excitation at 335 nm, whereas an excitation wavelength of 295 nm was used to record the fluorescence spectra of IDM-HSA and IBN-HSA complexes in the range of 310–400 nm.

3.2.9 Molecular modeling method

The structure of PM was constructed and geometry optimized with MMFF94 force field (Halgren, 1996) using Avogadro Software (Hanwell et al., 2012) and exported as a mol2 file. Docking, visualization and rendering simulation were performed using AutoDock 4.2 (Goodsell et al., 1996) and AutoDockTools 1.5.6 (Sanner, 1999) at the Academic Grid Malaysia Infrastructure. The crystal structure of HSA (PDB code 1BM0, 2.5 Å resolution) was downloaded from the Protein Data Bank (Berman et al., 2000). Water molecules were removed and the atomic coordinates of chain A of 1BM0 were stored in a separate file and used as input for AutoDockTools, where polar hydrogens, Kollman charges and solvation parameters were added. In the case of the ligand PM, nonpolar hydrogens were merged and rotatable bonds were defined. The two binding sites (subdomains IIA and IIIA) were defined with the help of two grids of 70 × 70 × 70 points each with a grid space of 0.375 Å, centered at coordinates x = 35.26, y = 32.41 and z = 36.46 for subsite IIA (site I) and x = 14.42, y = 23.55 and z = 23.31 for subsite IIIA (site II), respectively. The Lamarckian genetic algorithm with local search was used as the search engine, with a total of 100 runs for each binding site. In each run, a population of 150 individuals with 27 000 generations and 250 000 energy evaluations were employed. Operator weights for crossover, mutation and elitism were set at 0.8, 0.02 and 1, respectively. For the local search, default parameters were used. Cluster analysis was performed on docked results using a root-mean-square deviation (rmsd) tolerance of 2.0 Å. The protein–ligand complex was visualized and analyzed using AutoDockTools.

3.2.10 Interaction study of PM with different mammalian serum albumins

3.2.10.1 Fluorescence quenching titration and binding parameters

Binding of PM to different serum albumins was studied by titrating a fixed amount of serum albumin (3 μM) with increasing concentrations (0.9–4.5 μM with 0.9 μM intervals)

of PM. The total volume of the mixture in each tube was made to 3.0 ml with 60 mM sodium phosphate buffer, pH 7.4. The fluorescence spectra were recorded after 1 h incubation at room temperature, in the same way as described in the section 3.2.4. Data analysis was made for the determination of binding parameters, K_{sv} and K_a after inner filter effect correction following the procedures described in the section 3.2.6.2. The ΔG values of the binding reaction were obtained from the K_a values, using the following equation:

$$\Delta G = -RT \ln K_a \quad (6)$$

3.2.10.2 Warfarin displacement study

Equimolar concentrations (3 μM each) of WFN, Sudlow's site I marker and albumin were incubated for 1 h at room temperature (25 °C). Increasing concentrations (0−4.5 μM with 0.9 μM intervals) of PM were then added to WFN-albumin mixture and the fluorescence spectra were recorded in the wavelength range, 360−480 nm after 1 h incubation at room temperature, using an excitation wavelength of 335 nm.

3.2.11 Statistical analysis

Each of the individual experiments were conducted independently for three times and the data are presented as the mean standard deviation. Curve fitting and processing of statistical data were performed using OriginPro 8.5 software (originLab Corp., Northampton, MA, USA).

Flow Chart of the Research Work

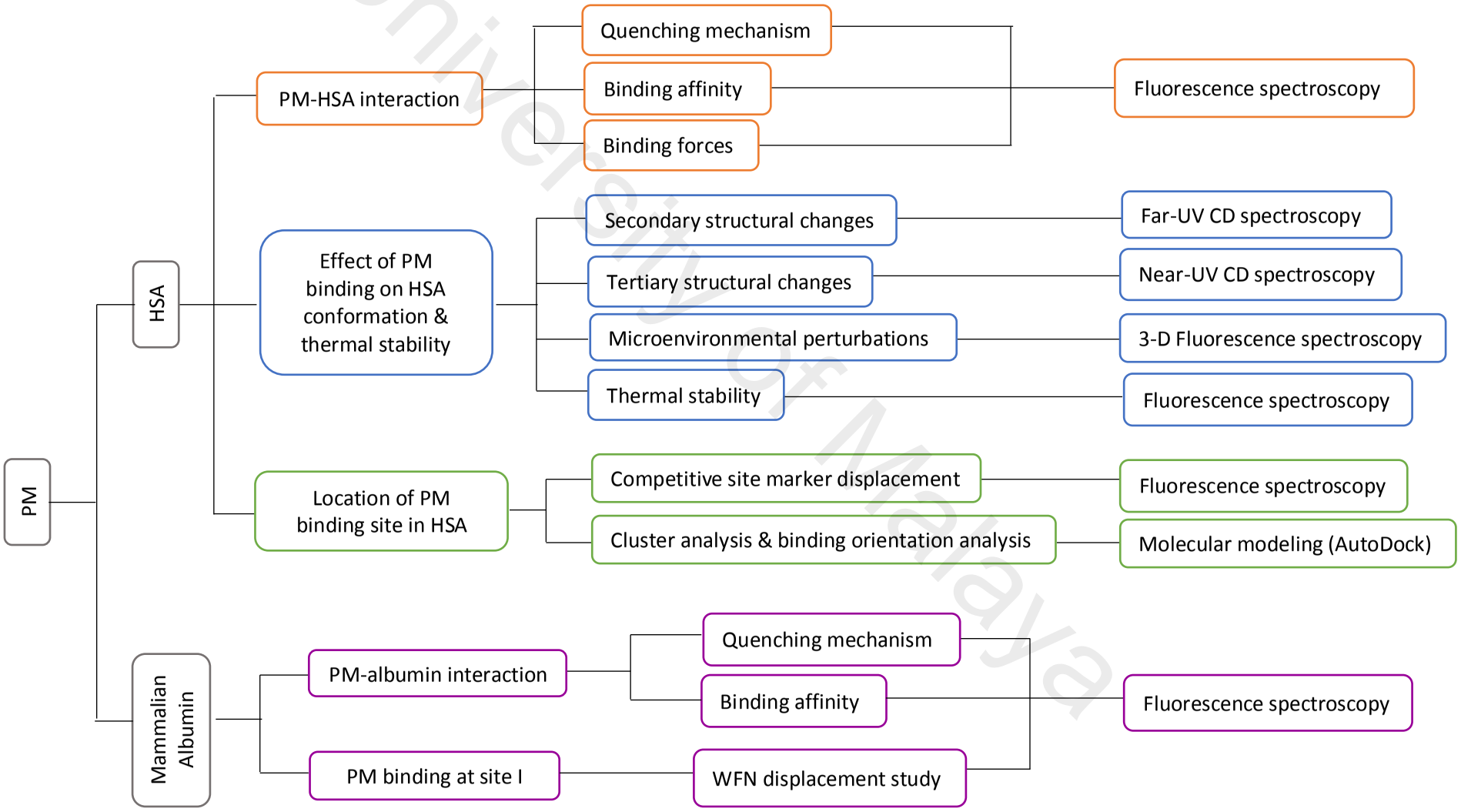

CHAPTER 4

Results and Discussion

CHAPTER 4

RESULTS AND DISCUSSION

4.1 PM-HSA interaction

Fluorescence spectroscopy is a useful tool for investigating ligand-protein interaction in terms of binding affinity, binding forces and mode of binding. The fluorescence spectrum of HSA mainly originates from tryptophan (Trp) residue, when an excitation wavelength of 295 nm is used (Lakowicz, 2006).

4.1.1 PM-induced quenching of HSA fluorescence

The protein (HSA) produced a fluorescence spectrum in the wavelength range, 310–400 nm with an emission maxima at 343 nm, when excited at 295 nm (Figure 4.1). It is important to note that free PM did not produce any fluorescence within this wavelength range (spectrum 'a' in Figure 4.1). Addition of increasing concentrations of PM to HSA led to a progressive decrease in the fluorescence intensity along with a blue shift of 3 nm in the emission maxima at the highest PM concentration (Figure 4.1). About 50 % decrease in the fluorescence intensity was observed at 7.2 μM PM concentration (inset of Figure 4.1). Such attenuation of the fluorescence signal (fluorescence quenching) can be ascribed to a number of molecular interactions, which include excited-state reactions, molecular rearrangements, energy transfer, ground-state complex formation and collision quenching (Lakowicz, 2006). The slight blue shift in the emission maxima implied that the polarity around the Trp residue was reduced (Steinhardt et al., 1971). This seems reasonable as the binding of PM with several hydrophobic groups to the Sudlow's site I of HSA, where the single Trp-214 is located, might have increased the hydrophobicity of the microenvironment around Trp residue. As shown in the sections 4.1.7 and 4.1.8, Sudlow's site I has been suggested to be the preferred binding site of PM. Similar blue

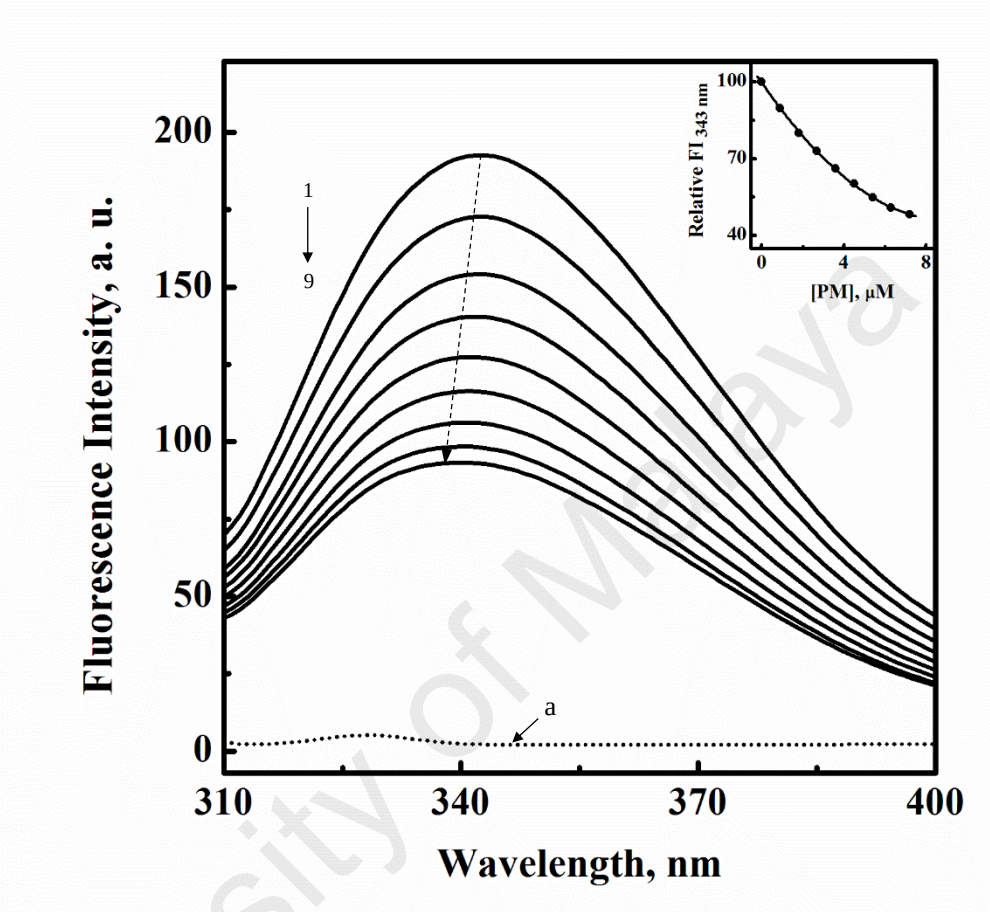

Figure 4.1: Fluorescence quenching spectra of HSA (3 μM) induced by increasing PM concentrations in 60 mM sodium phosphate buffer, pH 7.4 at 25 ℃. PM concentrations (spectra 1–9) were 0–7.2 μM with 0.9 μM intervals, while the excitation wavelength was 295 nm. Spectrum 'a' depicts the fluorescence spectrum of 7.2 μM PM. Arrow represents the blue shift in the emission maximum of HSA with increasing PM concentrations. The inset shows quenching of the fluorescence intensity of HSA at 343 nm ($FI_{343\ nm}$) with increasing PM concentrations.

shift in the emission maxima along with fluorescence quenching have also been observed upon interaction of other ligands with HSA (Sinisi et al., 2015; Sulkowska et al., 2008; Tunçet al., 2014).

4.1.2 Quenching mechanism

Quenching mechanism can be classified as either dynamic or static quenching. Molecular collisions between the fluorophore and the quencher are responsible for dynamic quenching, whereas static quenching is resulted from the complex formation between the fluorophore and the quencher (Lakowicz, 2006). These quenching mechanisms can be discriminated from each other based on their dependence on temperature. An increase in the bimolecular quenching rate constant is anticipated with increasing temperature due to increase in the rate of diffusion at higher temperature. On the other hand, value of the static quenching constant remains inversely proportional to temperature due to destabilization of the complex at higher temperature (Lakowicz, 2006). In order to ascertain the quenching mechanism involved in PM-HSA system, fluorescence quenching titration experiments were carried out at four different temperatures, *i.e.* 15, 25, 35 and 45 ℃. Analysis of the fluorescence quenching data according to Eq. 2 yielded the linear Stern-Volmer plots with correlation coefficient, $r \geq 0.996$ (Figure 4.2). The values of the Stern-Volmer constant, K_{sv}, as obtained from the slope of these plots are listed in Table 4.1. K_{sv} values correlated very well with temperature, T ($r = 0.9998$), showing a linear decrease in K_{sv} with increasing temperature (Figure 4.3) and obeyed the following straight line equation:

$$K_{sv} = -2793.7\ T + 220818 \qquad (6)$$

In view of the decrease in the K_{sv} value with temperature, PM-induced quenching of HSA fluorescence can be characterized as static quenching, which affirmed the formation of the complex between PM and HSA. Furthermore, the value of the quenching constant, k_q

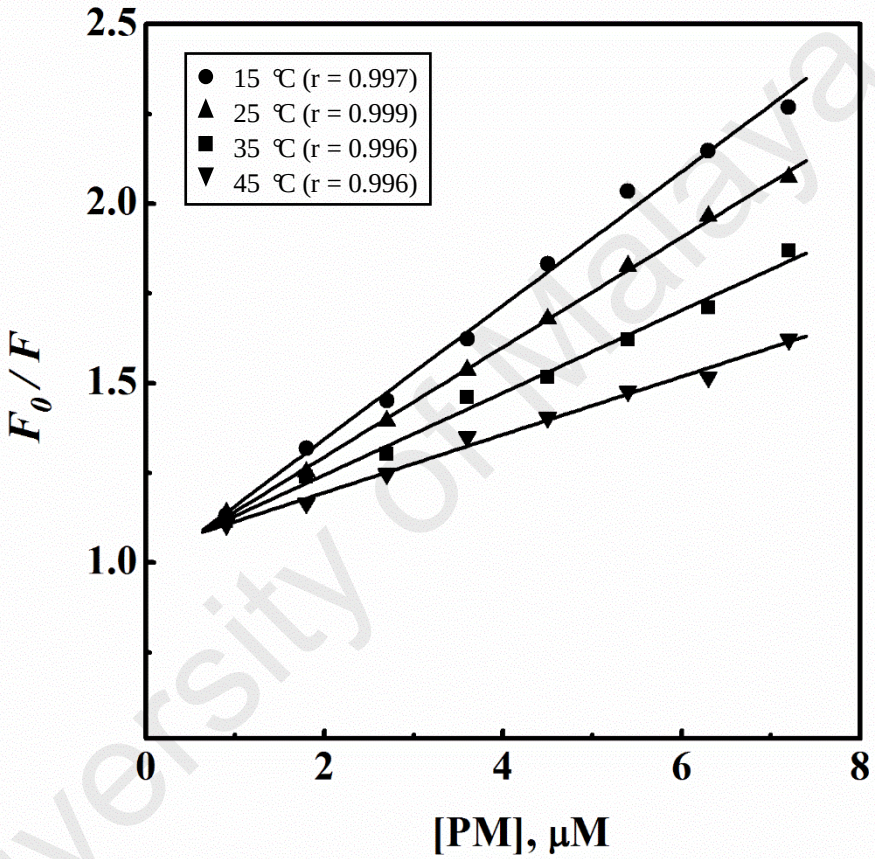

Figure 4.2: Stern-Volmer plots for the fluorescence quenching data of PM-HSA system at four different temperatures.

Table 4.1: Binding parameters for PM-HSA interaction at different temperatures.

T (℃)	K_{sv} (M^{-1})	k_q (M^{-1} s^{-1})	K_a (M^{-1})
15	$(1.80 \pm 0.04) \times 10^5$	$(3.68 \pm 0.04) \times 10^{13}$	$(2.35 \pm 0.06) \times 10^5$
25	$(1.50 \pm 0.01) \times 10^5$	$(3.28 \pm 0.01) \times 10^{13}$	$(2.09 \pm 0.06) \times 10^5$
35	$(1.23 \pm 0.08) \times 10^5$	$(2.18 \pm 0.08) \times 10^{13}$	$(1.39 \pm 0.05) \times 10^5$
45	$(0.95 \pm 0.10) \times 10^5$	$(1.57 \pm 0.10) \times 10^{13}$	$(1.00 \pm 0.08) \times 10^5$

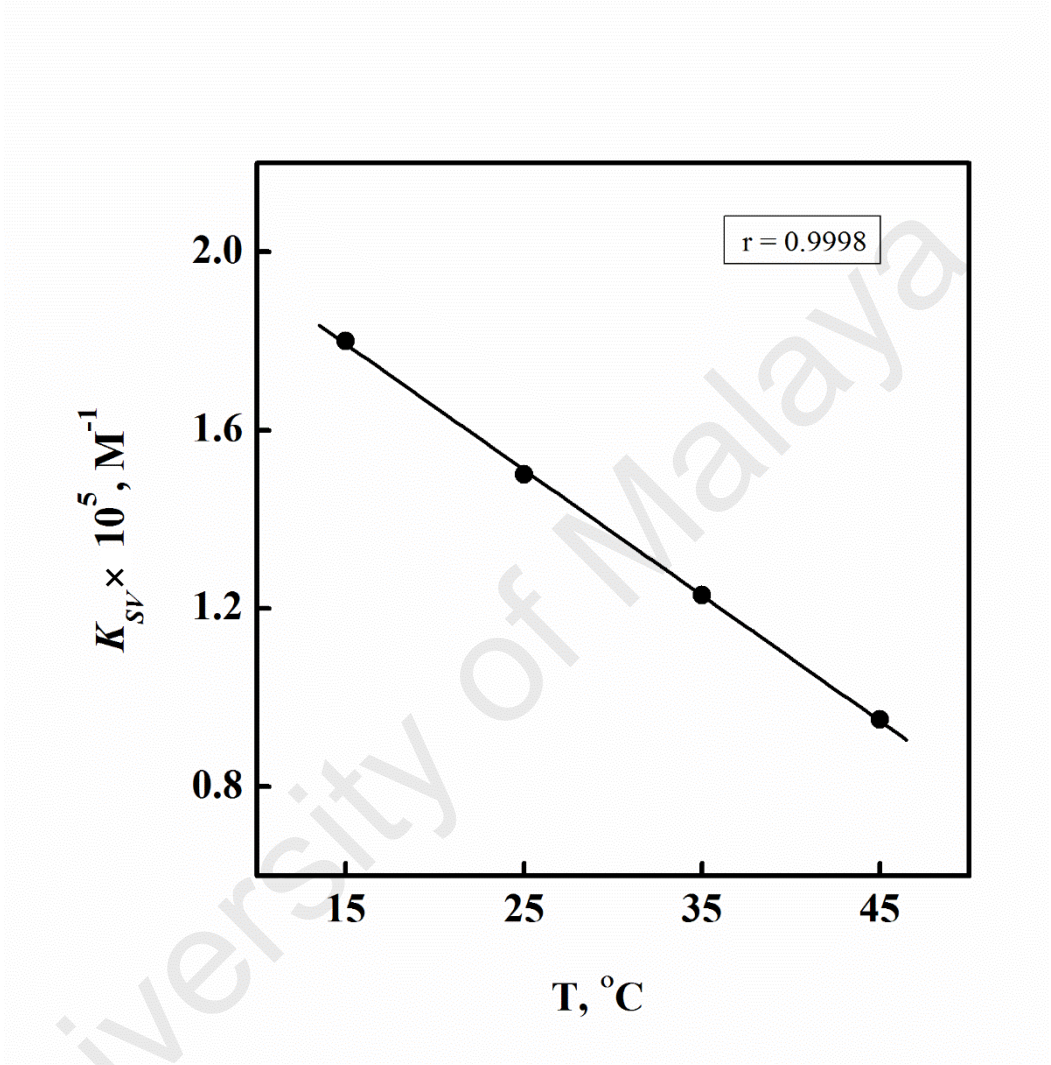

Figure 4.3: Plot showing the relationship between the Stern-Volmer constant (K_{SV}) and temperature (T).

calculated at different temperatures using Eq. 2 was found to fall in the order of magnitude of 10^{13} M^{-1} s^{-1} (Table 4.1). These values of k_q were much higher than the typical diffusion-controlled rate constant of the biomolecule (2×10^{10} M^{-1} s^{-1}), which further explained that the quenching was initiated by the formation of the complex between PM and HSA rather than through dynamic collisions (Lakowicz, 2006; Lakowicz and Weber, 1973).

4.1.3 Association constant, thermodynamic parameters and binding forces

The association constant (K_a) of PM-HSA interaction was determined at different temperatures using the double logarithmic plots, as shown in Figure 4.4. The K_a values had fallen in the order of magnitude of 10^5 M^{-1} (Table 4.1), which was suggestive of moderately strong binding affinity between PM and HSA (Qin et al., 2010; Zheng et al., 2016). Such binding affinity is physiologically significant in two ways. First, it allows the level of free PM in blood circulation under control, which may be toxic to other tissues. Secondly, such intermediate affinity would enable easy dissociation of PM at the target site for detoxification and clearance (Peters, 1995). The results show that the K_a value decreased with increasing temperature and was coincided with the static quenching mechanism (Lakowicz, 2006). The decrease in the K_a value with increasing temperature clearly suggested weakening of the PM-HSA complex at higher temperature (Feroz et al., 2012; Petitpas et al., 2001).

Treatment of the binding data according to van't Hoff plot (Figure 4.5), using Eq. 4 yielded the values of ΔH and ΔS of the binding reaction as -22.41 kJ mol^{-1} and 25.67 J mol^{-1} K^{-1}, respectively (Table 4.2). These values were used in Eq. 5 to compute the value of ΔG (Table 4.2). Negative sign of the ΔG values revealed the spontaneous nature of the binding process. Thermodynamic parameters, *i.e.* ΔH and ΔS are useful in investigating the nature of forces involved in ligand-protein interaction (Raffa, 2003). Generally, four types of non-covalent forces *viz.* hydrogen bonds, electrostatic, van der

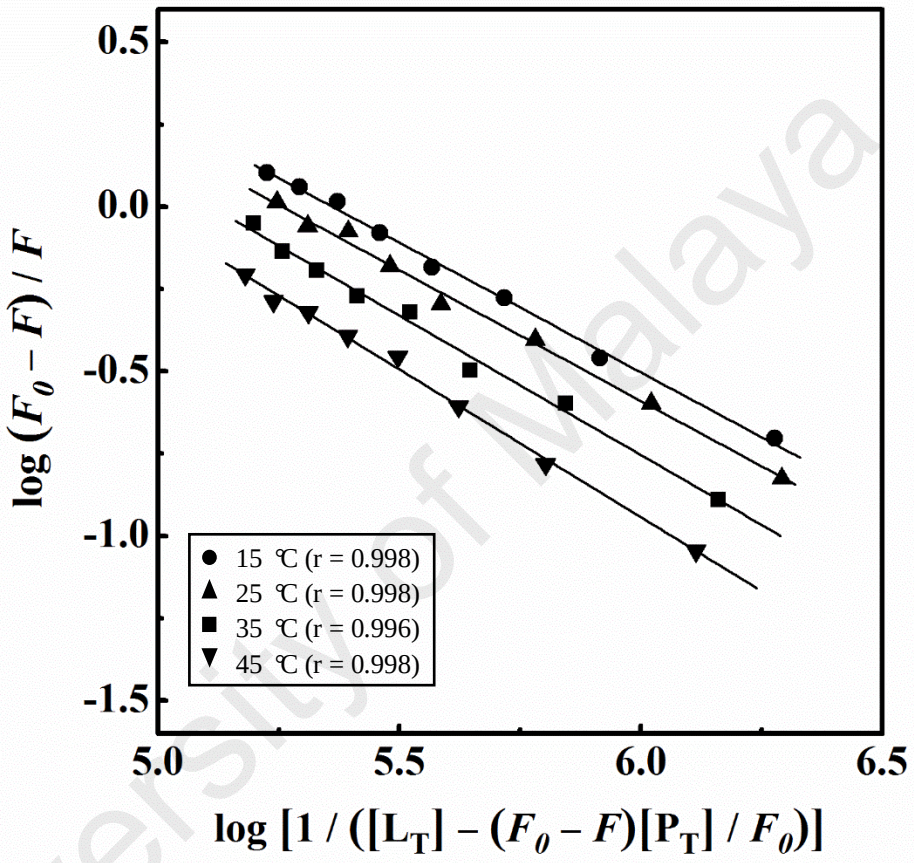

Figure 4.4: Plots of log $(F_0 - F) / F$ versus log $[1 / ([L_T] - (F_0 - F)[P_T] / F_0)]$ for the fluorescence quenching data of PM-HSA system at four different temperatures.

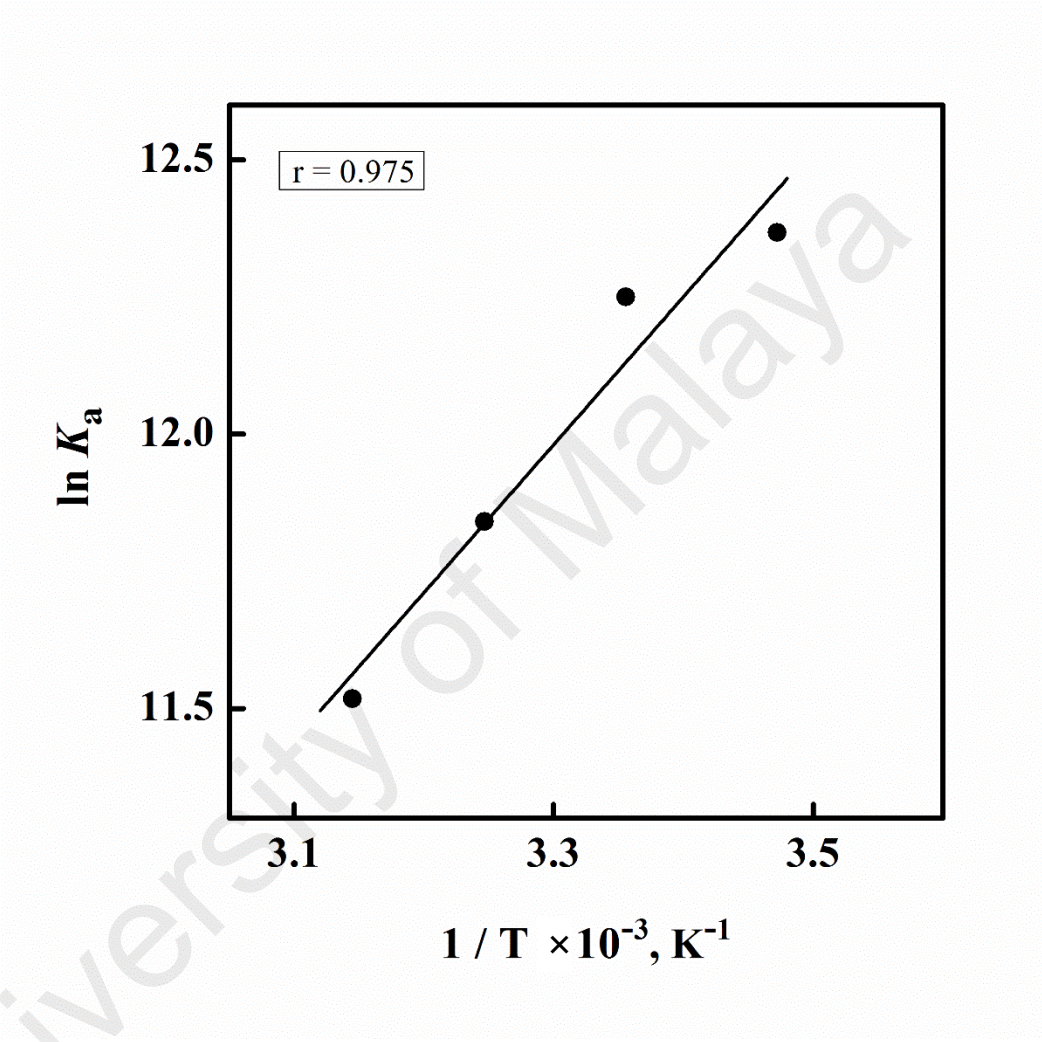

Figure 4.5: van't Hoff plot for PM-HSA interaction. Values of the association constant, K_a were obtained from the double logarithmic plot, shown in Figure 4.4.

Table 4.2: Thermodynamic parameters for PM-HSA interaction.

T (℃)	ΔS (J mol^{-1} K^{-1})	ΔH (kJ mol^{-1})	ΔG (kJ mol^{-1})
15	25.67	–22.41	– 29.80
25			– 30.06
35			– 30.31
45			– 30.57

Waals and hydrophobic interactions are believed to stabilize ligand-protein complexes (Olsson et al., 2008). According to Ross and Subramanian (1981), a positive sign for ΔS suggests the involvement of both hydrophobic and electrostatic interactions in the binding reaction. Since PM contains a benzene ring along with several other hydrophobic groups, which are liable to interact with the protein's hydrophobic residues, involvement of hydrophobic interactions between PM and HSA seems plausible. Dissolution of highly ordered domains of water around protein and ligand molecules might have increased the entropy upon ligand-protein complex formation. On the other hand, a significantly large negative value of ΔH ruled out the participation of electrostatic forces in PM-HSA complexation, as electrostatic forces are usually accompanied by a very small ΔH value (Ross and Subramanian, 1981). Absence of any ionizable group in PM further supports the exclusion of electrostatic forces in PM-HSA complexation. However, a single force cannot be presumed to be the sole force for the stabilization of the ligand-protein complex. Since hydrogen bond formation in low dielectric media has been found to be an exothermic process, which is always associated with a negative ΔH value (Ross and Subramanian, 1981), it is conceivable to think about the involvement of hydrogen bonding as an additional force in PM-HSA complex formation, based on the negative ΔH value of the interaction. This was well supported by our molecular docking results (section 4.1.8), showing hydrogen bonding pattern between PM and HSA.

4.1.4 PM-induced structural changes in HSA

The effect of PM-HSA interaction on the secondary and tertiary structures of HSA was studied using far-UV and near-UV CD spectroscopy.

Appearance of two minima at 208 and 222 nm in the far-UV CD spectrum of HSA (Figure 4.6) characterized the presence of α-helical structure (Taboada et al., 2006). A significant alteration in these signals in the presence of PM at 2:1 PM/HSA molar ratio

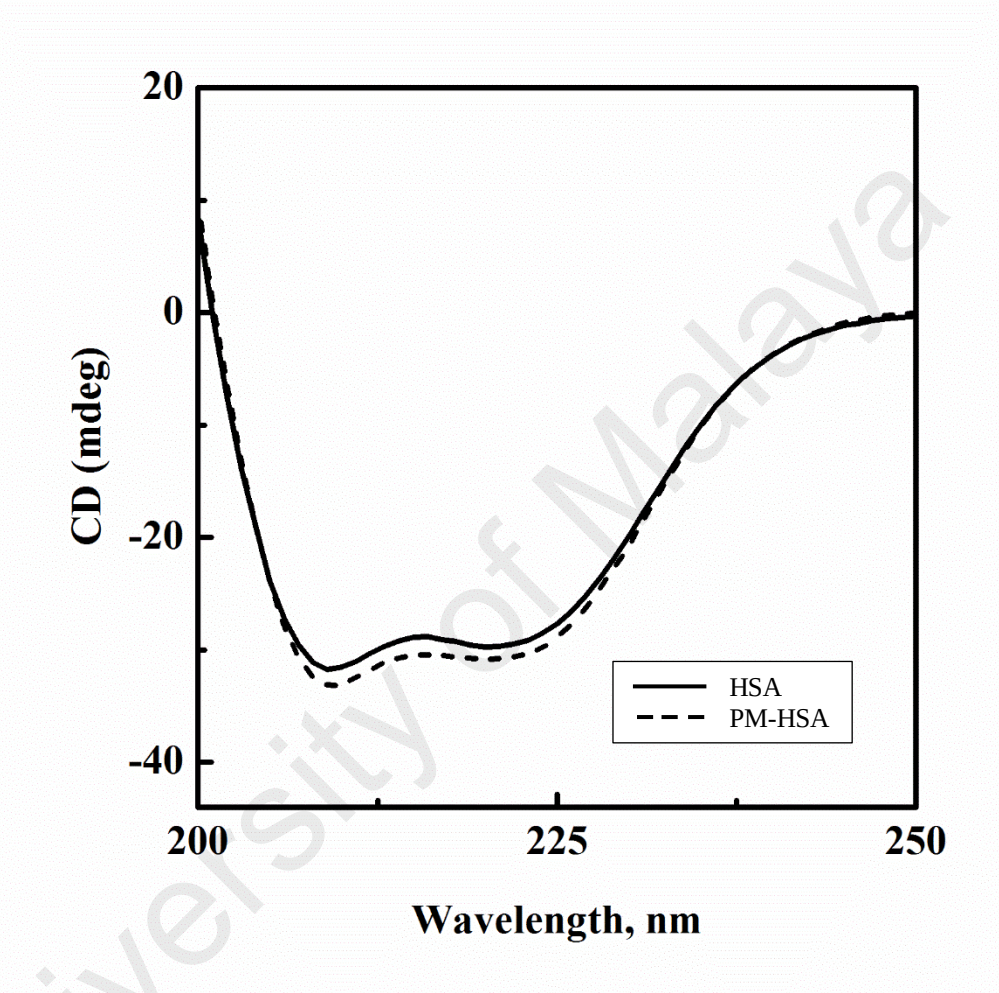

Figure 4.6: Far-UV CD spectra of HSA (3 μM) in the absence and the presence of 6 μM PM. The spectra were obtained in 60 mM sodium phosphate buffer, pH 7.4 at 25 ℃.

clearly suggested secondary structural changes in HSA due to PM binding. Secondary structural changes in HSA upon ligand binding have been reported earlier with other ligands (Chakraborty et al., 2015; Zhang et al., 2012).

Near-UV CD spectrum of HSA was characterized by the presence of minima at 263 and 269 nm and shoulders at 273 and 291 nm (Figure 4.7) due to disulfide and aromatic chromophores of HSA (Rogers and Hirst, 2004). Any change in the near-UV CD spectrum reflects the change in the tertiary structure of the protein. Interestingly, addition of PM to HSA in 1:1 molar ratio significantly affected the near-UV CD spectrum (Figure 4.7), which indicated PM-induced tertiary structural change as a result of PM binding to HSA. Several earlier reports have shown ligand-induced tertiary structural changes (Chakraborty et al., 2015; Ju árez et al., 2009).

4.1.5 PM-induced microenvironmental perturbations around protein fluorophores

Microenvironmental perturbations around aromatic fluorophores (Trp and Tyr) of HSA, induced by PM binding were investigated by comparing the 3-D fluorescence spectra of HSA in the absence and presence of PM. The 3-D fluorescence spectrum and corresponding contour map of HSA (Figure 4.8) showed the presence of peaks '1' and '2' due to Trp and Tyr residues. In addition, two minor peaks, *viz.* peaks 'a' and 'b', characterized as the Rayleigh scattering peak ($\lambda_{em} = \lambda_{ex}$) and the second-order scattering peak ($\lambda_{em} = 2\lambda_{ex}$), respectively, were also visible in the 3-D fluorescence spectrum (Ishtikhar et al., 2014). Qualitatively similar 3-D fluorescence spectra were observed in the presence of PM (Figures 4.9 and 4.10). However, both reduction in the fluorescence intensity and blue shift in the emission maxima were noticed in the presence of PM, being more pronounced at higher PM/HSA (2:1) molar ratio (Figure 4.10). Peak '1' (λ_{ex} = 280 nm) experienced 14 % and 30 % decrease in the fluorescence intensity at PM/HSA molar ratios of 1:1 and 2:1, respectively, whereas reduction in the fluorescence intensity of peak

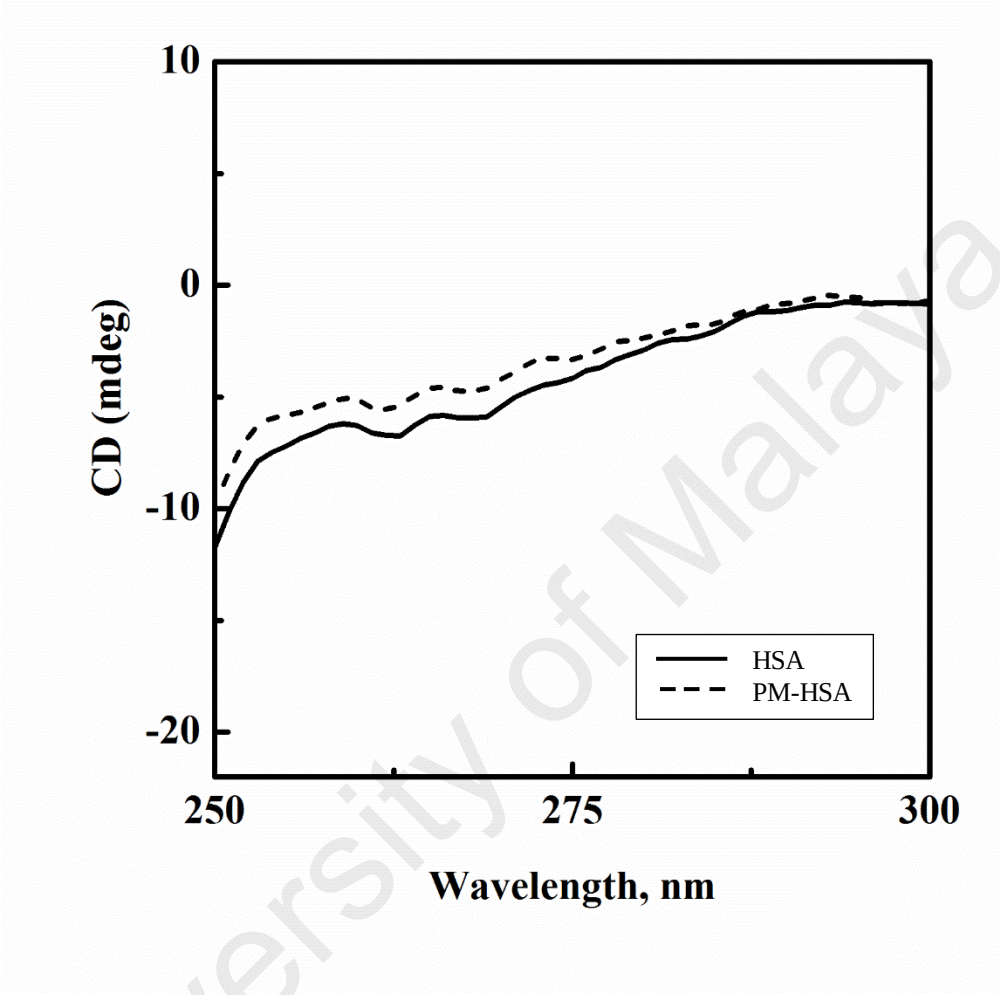

Figure 4.7: Near-UV CD spectra of HSA (10 µM) in the absence and the presence of 10 µM PM. The spectra were obtained in 60 mM sodium phosphate buffer, pH 7.4 at 25 ℃.

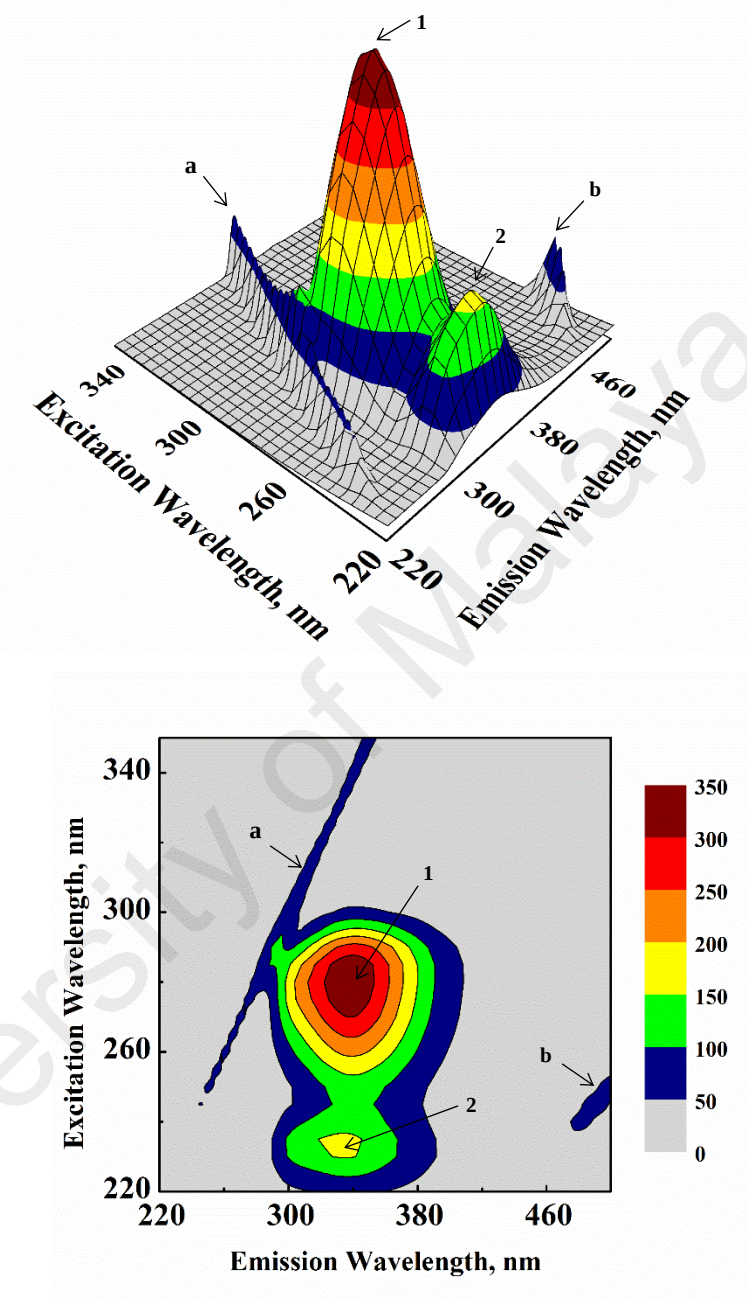

Figure 4.8: Three-dimensional fluorescence spectrum (top) and corresponding contour map (bottom) of 3 μM HSA, as obtained in 60 mM sodium phosphate buffer, pH 7.4 at 25 ℃.

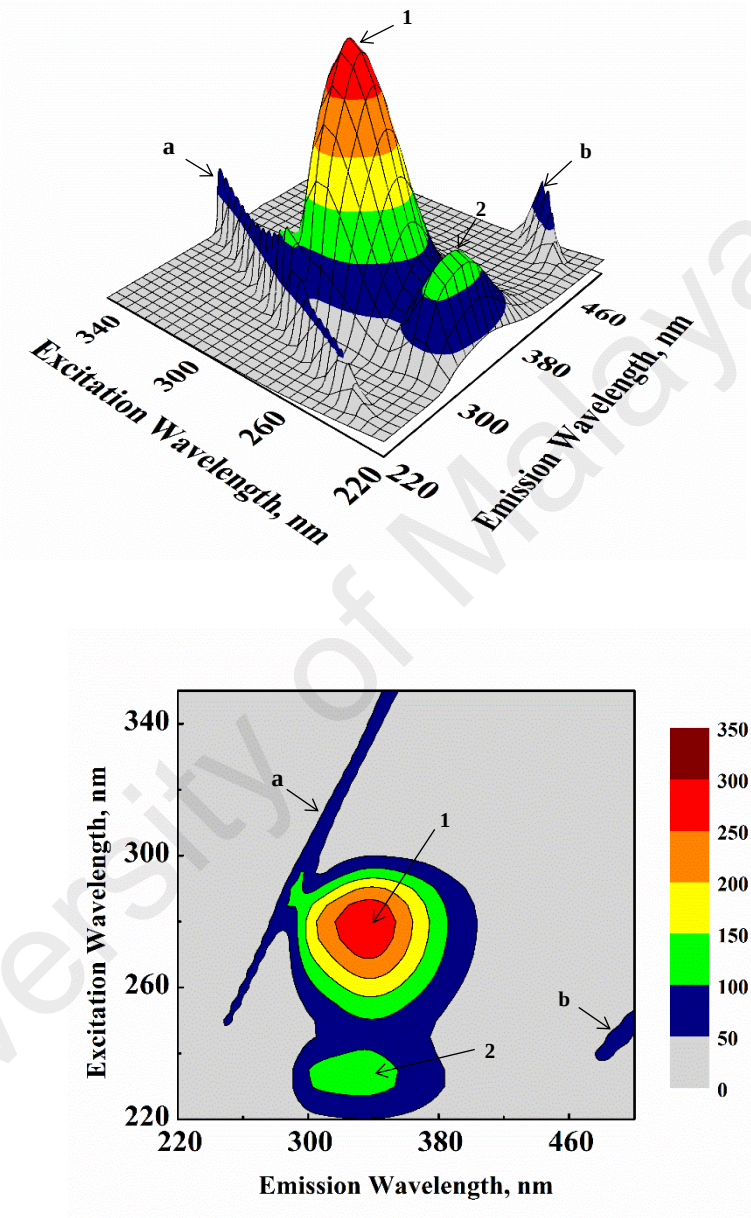

Figure 4.9: Three-dimensional fluorescence spectrum (top) and corresponding contour map (bottom) of 1:1 PM-HSA system. The spectrum was obtained in 60 mM sodium phosphate buffer, pH 7.4 at 25 ℃, using a protein concentration of 3 μM.

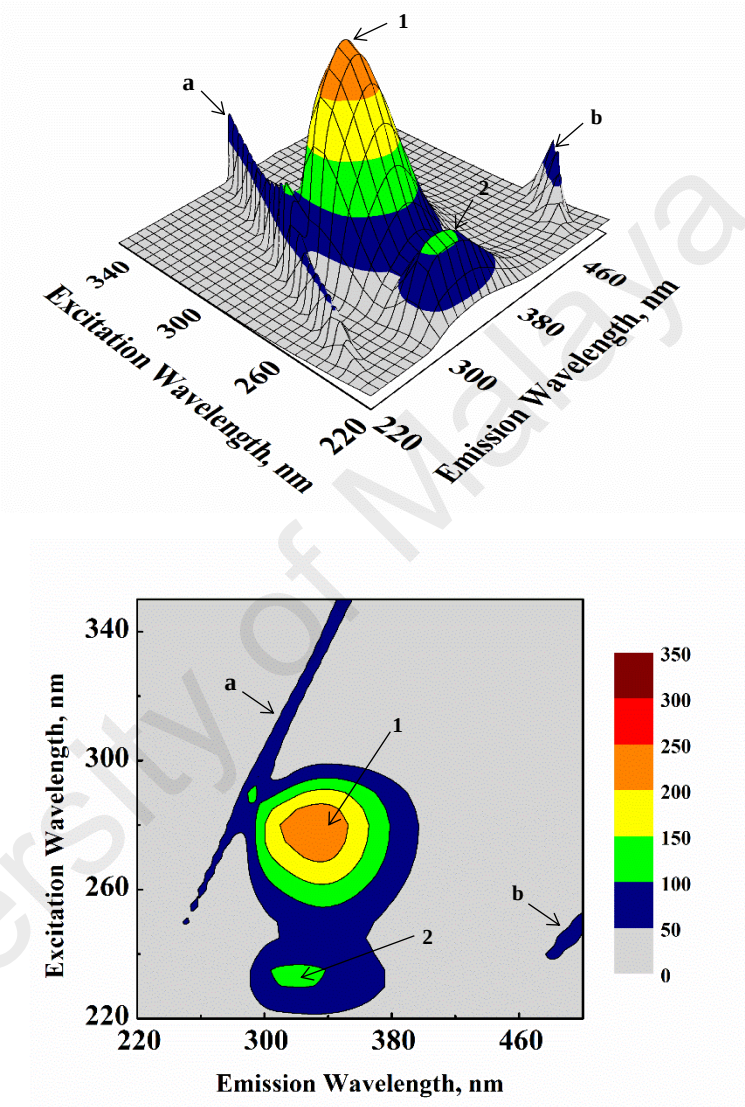

Figure 4.10: Three-dimensional fluorescence spectrum (top) and corresponding contour map (bottom) of 2:1 PM-HSA system. The spectrum was obtained in 60 mM sodium phosphate buffer, pH 7.4 at 25 ℃, using a protein concentration of 3 μM.

'2' (λ_{ex} = 235 nm) was found to be 20 % and 32 %, respectively, at the same molar ratios (Table 4.3). Such decrease in the fluorescence intensity experienced in both peaks '1' and '2' was also associated with 2 and 5 nm blue shift in peak '1' and 5 and 15 nm blue shift in peak '2' at PM/HSA molar ratios of 1:1 and 2:1, respectively. Blue shift in the emission maxima clearly suggested the changes in the microenvironment from polar to non-polar in the presence of PM. These changes in the fluorescence characteristics suggested that binding of PM to HSA produced significant microenvironmental perturbations around Trp and Tyr residues of HSA.

4.1.6 PM-induced thermal stabilization of HSA

In order to study the effect of PM binding on the thermal stability of HSA, fluorescence intensity of HSA at 343 nm was monitored at different temperatures (25–100 ℃) in the absence and the presence of PM (PM/HSA molar ratio of 2:1). A progressive decrease in the fluorescence intensity was observed up to 70 ℃, followed by a slow decrease beyond it (Figure 4.11). This result was similar to the thermal stability profile of HSA reported earlier (Flora et al., 1998; Picó, 1997). Presence of PM in the incubation mixture showed significant protection of HSA from thermal-induced destabilization throughout the temperature range studied (Figure 4.11). Quantitatively, around 55 % decrease in the fluorescence intensity at 343 nm was observed at 100 ℃ in the presence of PM against 75 % quenching noted in its absence. These results clearly suggested increased thermal stability of HSA in the presence of PM due to stabilization of the complex by non-covalent forces, which required higher temperature to be broken down (Yeggoni et al., 2015). This provided another evidence in support of the formation of PM-HSA complex.

4.1.7 Identification of the PM binding site on HSA

The two principal ligand binding sites of HSA, namely Sudlow's sites I and II are located in the hydrophobic cavities in subdomains IIA and IIIA, respectively (Carter et

Table 4.3: Three-dimensional fluorescence spectral characteristics of HSA and PM-HSA system.

System	Peak no.	Peak position [$\lambda_{ex}/\lambda_{em}$, nm/nm]	Intensity
HSA	a	220/220 → 350/350	18.8 → 73.2
	b	250/500	85.6
	1	280/338	343.9
	2	235/333	160.4
[PM]:[HSA]= 1 : 1	a	220/220 → 350/350	19.5 → 80.1
	b	250/500	83.9
	1	280/336	295.7
	2	235/328	128.9
[PM]:[HSA]= 2 : 1	a	220/220 → 350/350	19.4 → 80.2
	b	250/500	79.1
	1	280/333	239.8
	2	235/318	109.0

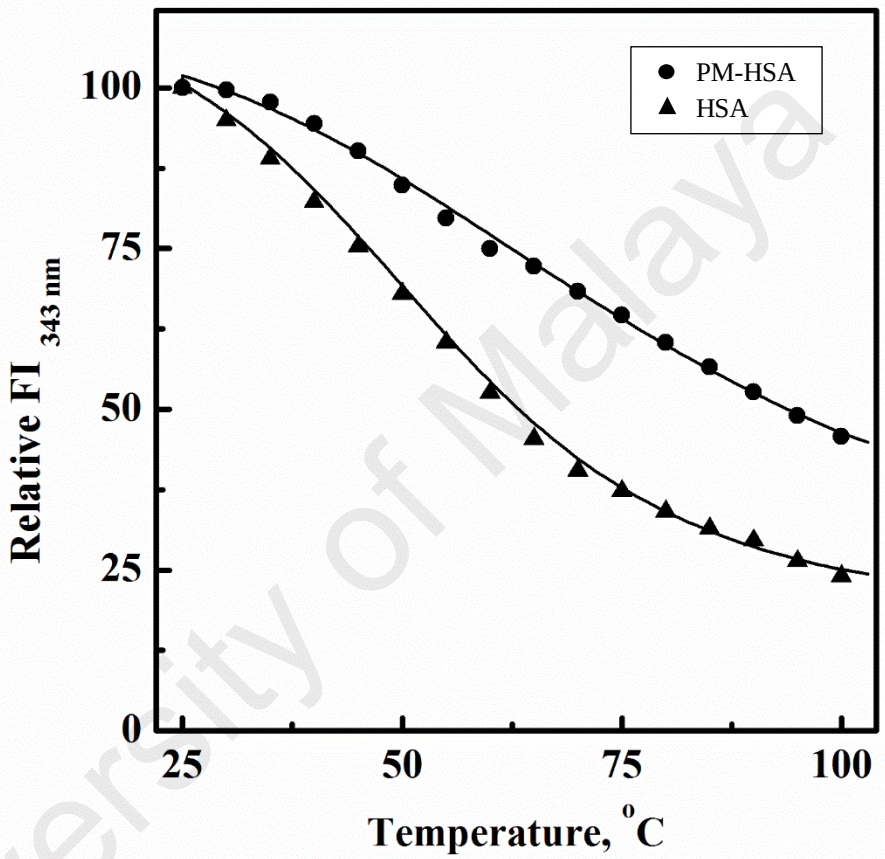

Figure 4.11: Thermal stability profiles of HSA and 2:1 PM-HSA system, as studied by fluorescence measurements at 343 nm in the temperature range, 25–100 ℃. The fluorescence measurements were made in 60 mM sodium phosphate buffer, pH 7.4, using a protein concentration of 3 μM and excitation wavelength of 295 nm.

al., 1989; Sudlow et al., 1975). Heterocyclic compounds such as warfarin, indomethacin and phenybutazone tend to bind at site I, whereas smaller aromatic compounds *viz.* ibuprofen, ketoprofen and diazepam generally have high affinity for site II (Curry, 2002). These compounds are widely used as the site markers due to their high affinities towards these binding sites. In order to identify the binding site of PM on HSA, competitive experiments were carried out using WFN and IDM as the site I markers and IBN as the site II marker.

The displacing action of PM on WFN-HSA (1:1) complex was studied by monitoring the change in the fluorescence spectrum of the WFN-HSA complex, which was characterized by the presence of an emission maxima at 383 nm upon excitation at 335 nm (spectrum '1' in Figure 4.12). This method seems reliable since the free forms of HSA and PM as well as the PM-HSA complex did not produce significant fluorescence spectra within the wavelength range, 360–480 nm (spectra 'b'–'d' in Figure 4.12). Even free WFN (spectrum 'a') produced relatively weaker signal at 383 nm compared to WFN-HSA complex. Addition of increasing PM concentrations to the WFN-HSA complex produced a decreasing trend in the fluorescence spectra (spectra '2'–'8' in Figure 4.12). Nearly 40 % decrease in the fluorescence intensity was observed at the highest PM concentration (6.3 μM) used (inset of Figure 4.12), which clearly reflected the WFN displacing action of PM from its binding site on HSA, *i.e*. site I.

In order to ascertain the location of the PM binding site, fluorescence quenching spectra of PM-HSA complex were recorded both in the absence and the presence of other site markers, IDM (for site I) and IBN (for site II), using an excitation wavelength of 295 nm (Figure 4.13). To compare the effect of IDM and IBN on PM-HSA system, the fluorescence quenching data were analyzed using Eq. 3 and the corresponding K_a values were determined from the double logarithmic plots (Figure 4.14). The K_a value of the PM-HSA system (2.09×10^5 M^{-1}) was significantly reduced to nearly half (1.11×10^5

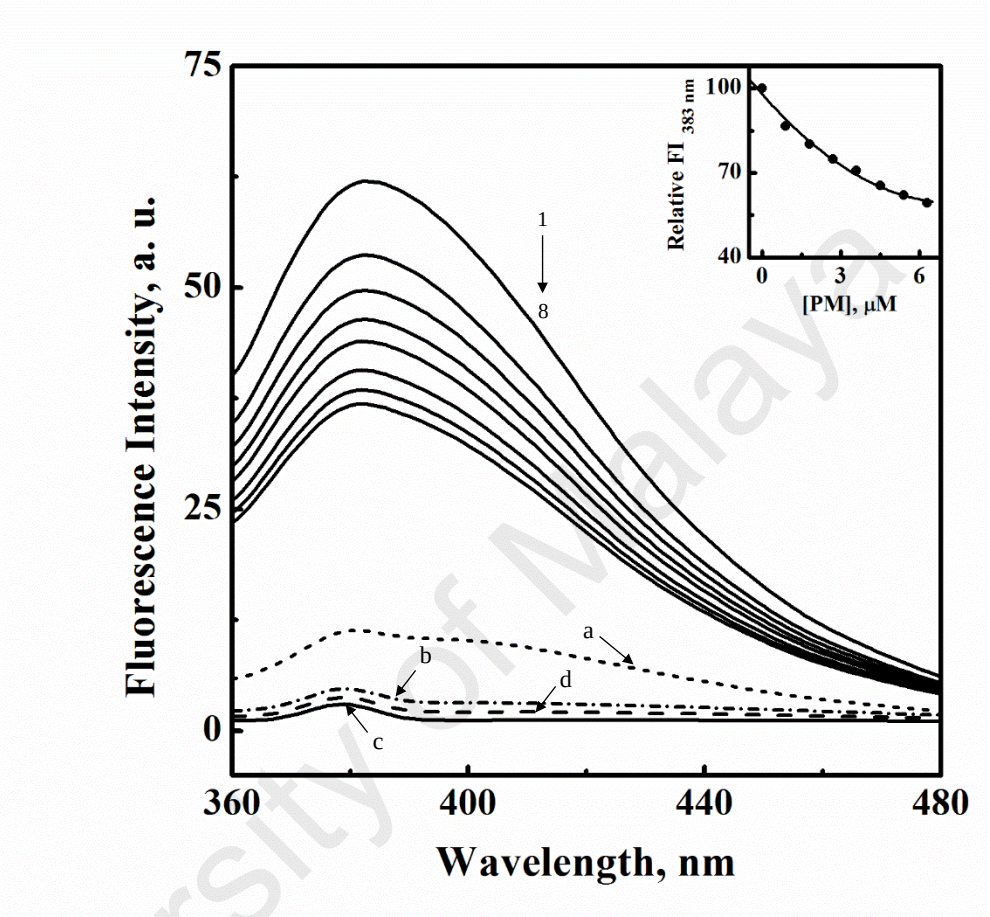

Figure 4.12: Quenching of the fluorescence spectrum of 1:1 WFN–HSA complex (spectrum 1) induced by increasing PM concentrations (λ_{ex} = 335 nm). The PM concentrations used were 0.9–6.3 µM with 0.9 µM intervals (spectra 2–8). The fluorescence spectra, obtained with 3 µM WFN (spectrum 'a'), 3 µM HSA (spectrum 'b'), 6 µM PM (spectrum 'c') and 2:1 PM–HSA complex (spectrum 'd') are also shown. The inset shows quenching of the fluorescence intensity of WFN-HSA complex at 383 nm ($FI_{383\ nm}$) with increasing PM concentrations.

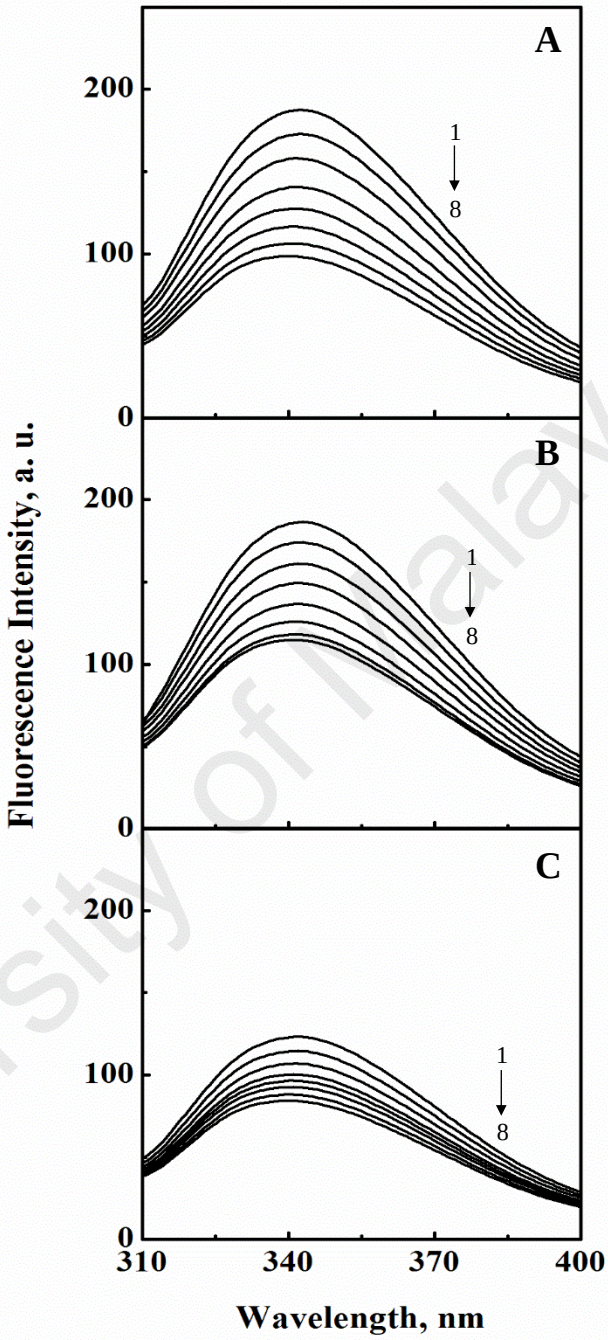

Figure 4.13: Fluorescence quenching spectra of HSA (A), 1:1 IBN-HSA complex (B) and 1:1 IDM-HSA complex (C) in the absence (spectrum 1) and the presence (spectra 2–8) of increasing PM concentrations (0.9–6.3 μM with 0.9 μM intervals), obtained in 60 mM sodium phosphate buffer, pH 7.4 at 25 ℃.

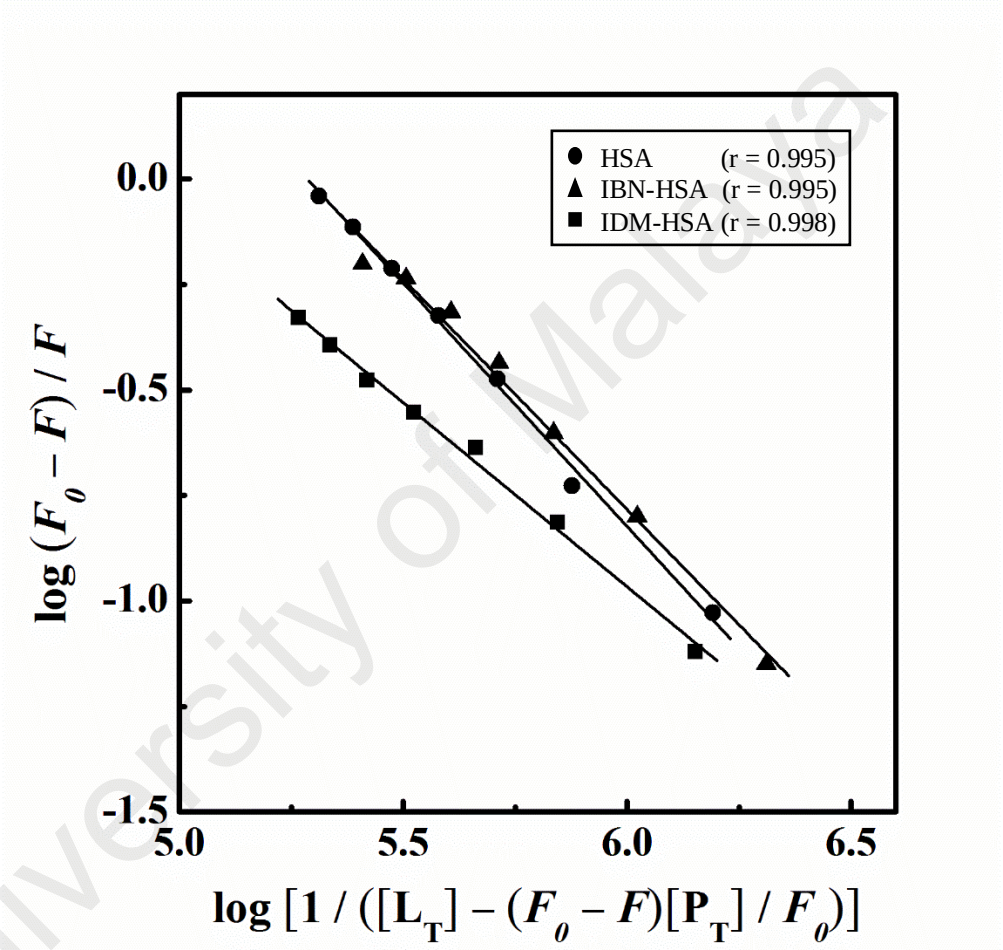

Figure 4.14: Double logarithmic plots for the fluorescence quenching data, obtained with HSA (3 μM), 1:1 IBN-HSA complex and 1:1 IDM-HSA complex with increasing PM concentrations, as shown in Figure 4.13 A, B and C, respectively.

M^{-1}) in the presence of IDM, but showed no significant variation (1.92×10^5 M^{-1}) in the presence of IBN (Table 4.4). From these results, it can be deduced that the binding affinity of PM towards HSA was significantly affected by the presence of IDM, whereas no significant change in the binding affinity was noticed in the presence of IBN. Therefore, site I seems to be the preferred binding site of PM, which was further supported by the molecular modeling results.

4.1.8 Molecular modeling

A molecular modeling study was conducted to predict the binding site of PM on HSA and to confirm the results of the displacement experiments described above. A total of 17 multimember conformational clusters were obtained for site I from 100 docking runs. The highest populated cluster had 42 out of 100 conformations with the lowest mean binding energy as −33.4 kJ mol^{-1} (Figure 4.15A). For the binding site II, 10 multimember conformational clusters, possessing lowest mean binding energy of −23.6 kJ mol^{-1} were identified, with the highest populated cluster having 42 members out of 100 conformations (Figure 4.15B). As the docking energy of the most favorable docking conformation in site II was larger than the one in site I, it revealed that PM showed a binding preference for the drug binding site I (subdomain IIA) of HSA.

The results of these docking studies were in good agreement with the displacement experiments discussed above. The predicted binding model with the lowest docking energy (−33.4 kJ mol^{-1}) was then used for binding orientation analysis (Figure 4.16). The binding site (defined by the amino acid residues within 5 Å distance from the ligand) was found to be deep inside the protein structure and mostly located in a hydrophobic cleft, lined by the following amino acid residues: Tyr-150, Glu-153, Lys-195, Gln-196, Lys-199, Trp-214, Arg-218, Leu-219, Arg-222, Phe-223, Leu-238, Val-241, His-242, Arg-257, Ser-287, Ile-290, Ala-291 and Glu-292. Presence of hydrophobic amino acid

Table 4.4: Association constants for the site marker displacement study of PM-HSA interaction.

Site marker	K_a ($\times 10^5$ M^{-1})	r
-	2.09 ± 0.06	0.995
IBN	1.92 ± 0.07	0.995
IDM	1.11 ± 0.06	0.998

r is the correlation coefficient.

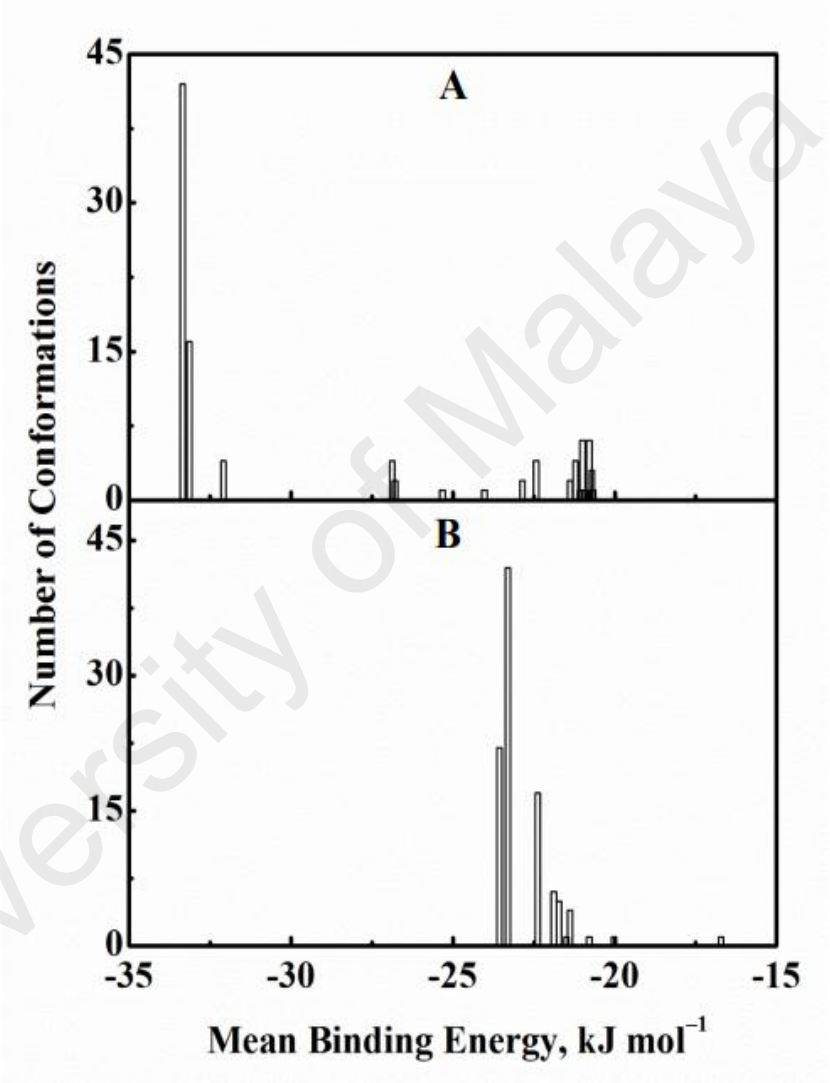

Figure 4.15: Cluster analyses of the AutoDock docking runs of PM in the drug binding site I (A) and site II (B) of HSA (1BM0).

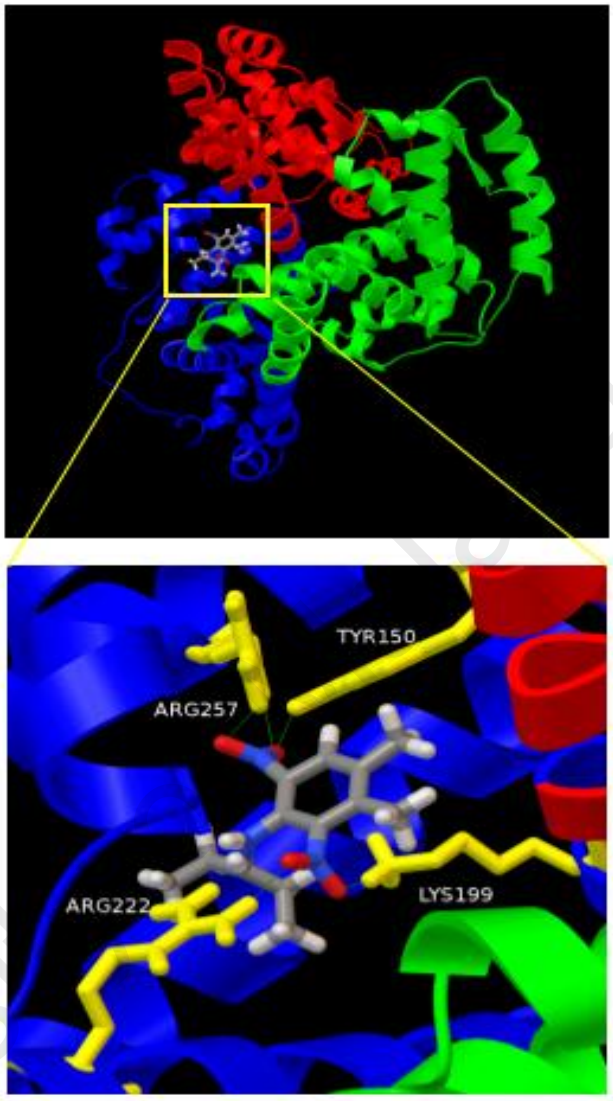

Figure 4.16: Predicted orientation of the lowest docking energy conformation of PM (rendered in ball and stick) in the binding site I (subdomain IIA) of HSA. The different domains, namely, domain I, II and III of HSA are shown in red, blue and green, respectively. The zoomed-in view of the binding site shows the hydrogen bonds (green lines) formed between the amino acid residues of HSA (rendered in yellow ball and stick) and PM in the binding site I.

residues at the binding site of HSA might have contributed towards the stability of the ligand-HSA complex through hydrophobic interactions. However, the presence of several polar amino acid residues within the proximity of the bound ligand indicated that the interaction between the ligand and HSA at this site cannot be presumed to be exclusively hydrophobic in nature. Furthermore, five hydrogen bonds were predicted in the PM-HSA complex docking conformation at site I, against three hydrogen bonds at site II (Table 4.5). These results further supported the involvement of both hydrogen bonds and hydrophobic interactions in PM-HSA complex formation.

4.2 Interaction of PM with different mammalian serum albumins

4.2.1 PM-induced quenching of albumin fluorescence

The fluorescence quenching results of different serum albumins, *i.e.* BSA, SSA, PSA, HSA and RbSA, obtained in the presence of increasing PM concentrations are shown in Figure 4.17A–E. Quantitative differences in the values of the fluorescence intensity, obtained with these albumins can be ascribed to the number of Trp residues in these proteins, that contribute towards the fluorescence intensity upon excitation at 295 nm (Lakowicz, 2006). BSA, SSA and PSA with two Trp residues produced higher fluorescence intensity (Figure 4.17A–C, Table 4.6) compared to HSA and RbSA (Figure 4.17D–E, Table 4.6), which possess single Trp residue (Pajot, 1976). On the other hand, the emission maxima of these albumins were found to fall in the range, 341–345 nm, characteristic of Trp residue(s) (Table 4.6) (Vivian and Callis, 2001).

As evident from Figure 4.17A–E, addition of PM to these albumins produced quenching in the fluorescence intensity in a concentration dependent manner. Such quenching was suggestive of the binding of PM to these albumins, as similar quenching was observed with the binding of many ligands to serum albumins (Han et al., 2009; Feroz et al., 2015; Kamtekar et al., 2013; Samari et al., 2012). Values of the fluorescence

Table 4.5: Predicted hydrogen bonds between interacting atoms of the amino acid residues of HSA (1BM0) and PM at site I and site II.

HSA binding site	Protein atom	Ligand atom	Distance (Å)
Site I	TYR-150: HH	O (nitro, C_6)	1.98
	LYS-199: HZ1	O (nitro, C_2)	2.19
	ARG-222: HH21	O (nitro, C_2)	1.97
	ARG-257: HE	O (nitro, C_6)	2.15
	ARG-257: HH22	O (nitro, C_6)	1.95
Site II	LYS-413: HZ3	O (nitro, C_2)	2.20
	LYS-414: HZ1	O (nitro, C_6)	1.55
	LYS-414: HZ2	O (nitro, C_6)	2.05

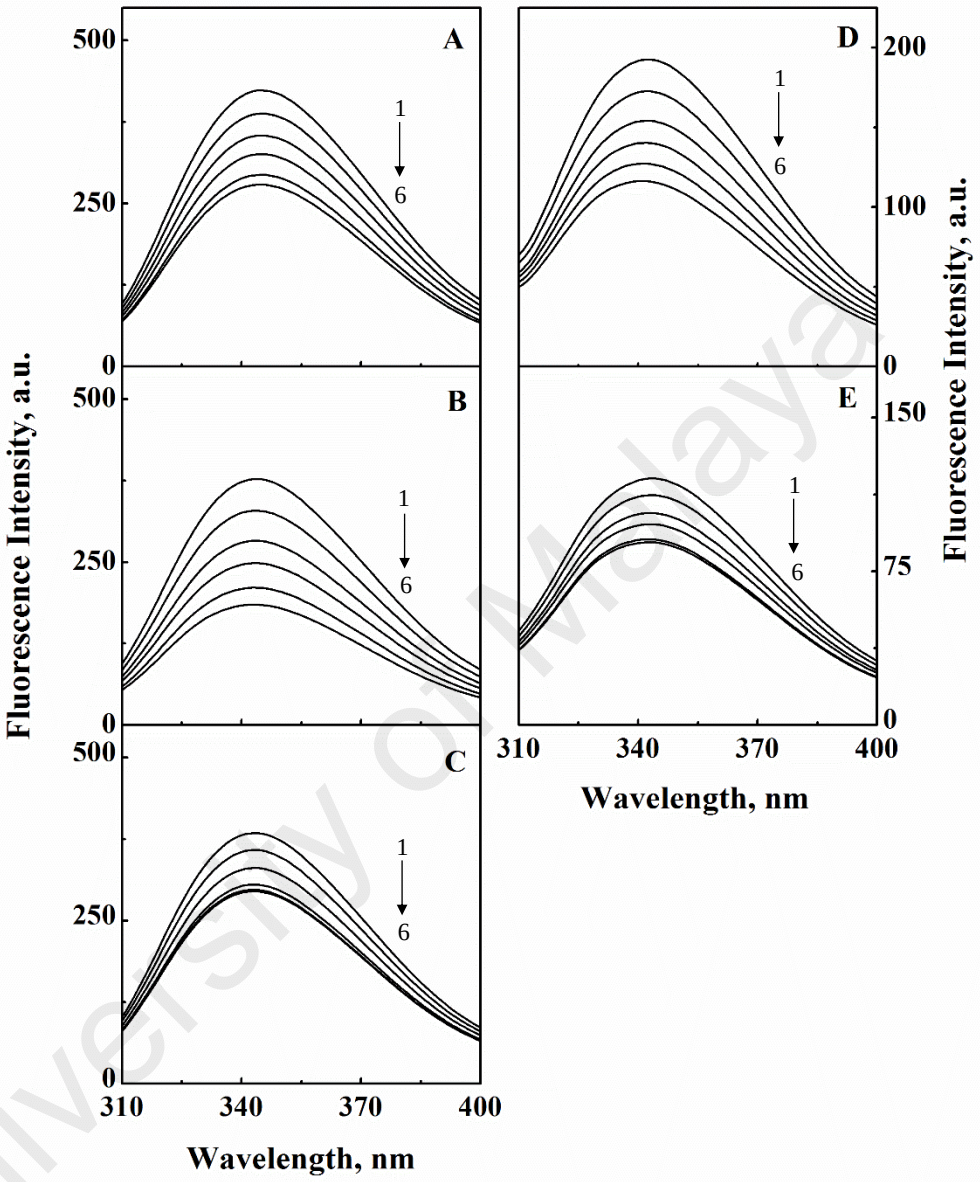

Figure 4.17: Fluorescence quenching spectra of different serum albumins (3 μM) induced by increasing PM concentrations in 60 mM sodium phosphate buffer, pH 7.4 at 25 ℃. PM concentrations (spectra 1–6) were 0–4.5 μM with 0.9 μM intervals, while the excitation wavelength was 295 nm. (A) BSA, (B) SSA, (C) PSA, (D) HSA and (E) RbSA.

intensity at the emission maxima, obtained at different PM concentrations were transformed into the relative fluorescence intensity by taking the fluorescence intensity of these albumins in the absence of PM as 100. Figure 4.18 shows change in the relative fluorescence intensity at the emission maxima with increasing PM concentrations, obtained with different serum albumins. All these albumins showed gradual decrease in the fluorescence intensity with increasing PM concentrations. However, a comparison of the quenching pattern, obtained with these albumins suggests lesser extent of the fluorescence quenching with PSA and RbSA compared to that observed with SSA, HSA and BSA at the highest PM/albumin molar ratio (1.5:1). Quantitatively, about 51 %, 39 % and 36 % quenching was observed with SSA, HSA and BSA, respectively, compared to PSA and RbSA, showing 19 % and 26 % quenching, respectively (Figure 4.18, Table 4.6).

4.2.2 Binding parameters for PM-albumin interaction

In order to find out the source of PM-induced quenching, fluorescence quenching data were treated according to Eq. 2 and the K_{SV} values were obtained from the slope of the linear Stern-Volmer plots (Figure 4.19). In line to the quenching pattern (Table 4.6), BSA, SSA and HSA showed higher K_{SV} values compared to those obtained with PSA and RbSA (Table 4.7). Substitution of K_{SV} values in Eq. 2 yielded the values of bimolecular quenching constant, k_q. These k_q values had fallen in the order of 10^{13} M^{-1} s^{-1} for BSA, SSA and HSA and 10^{12} M^{-1} s^{-1} for PSA and RbSA. Values of k_q higher than 10^{10} M^{-1} s^{-1} (diffusion-controlled limit) simply reflects complex formation (Lakowicz, 2006). Thus, it appears that PM-induced fluorescence quenching might have been resulted from static quenching mechanism, which supports the complex formation.

Binding affinity of PM towards different serum albumins was determined by analyzing the fluorescence quenching data according to Eq. 3. The values of the association constant, K_a for different PM-albumin systems were obtained from the resulting double logarithmic

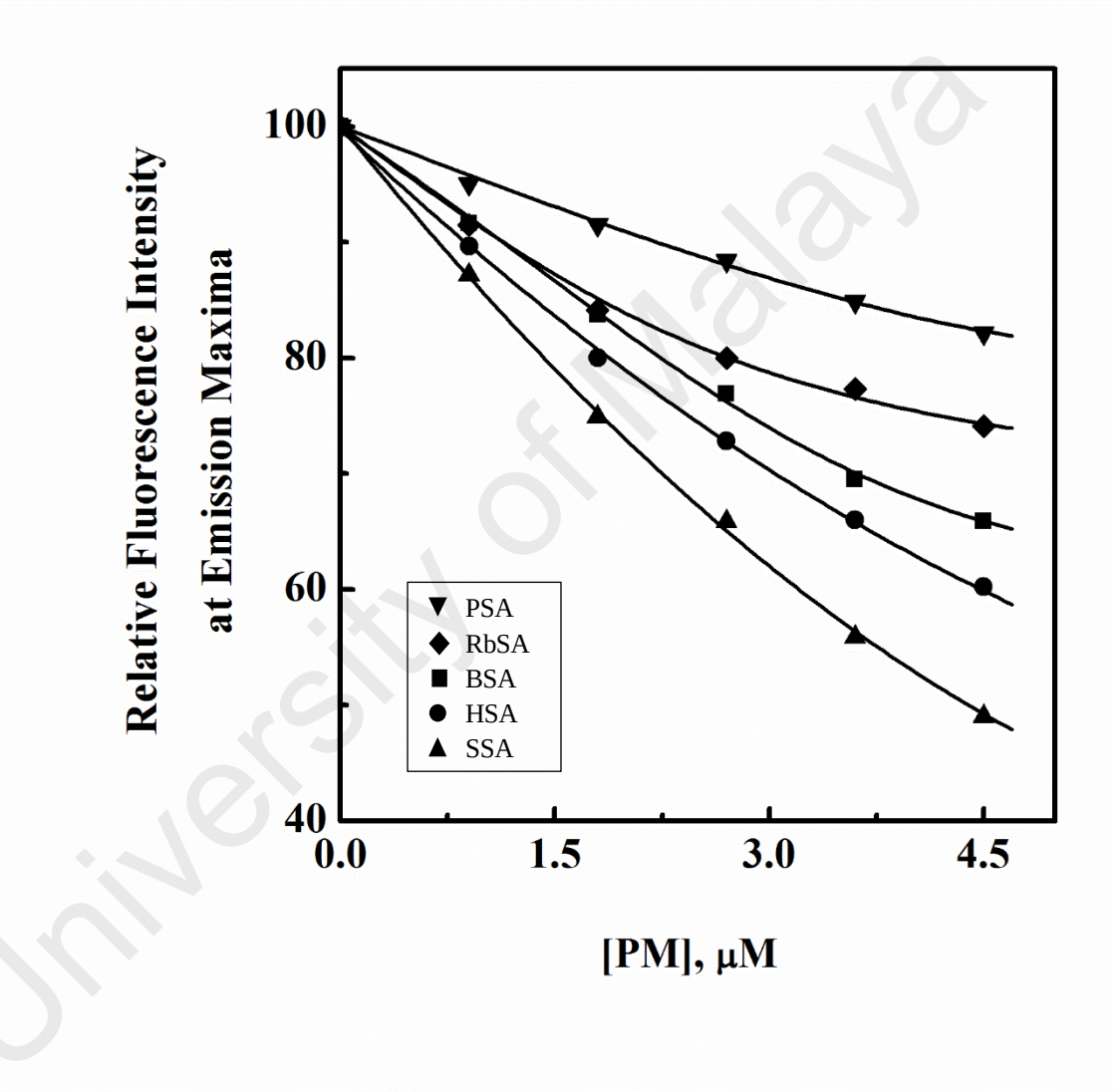

Figure 4.18: Plot showing a comparison of the fluorescence quenching of different serum albumins at their emission maxima with increasing PM concentrations.

Table 4.6: Fluorescence characteristics of different serum albumins in the absence and the presence of PM.

Albumin	Emission maxima (nm)	Intensity (a.u.)	% Quenching ([PM]/[Albumin]=1.5:1)
BSA	345	424	36.3 ± 2.6
SSA	341	378	50.9 ± 2.3
PSA	343	384	19.4 ± 1.6
HSA	343	193	38.7 ± 1.5
RbSA	343	125	26.0 ± 1.6

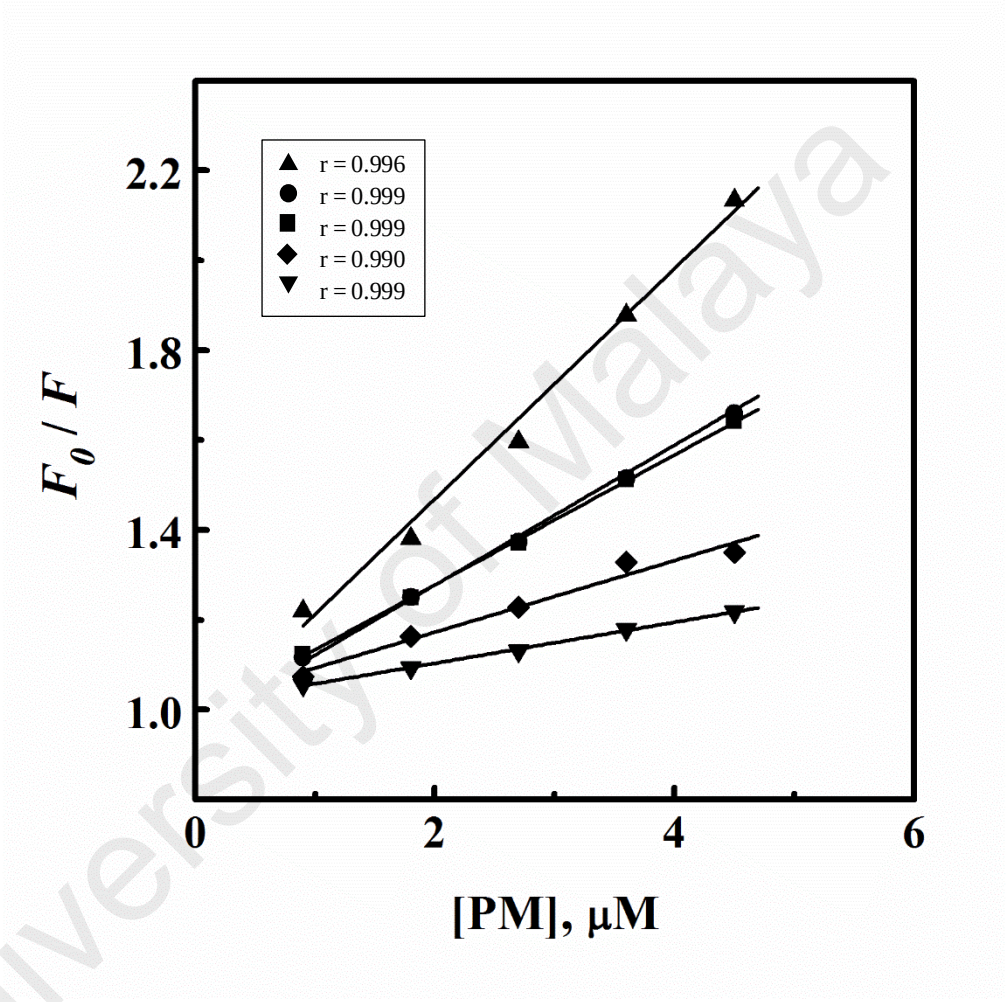

Figure 4.19: Stern-Volmer plots for the fluorescence quenching of different serum albumins by PM. The symbols used for various serum albumins are the same as used in Figure 4.18.

Table 4.7: Binding parameters and free energy change for the interaction between PM and different serum albumins.

Albumin	K_{SV} (M^{-1})	K_a (M^{-1})	ΔG (kJ mol^{-1})
BSA	$(1.29 \pm 0.14) \times 10^5$	$(1.71 \pm 0.15) \times 10^5$	–29.86
SSA	$(2.44 \pm 0.04) \times 10^5$	$(3.27 \pm 0.24) \times 10^5$	–31.46
PSA	$(5.57 \pm 0.30) \times 10^4$	$(8.88 \pm 0.08) \times 10^4$	–28.23
HSA	$(1.51 \pm 0.01) \times 10^5$	$(2.18 \pm 0.12) \times 10^5$	–30.46
RbSA	$(8.10 \pm 0.14) \times 10^4$	$(9.74 \pm 0.31) \times 10^4$	–28.46

plots (Figure 4.20) and are given in Table 4.7. Based on the PM binding affinity, these albumins can be arranged in the order: SSA > HSA > BSA > RbSA > PSA. Although the sequence and protein characteristics of these albumins show high degree of similarity (Michaud et al., 2009), binding affinity of ligands varies considerably among the species according to the degree of phylogenetic relationship (Day and Myszka, 2003). Such species differences in ligand-albumin interaction have been reported earlier (Kosa et al., 1997; Feroz et al., 2015; Tayyab et al., 2003). The Gibbs free energy change (ΔG) of the binding reaction was calculated using Eq. 6 (Table 4.7) and the negative values of ΔG for all PM-albumin systems suggested that the binding reactions were feasible (Ross and Subramanian, 1981).

4.2.3 Warfarin displacement results

As PM was found to bind to site I of HSA, based on site marker displacement and molecular modeling results described above (sections 4.1.7 and 4.1.8), a comparison for the WFN displacing action of PM on the complexes of WFN with other albumins was made. Spectrum 1 in Figure 4.21 shows the fluorescence spectrum of WFN-SSA complex, when excited at 335 nm. The spectrum was characterized by the presence of an emission maxima at 383 nm. Addition of increasing concentrations of PM displaced WFN from its binding site, as reflected from the progressive decrease in the fluorescence intensity (spectra 2-6 in Figure 4.21). In this range of wavelength, the fluorescence signals produced by SSA, PM and PM-HSA mixture (spectra 'b'–'d' in Figure 4.21) were insignificant. Even free WFN (spectrum 'a' in Figure 4.21) produced relatively weaker signal at 383 nm compared to WFN-SSA complex. WFN displacement results, obtained with other serum albumins, *i.e*. BSA (Figure 4.22), PSA (Figure 4.23), RbSA (Figure 4.24) and HSA (Figure 4.12) were qualitatively similar to those obtained with SSA, but showed significant differences in the extent of fluorescence quenching. This can be clearly seen from the decrease in the relative fluorescence intensity of different WFN-

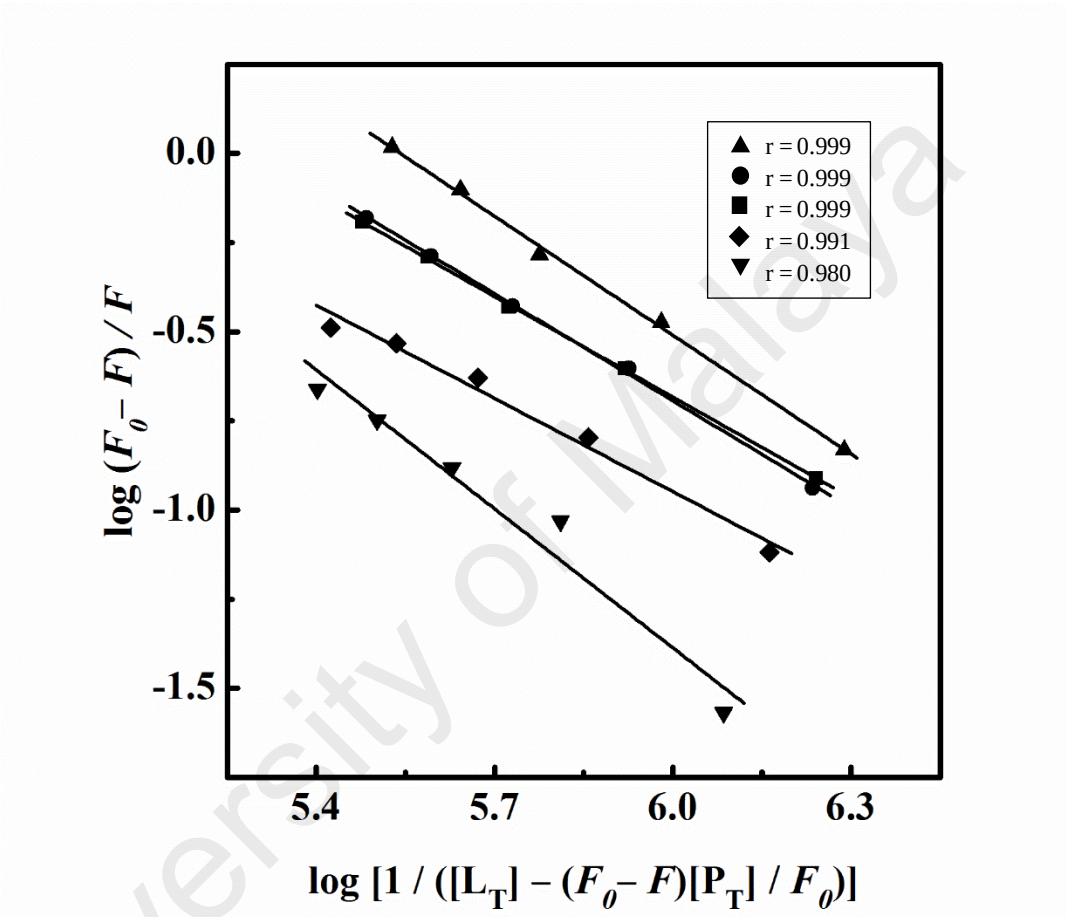

Figure 4.20: Double logarithmic plots for the fluorescence quenching of different serum albumins by PM. The symbols used for various serum albumins are the same as used in Figure 4.18.

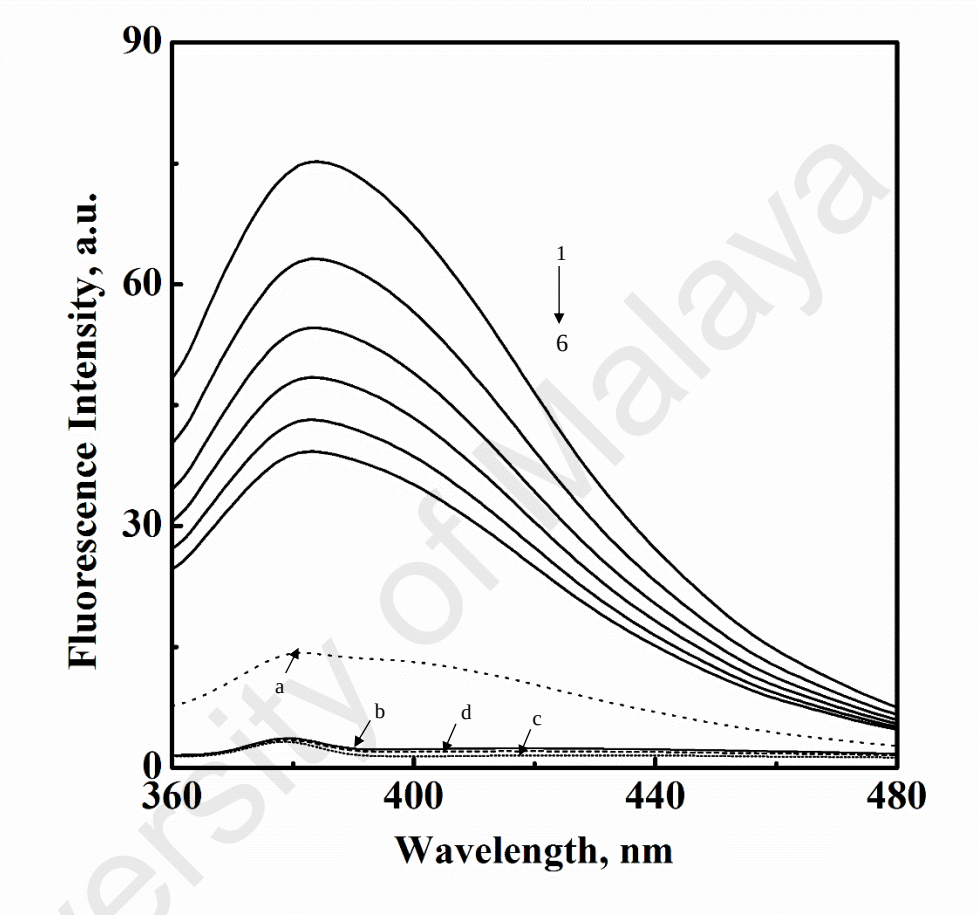

Figure 4.21: Fluorescence spectra of 1:1 WFN-SSA complex (spectrum 1) in the presence of increasing PM concentrations (λ_{ex} = 335 nm). The PM concentrations were 0.9–4.5 µM with 0.9 µM intervals (spectra 2–6). The spectra labelled as 'a', 'b', 'c' and 'd' refer to the fluorescence spectra of WFN (3 µM), SSA (3 µM), PM (4.5 µM) and PM-SSA (1.5:1) complex, respectively.

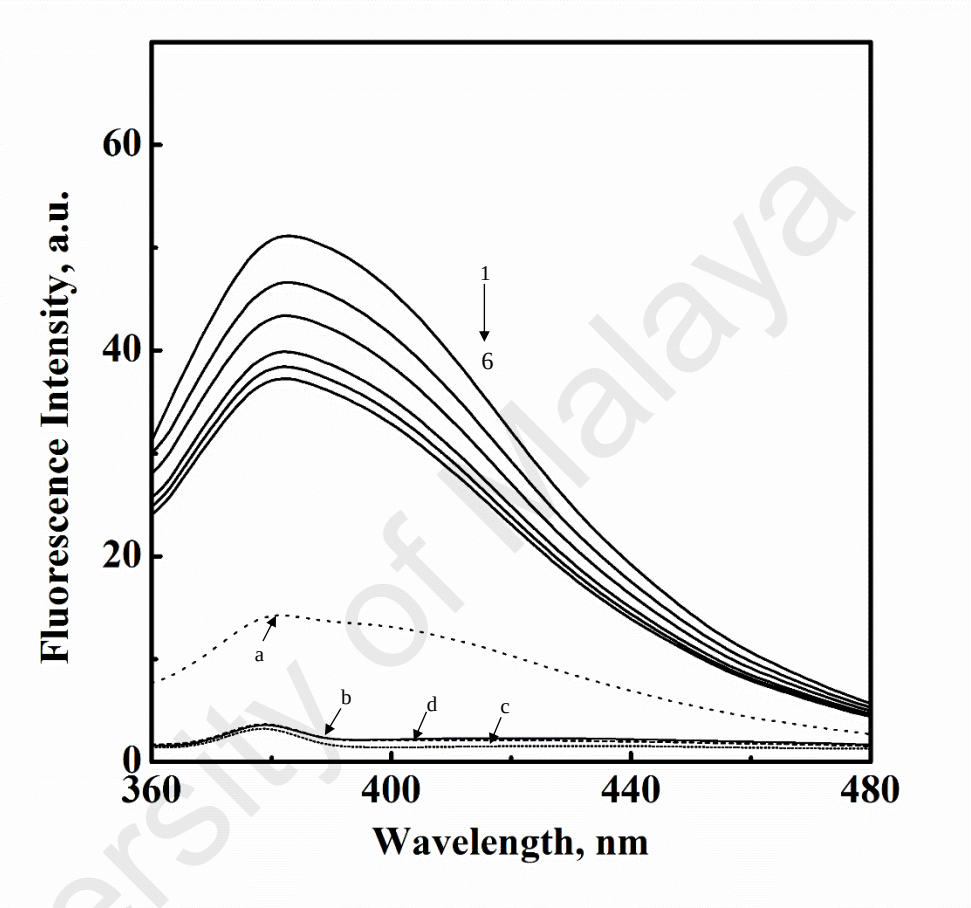

Figure 4.22: Fluorescence spectra of 1:1 WFN-BSA complex (spectrum 1) in the presence of increasing PM concentrations (λ_{ex} = 335 nm). The PM concentrations were 0.9–4.5 µM with 0.9 µM intervals (spectra 2–6). The spectra labelled as 'a', 'b', 'c' and 'd' refer to the fluorescence spectra of WFN (3 µM), BSA (3 µM), PM (4.5 µM) and PM-BSA (1.5:1) complex, respectively.

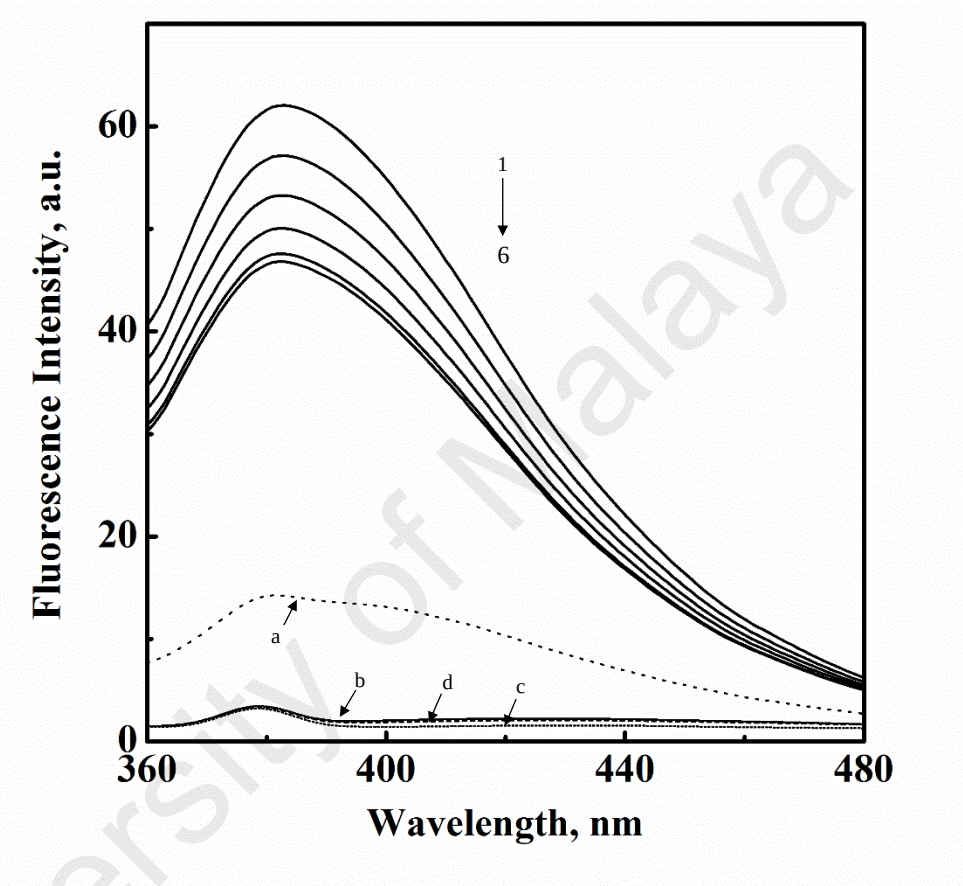

Figure 4.23: Fluorescence spectra of 1:1 WFN-PSA complex (spectrum 1) in the presence of increasing PM concentrations (λ_{ex} = 335 nm). The PM concentrations were 0.9–4.5 µM with 0.9 µM intervals (spectra 2–6). The spectra labelled as 'a', 'b', 'c' and 'd' refer to the fluorescence spectra of WFN (3 µM), PSA (3 µM), PM (4.5 µM) and PM-PSA (1.5:1) complex, respectively.

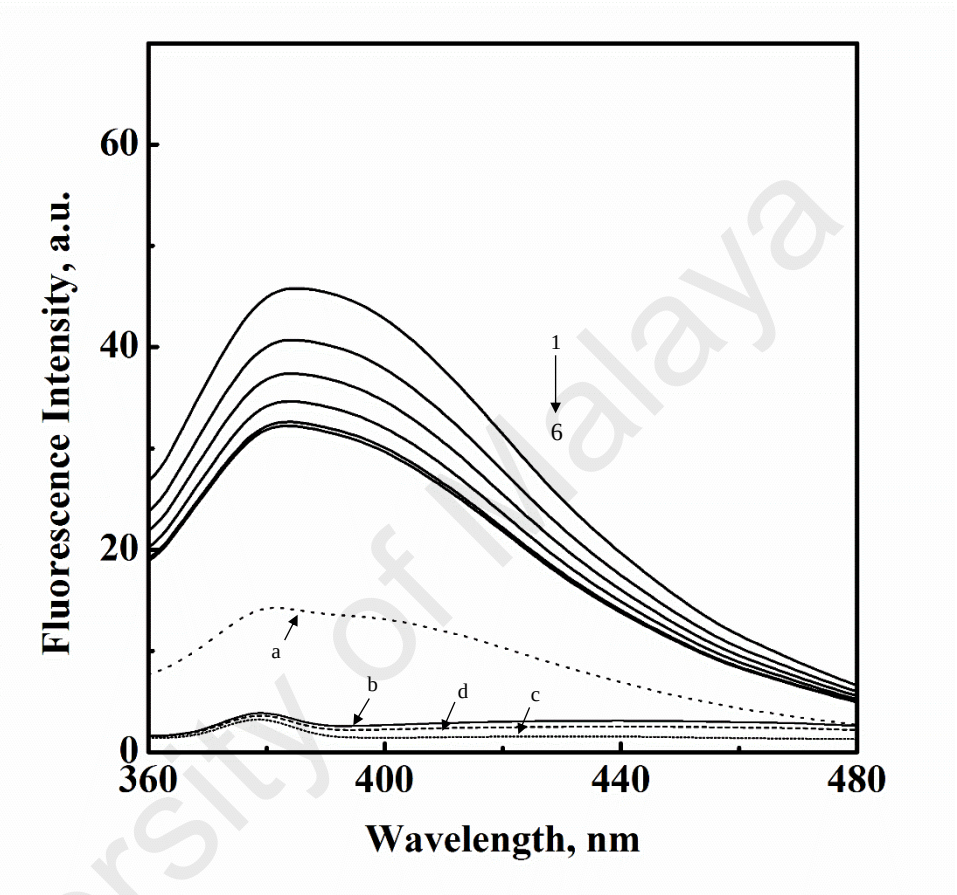

Figure 4.24: Fluorescence spectra of 1:1 WFN-RbSA complex (spectrum 1) in the presence of increasing PM concentrations (λ_{ex} = 335 nm). The PM concentrations used were 0.9–4.5 µM with 0.9 µM intervals (spectra 2–6). The spectra labelled as 'a', 'b', 'c' and 'd' refer to the fluorescence spectra of WFN (3 µM), RbSA (3 µM), PM (4.5 µM) and PM-RbSA (1.5:1) complex, respectively.

albumin (1:1) complexes at 383 nm with increasing PM concentrations, as shown in Figure 4.25. Values of the percentage fluorescence quenching of different WFN-albumin complexes induced by the highest PM concentration (4.5 μM) are listed in Table 4.8. Complexes of WFN with BSA and RbSA showed close similarity to HSA in terms of percentage quenching, as 27 % and 31 % quenching were observed with BSA and RbSA, respectively, against 34 % quenching observed with HSA. On the other hand, SSA showed relatively higher degree (48 %) of quenching, whereas a lesser degree (23 %) of quenching was displayed by PSA.

A comparison of the PM binding properties of various serum albumins as well as WFN displacement results showed close similarity between BSA and HSA.

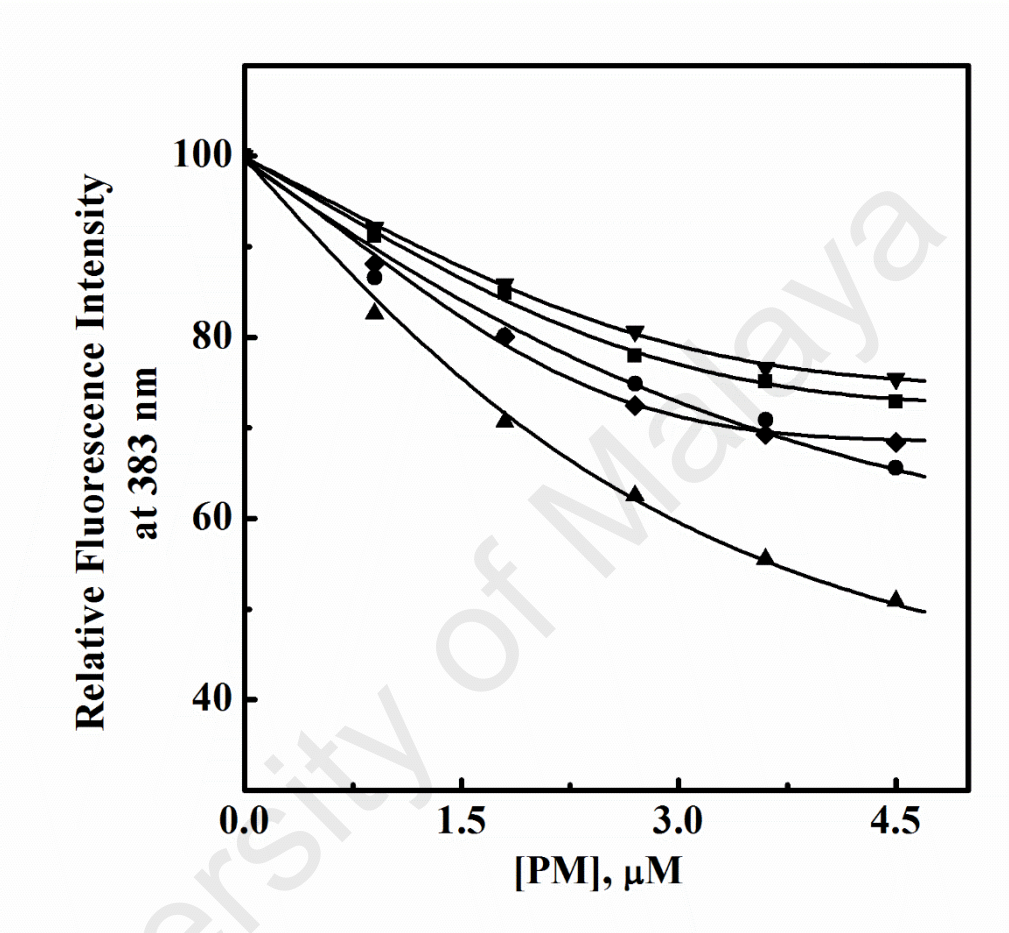

Figure 4.25: Plots showing quenching of the fluorescence intensity at 383 nm of different 1:1 WFN-albumin complexes with increasing PM concentrations. The symbols used for various serum albumins are the same as used in Figure 4.18.

Table 4.8: Fluorescence quenching of different WFN-albumin (1:1) complexes in the presence of 4.5 μM PM.

Albumin	% Quenching
BSA	27.4 ± 0.2
SSA	47.8 ± 1.4
PSA	23.3 ± 1.3
HSA	34.0 ± 0.5
RbSA	31.0 ± 1.1

CHAPTER 5

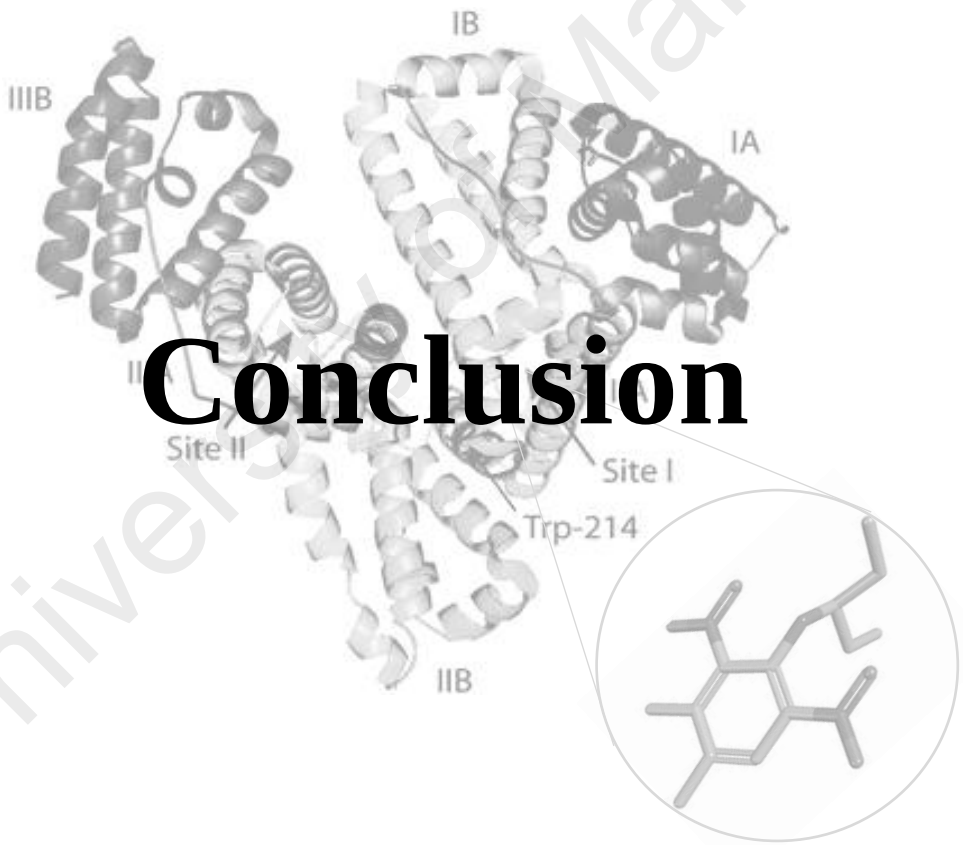

Conclusion

CHAPTER 5

CONCLUSION

Spectroscopic results showed moderately strong binding affinity between PM and HSA. Both hydrophobic interactions and hydrogen bonds were involved in stabilizing the PM-HSA complex. While changes in the secondary and tertiary structures of HSA were noticed upon complexation, protein's thermal stability was increased. Sudlow's site I, located in subdomain IIA was found to be the preferred binding site of PM on HSA. Based on the results obtained with other serum albumins, BSA was found to be closely similar to HSA, as evident from the PM-induced fluorescence quenching pattern, binding affinity as well as WFN displacement results. Thus, bovine can be considered as a suitable animal model for further exploration on toxicological effects of PM. These results may be useful in understanding the toxicity of PM in human subject.

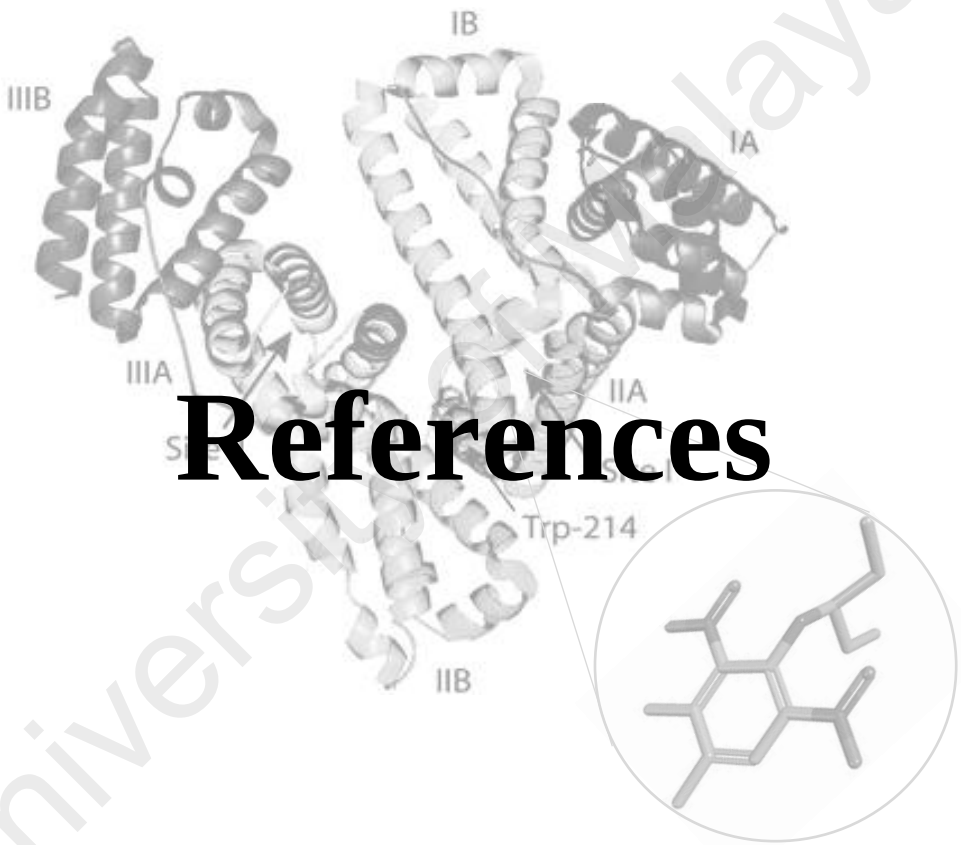

References

REFERENCES

Abd-Algadir, M. I., Idris, O. F., & Elkhier, M. K. (2011). Effect of pendimethalin herbicide on fish (*Tilapia nilotica*) skeletal muscles, gills and its influence on human. *World Journal of Life Sciences and Medical Research*, *1*(1), 5-10.

Abou-Zied, O. K., & Al-Shihi, O. I. (2008). Characterization of subdomain IIA binding site of human serum albumin in its native, unfolded, and refolded states using small molecular probes. *Journal of the American Chemical Society*, *130*(32), 10793-10801.

Ahmed, S., & Chauhan, B. S. (2014). Performance of different herbicides in dry-seeded rice in Bangladesh. *The Scientific World Journal*, *14 pp*.

Appleby, A. P., & Valverde, B. E. (1989). Behavior of dinitroaniline herbicides in plants. *Weed Technology*, *3*(1), 198-206.

Asman, W. A., Jørgensen, A., Bossi, R., Vejrup, K. V., Mogensen, B. B., & Glasius, M. (2005). Wet deposition of pesticides and nitrophenols at two sites in Denmark: Measurements and contributions from regional sources. *Chemosphere*, *59*(7), 1023-1031.

Barba-Brioso, C., Fernández-Caliani, J. C., Miras, A., Cornejo, J., & Galán, E. (2010). Multi-source water pollution in a highly anthropized wetland system associated with the estuary of Huelva (SW Spain). *Marine Pollution Bulletin*, *60*(8), 1259-1269.

Berman, H. M., Westbrook, J., Feng, Z., Gilliland, G., Bhat, T. N., Weissig, H., ... & Bourne, P. E. (2000). The protein data bank. *Nucleic Acids Research*, *28*(1), 235-242.

Bertucci, C., & Domenici, E. (2002). Reversible and covalent binding of drugs to human serum albumin: Methodological approaches and physiological relevance. *Current Medicinal Chemistry*, *9*(15), 1463-1481.

Bi, S., Ding, L., Tian, Y., Song, D., Zhou, X., Liu, X., & Zhang, H. (2004). Investigation of the interaction between flavonoids and human serum albumin. *Journal of Molecular Structure*, *703*(1), 37-45.

Bos, O. J., Remijn, J. P., Fischer, M. J., Wilting, J., & Janssen, L. H. (1988). Location and characterization of the warfarin binding site of human serum albumin: A comparative study of two large fragments. *Biochemical Pharmacology*, *37*(20), 3905-3909.

Brown, J. R., & Shockley, P. (1982). Serum albumin: Structure and characterization of its ligand binding sites. In P. C. Jost & O. H. Griffith (Eds.), *Lipid-Protein Interactions* (pp. 25-68). New York: Wiley.

Brown, W. M., Dziegielewska, K. M., Foreman, R. C., & Saunders, N. R. (1989). Nucleotide and deduced amino acid sequence of sheep serum albumin. *Nucleic Acids Research*, *17*(24), 10495-10495.

Capel, P. D., Lin, M., & Wotzka, P. J. (1998). Wet Atmospheric Deposition of Pesticides in Minnesota, Water-Resources Investigations Report 97-4026, U.S. Geological Survey, 1989-1994.

Carter, D. C., He, X. M., Munson, S. H., Twigg, P. D., Gernert, K. M., Broom, M. B., & Miller, T. Y. (1989). Three-dimensional structure of human serum albumin. *Science*, *244*(4909), 1195-1199.

Carter, D. C., & Ho, J. X. (1994). Structure of serum albumin. *Advances in Protein Chemistry*, *45*, 153-203.

Chakraborty, B., Mitra, P., & Basu, S. (2015). Spectroscopic exploration of drug–protein interaction: A study highlighting the dependence of the magnetic field effect on inter-radical separation distance formed during photoinduced electron transfer. *RSC Advances*, *5*(99), 81533-81545.

Chuang, V. T. G., & Otagiri, M. (2001). Flunitrazepam, a 7-nitro-1, 4-benzodiazepine that is unable to bind to the indole-benzodiazepine site of human serum albumin. *Biochimica et Biophysica Acta-Protein Structure and Molecular Enzymology*, *1546*(2), 337-345.

Cicchetti, F., Drouin-Ouellet, J., & Gross, R. E. (2009). Environmental toxins and Parkinson's disease: What have we learned from pesticide-induced animal models? *Trends in Pharmacological Sciences*, *30*(9), 475-483.

CORPEP. (2010). Les pesticides dans les eaux superficielles bretonnes—bilan 2009. 24 pp.

Curry, S. (2002). Beyond expansion: Structural studies on the transport roles of human serum albumin. *Vox Sanguinis*, *83*(s1), 315-319.

Curry, S., Mandelkow, H., Brick, P., & Franks, N. (1998). Crystal structure of human serum albumin complexed with fatty acid reveals an asymmetric distribution of binding sites. *Nature Structural & Molecular Biology*, *5*(9), 827-835.

Carter, D.C., He, X.M., Munson, S.H., Twigg, P.D., Gernert, K.M., Broom, M.B., & Miller, T.Y. (1989). Three-dimensional structure of human serum albumin, *Science 244*, 1195-1198.

Danion, M., Le Floch, S., Castric, J., Lamour, F., Cabon, J., & Quentel, C. (2012). Effect of chronic exposure to pendimethalin on the susceptibility of rainbow trout, *Oncorhynchus mykiss L.*, to viral hemorrhagic septicemia virus (VHSV). *Ecotoxicology and Environmental Safety, 79*, 28-34.

Danion, M., Le Floch, S., Lamour, F., & Quentel, C. (2014). Effects of *in vivo* chronic exposure to pendimethalin on EROD activity and antioxidant defenses in rainbow trout (*Oncorhynchus mykiss*). *Ecotoxicology and Environmental Safety, 99*, 21-27.

Davidson, M. K., Lindsey, J. R., & Davis, J. K. (1987). Requirements and selection of an animal model. *Israel Journal of Medical Sciences*, *23*(6), 551-555.

Day, Y. S., & Myszka, D. G. (2003). Characterizing a drug's primary binding site on albumin. *Journal of Pharmaceutical Sciences*, *92*(2), 333-343.

Dimitrov, B. D., Gadeva, P. G., Benova, D. K., & Bineva, M. V. (2006). Comparative genotoxicity of the herbicides roundup, stomp and reglone in plant and mammalian test systems. *Mutagenesis*, *21*(6), 375-382.

Dockal, M., Carter, D. C., & Rüker, F. (1999). The three recombinant domains of human serum albumin. Structural characterization and ligand binding properties. *Journal of Biological Chemistry*, *274*(41), 29303-29310.

Dubois-Presle, N., Lapicque, F., Maurice, M. H., Fournel-Gigleux, S., Magdalou, J., Abiteboul, M., ... & Netter, P. (1995). Stereoselective esterase activity of human serum albumin toward ketoprofen glucuronide. *Molecular Pharmacology*, *47*(3), 647-653.

Dugaiczyk, A., Law, S. W., & Dennison, O. E. (1982). Nucleotide sequence and the encoded amino acids of human serum albumin mRNA. *Proceedings of the National Academy of Sciences of the United States of America*, *79*(1), 71-75.

Edwards, C. A., & Adams, R. S. (1970). Persistent pesticides in the environment. *Critical Reviews in Environmental Science and Technology*, *1*(1-4), 7-67.

El-Sharkawy, N. I., Reda, R. M., & El-Araby, I. E. (2011). Assessment of stomp® (pendimethalin) toxicity on *Oreochromis niloticus*. *Journal of American Science, 7*(10), 568-576.

Ericsson, A. C., Crim, M. J., & Franklin, C. L. (2013). A brief history of animal modeling, *Missouri Medicine, 110*(3), 201–205.

Evans, T. W. (2002). Review article: Albumin as a drug—Biological effects of albumin unrelated to oncotic pressure. *Alimentary Pharmacology & Therapeutics*, *16*(s5), 6-11.

Fehske, K. J., Schläfer, U., Wollert, U., & Müller, W. E. (1982). Characterization of an important drug binding area on human serum albumin including the high-affinity binding sites of warfarin and azapropazone. *Molecular Pharmacology*, *21*(2), 387-393.

Feroz, S. R., Mohamad, S. B., Bujang, N., Malek, S. N., & Tayyab, S. (2012). Multispectroscopic and molecular modeling approach to investigate the interaction of flavokawain B with human serum albumin. *Journal of Agricultural and Food Chemistry*, *60*(23), 5899-5908.

Feroz, S. R., Rumana, A., Malek, S. N., & Tayyab, S. (2015). A comparative analysis on the binding characteristics of various mammalian albumins towards a multitherapeutic agent, pinostrobin. *Experimental Animals*, *64*(2), 101-108.

Figge, J., Rossing, T. H., & Fencl, V. (1991). The role of serum proteins in acid-base equilibria. *The Journal of Laboratory and Clinical Medicine*, *117*(6), 453-467.

Flora, K., Brennan, J. D., Baker, G. A., Doody, M. A., & Bright, F. V. (1998). Unfolding of acrylodan-labeled human serum albumin probed by steady-state and time-resolved fluorescence methods. *Biophysical Journal*, *75*(2), 1084-1096.

Ghuman, J., Zunszain, P. A., Petitpas, I., Bhattacharya, A. A., Otagiri, M., & Curry, S. (2005). Structural basis of the drug-binding specificity of human serum albumin. *Journal of Molecular Biology*, *353*(1), 38-52.

Gianazza, E., Frigerio, A., Astrua-Testori, S., & Righetti, P. G. (1984). The behavior of serum albumin upon isoelectric focusing on immobilized pH gradients. *Electrophoresis*, *5*(5), 310-312.

Gianessi, L.P., & Reigner, N.P. (2007). The value of herbicides in US crop production. *Weed Technology*, *21*(2), 559-566.

Gilliam, C. H., Eakes, D. J., & Olive, J. W. (1993). Herbicide use during propagation affects root initiation and development. *Journal of Environmental Horticulture*, *11*(4), 157-159.

Glaumann, H. (1970). Studies on the synthesis and transport of albumin in microsomal subfractions from rat liver. *Biochimica et Biophysica Acta-Nucleic Acids and Protein Synthesis*, *224*(1), 206-218.

Gonçalves, C. M., Esteves da Silva, J. C., & Alpendurada, M. F. (2007). Evaluation of the pesticide contamination of groundwater sampled over two years from a

vulnerable zone in Portugal. *Journal of Agricultural and Food Chemistry*, *55*(15), 6227-6235.

Goodsell, D. S., Morris, G. M., & Olson, A. J. (1996). Automated docking of flexible ligands: Applications of AutoDock. *Journal of Molecular Recognition*, *9*(1), 1-5.

Halgren, T. A. (1996). Merck molecular force field. I. Basis, form, scope, parameterization, and performance of MMFF94. *Journal of Computational Chemistry*, *17*(5-6), 490-519.

Han, X. L., Mei, P., Liu, Y., Xiao, Q., Jiang, F. L., & Li, R. (2009). Binding interaction of quinclorac with bovine serum albumin: A biophysical study. *Spectrochimica Acta Part A: Molecular and Biomolecular Spectroscopy*, *74*(3), 781-787.

Hanwell, M. D., Curtis, D. E., Lonie, D. C., Vandermeersch, T., Zurek, E., & Hutchison, G. R. (2012). Avogadro: An advanced semantic chemical editor, visualization, and analysis platform. *Journal of Cheminformatics*, *4*(17), 17 pp.

Harper, M. E., & Dugaiczyk, A. (1983). Linkage of the evolutionarily-related serum albumin and alpha-fetoprotein genes within q11-22 of human chromosome 4. *American Journal of Human Genetics*, *35*(4), 565-572.

Hartwig, N. L. (1996). Introduction to Weeds and Herbicides. The Pennsylvania State University, Pennsylvania, USA.

He, X. M., & Carter, D. C. (1992). Atomic structure and chemistry of human serum albumin. *Nature*, *358*(6383), 209-215.

Holowachuk, E. W. (1991). cDNA sequence of bovine preproalbumin. Gene. Bank. Database Accession # M73993.

Huang, X., & Miller, W. (1991). A time-efficient, linear-space local similarity algorithm. *Advances in Applied Mathematics*, *12*(3), 337-357.

Hughes, W. L. (1954). The proteins of blood plasma. In H. Neurath & K. Bailey (Eds.), *The proteins*. (pp. 663-754). New York: Academic Press.

Hunter, M. J. (1966). A method for the determination of protein partial specific volumes. *The Journal of Physical Chemistry*, *70*(10), 3285-3292.

Ishtikhar, M., Khan, S., Badr, G., Mohamed, A. O., & Khan, R. H. (2014). Interaction of the 5- fluorouracil analog 5-fluoro-2′-deoxyuridine with 'N'and 'B'isoforms of human serum albumin: A spectroscopic and calorimetric study. *Molecular BioSystems*, *10*(11), 2954-2964.

Juárez, J., Taboada, P., & Mosquera, V. (2009). Existence of different structural intermediates on the fibrillation pathway of human serum albumin. *Biophysical Journal*, *96*(6), 2353-2370.

Kamtekar, N., Pandey, A., Agrawal, N., Pissurlenkar, R. R., Borana, M., & Ahmad, B. (2013). Interaction of multimicrobial synthetic inhibitor 1, 2-bis (2-benzimidazolyl)-1, 2-ethanediol with serum albumin: Spectroscopic and computational studies. *PloS One*, *8*(1), e53499.

Khan, J. M., Chaturvedi, S. K., & Khan, R. H. (2013). Elucidating the mode of action of urea on mammalian serum albumins and protective effect of sodium dodecyl sulfate. *Biochemical and Biophysical Research Communications*, *441*(3), 681-688.

Knudsen, A., Pedersen, A. O., & Brodersen, R. (1986). Spectroscopic properties of bilirubin-human serum albumin complexes: A stoichiometric analysis. *Archives of Biochemistry and Biophysics*, *244*(1), 273-284.

Kosa, T., Maruyama, T., & Otagiri, M. (1997). Species differences of serum albumins: I. Drug binding sites. *Pharmaceutical Research*, *14*(11), 1607-1612.

Kragh-Hansen, U. (1985). Relations between high-affinity binding sites of markers for binding regions on human serum albumin. *Biochemical Journal*, *225*(3), 629-638.

Kragh-Hansen, U. (1988). Evidence for a large and flexible region of human serum albumin possessing high affinity binding sites for salicylate, warfarin, and other ligands. *Molecular Pharmacology*, *34*(2), 160-171.

Kragh-Hansen, U., Chuang, V. T. G., & Otagiri, M. (2002). Practical aspects of the ligand-binding and enzymatic properties of human serum albumin. *Biological and Pharmaceutical Bulletin*, *25*(6), 695-704.

Lakowicz, J. R. (2006). Principles of fluorescence spectroscopy. (3rd ed.). *New York*: Plenum Press.

Lakowicz, J. R., & Weber, G. (1973). Quenching of fluorescence by oxygen. Probe for structural fluctuations in macromolecules. *Biochemistry*, *12*(21), 4161-4170.

Larson, S. J., Gilliom, R. J., & Capel, P. D. (1999). Pesticides in streams of the United States: Initial results from the national water-quality assessment program (No. 98-4222). Virginia, DC: US Dept. of the Interior, US Geological Survey.

Lie, S. O., & Bratlid, D. (1970). The protective effect of albumin on bilirubin toxicity on human fibroblasts. *Scandinavian Journal of Clinical and Laboratory Investigation*, *26*(1), 37-41.

Lokke, H.E. (1999). Rapport fra underudvalget om miljø og sundhed. Bichel–Udvalget, Copenhagen.

Longsworth, L. G., & Jacobsen, C. F. (1949). An electrophoretic study of the binding of salt ions by β-lactoglobulin and bovine serum albumin. *The Journal of Physical Chemistry*, *53*(1), 126-134.

Mallory-Smith, C. A., & Retzinger Jr, E. J. (2003). Revised classification of herbicides by site of action for weed resistance management strategies. *Weed Technology*, *17*(3), 605-619.

Martinez, M. N. (2011). Factors influencing the use and interpretation of animal models in the development of parenteral drug delivery systems. *The American Association of Pharmaceutical Scientists Journal*, *13*(4), 632-649.

Megadi, V. B., Tallur, P. N., Hoskeri, R. S., Mulla, S. I., & Ninnekar, H. Z. (2010). Biodegradation of pendimethalin by *Bacillus circulans*. *Indian Journal of Biotechnology*, *9*, 173-177.

Michaud, F. T., Garnier, A., Lemieux, L., & Duchesne, C. (2009). Multivariate analysis of single quadrupole LC-MS spectra for routine characterization and quantification of intact proteins. *Proteomics*, *9*(3), 512-520.

Minghetti, P. P., Ruffner, D. E., Kuang, W. J., Dennison, O. E., Hawkins, J. W., Beattie, W. G., & Dugaiczyk, A. (1986). Molecular structure of the human albumin gene is revealed by nucleotide sequence within q11-22 of chromosome 4. *Journal of Biological Chemistry*, *261*(15), 6747-6757.

Nayak, B. S., Prusty, J. C., & Mohanty, S. K. (1994). Effect of herbicides on bacteria, fungi and actinomycetes in sesame (*Sesamum indicum*) soil. *Indian Journal of Agricultural Sciences*, *64*, 888-890.

Olsson, T. S., Williams, M. A., Pitt, W. R., & Ladbury, J. E. (2008). The thermodynamics of protein–ligand interaction and solvation: Insights for ligand design. *Journal of Molecular Biology*, *384*(4), 1002-1017.

Oncley, J. L., Scatchard, G., & Brown, A. (1947). Physical-chemical characteristics of certain of the proteins of normal human plasma. *The Journal of Physical Chemistry*, *51*(1), 184-198.

Otagiri, M. (2005). A molecular functional study on the interactions of drugs with plasma proteins. *Drug Metabolism and Pharmacokinetics*, *20*(5), 309-323.

Painter, L., Harding, M., & Beeby, P. (1998). Synthesis and interaction with human serum albumin of the first 3, 18-disubstituted derivative of bilirubin. *Journal of the Chemical Society, Perkin Transactions 1*, (18), 3041-3044.

Pajot, P. (1976). Fluorescence of proteins in 6-M guanidine hydrochloride. *European Journal of Biochemistry, 63*(1), 263-269.

Parka, S. J., & Soper, O. F. (1977). The physiology and mode of action of the dinitroaniline herbicides. *Weed Science, 25*, 79-87.

Patel, S., Bajpayee, M., Pandey, A. K., Parmar, D., & Dhawan, A. (2007). *In vitro* induction of cytotoxicity and DNA strand breaks in CHO cells exposed to cypermethrin, pendimethalin and dichlorvos. *Toxicology in vitro, 21*(8), 1409-1418.

Peters, T. Jr. (1996). *All about albumin: Biochemistry, genetics, and medical applications*. San Diego: Academic Press.

Peters, T. Jr., & Davidson, L. K. (1982). The biosynthesis of rat serum albumin. In vivo studies on the formation of the disulfide bonds. *Journal of Biological Chemistry*, *257*(15), 8847-8853.

Peters, T. Jr., Fleischer, B., & Fleischer, S. (1971). The biosynthesis of rat serum albumin IV. Apparent passage of albumin through the Golgi apparatus during secretion. *Journal of Biological Chemistry*, *246*(1), 240-244.

Peters, T. Jr. (1985). Serum albumin. *Advances in Protein Chemistry*, 37, 161-245.

Petitpas, I., Bhattacharya, A. A., Twine, S., East, M., & Curry, S. (2001). Crystal structure analysis of warfarin binding to human serum albumin anatomy of drug site I. *Journal of Biological Chemistry*, *276*(25), 22804-22809.

Picó, G. A. (1997). Thermodynamic features of the thermal unfolding of human serum albumin. *International Journal of Biological Macromolecules*, *20*(1), 63-73.

Poleksic, V., Karan, V., Vidmanic, L., Elezovic, I., & Tutundžić, V. (1995). Field study of the indirect effects of a herbicide pendimethalin on freshwater communities. *Toxicology Letters, 78*, 67-67.

Poór, M., Li, Y., Matisz, G., Kiss, L., Kunsági-Máté, S., & Kőszegi, T. (2014). Quantitation of species differences in albumin–ligand interactions for bovine, human and rat serum albumins using fluorescence spectroscopy: A test case with some Sudlow's site I ligands. *Journal of Luminescence, 145*, 767-773.

Promkaew, N., Soontornchainaksaeng, P., Jampatong, S., & Rojanavipart, P. (2010). Toxicity and genotoxicity of pendimethalin in maize and onion. *Kasetsart Journal: Natural Science, 44*, 1010-1015.

Qin, P., Liu, R., Pan, X., Fang, X., & Mou, Y. (2010). Impact of carbon chain length on binding of perfluoroalkyl acids to bovine serum albumin determined by spectroscopic methods. *Journal of Agricultural and Food Chemistry*, *58*(9), 5561-5567.

Quinlan, G. J., Martin, G. S., & Evans, T. W. (2005). Albumin: Biochemical properties and therapeutic potential. *Hepatology*, *41*(6), 1211-1219.

Raffa, R.B. (2003). Experimental approaches to determine the thermodynamics of protein-ligand interactions, In H.J. Böhm, G. Schneider (Eds.), *Protein-ligand interactions: From molecular recognition to drug design* (pp. 51-72). Weinheim: Wiley-VCH Verlag.

Riley, M. B., Keese, R. J., Camper, N. D., Whitwell, T., & Wilson, P. C. (1994). Pendimethalin and oxyfluorfen residues in pond water and sediment from container plant nurseries. *Weed Technology*, *8*(2), 299-303.

Ringot, D., Chango, A., Schneider, Y. J., & Larondelle, Y. (2006). Toxicokinetics and toxicodynamics of ochratoxin A, an update. *Chemico-Biological Interactions*, *159*(1), 18-46.

Rogers, D. M., & Hirst, J. D. (2004). First-principles calculations of protein circular dichroism in the near ultraviolet. *Biochemistry*, *43*(34), 11092-11102.

Ross, P. D., & Subramanian, S. (1981). Thermodynamics of protein association reactions: Forces contributing to stability. *Biochemistry*, *20*(11), 3096-3102.

Samari, F., Hemmateenejad, B., Shamsipur, M., Rashidi, M., & Samouei, H. (2012). Affinity of two novel five-coordinated anticancer Pt (II) complexes to human and bovine serum albumins: A spectroscopic approach. *Inorganic Chemistry*, *51*(6), 3454-3464.

Sanner, M. F. (1999). Python: A programming language for software integration and development. *Journal of Molecular Graphics and Modelling*, *17*(1), 57-61.

Scheider, W., Dintzis, H. M., & Oncley, J. L. (1976). Changes in the electric dipole vector of human serum albumin due to complexing with fatty acids. *Biophysical Journal*, *16*(5), 417-431.

Sherwani, S. I., Arif, I. A., & Khan, H. A. (2015). Modes of action of different classes of herbicides. In A. Price, J. Kelton, & L. Sarunaite (Eds.), *Herbicides, physiology of action, and safety* (pp. 165-186). InTechOpen.

Simon, G. A., & Maibach, H. I. (2000). The pig as an experimental animal model of percutaneous permeation in man: Qualitative and quantitative observations–An overview. *Skin Pharmacology and Physiology*, *13*(5), 229-234.

Sinisi, V., Forzato, C., Cefarin, N., Navarini, L., & Berti, F. (2015). Interaction of chlorogenic acids and quinides from coffee with human serum albumin. *Food Chemistry*, *168*, 332-340.

Stamler, J. S., Jaraki, O., Osborne, J., Simon, D. I., Keaney, J., Vita, J., ... & Loscalzo, J. (1992). Nitric oxide circulates in mammalian plasma primarily as an *S*-nitroso adduct of serum albumin. *Proceedings of the National Academy of Sciences of the United States of America*, *89*(16), 7674-7677.

Starrett, S. K., Christians, N. E., & Austin, T. A. (1996). Movement of pesticides under two irrigation regimes applied to turfgrass. *Journal of Environmental Quality*, *25*(3), 566-571.

Steinhardt, J., Krijn, J., & Leidy, J. G. (1971). Differences between bovine and human serum albumins. Binding isotherms, optical rotatory dispersion, viscosity, hydrogen ion titration, and fluorescence effects. *Biochemistry*, *10*(22), 4005-4015.

Strandberg, M., & Scott-Fordsmand, J. J. (2004). Effects of pendimethalin at lower trophic levels—A review. *Ecotoxicology and Environmental Safety*, *57*(2), 190-201.

Sudlow, G., Birkett, D. J., & Wade, D. N. (1975). The characterization of two specific drug binding sites on human serum albumin. *Molecular Pharmacology*, *11*(6), 824-832.

Sugio, S., Kashima, A., Mochizuki, S., Noda, M., & Kobayashi, K. (1999). Crystal structure of human serum albumin at 2.5 Å resolution. *Protein Engineering*, *12*(6), 439-446.

Sułkowska, A., Maciążek-Jurczyk, M., Bojko, B., Rownicka, J., Zubik-Skupień, I., Temba, E., ... & Sułkowski, W. W. (2008). Competitive binding of phenylbutazone and colchicine to serum albumin in multidrug therapy: A spectroscopic study. *Journal of Molecular Structure*, *881*(1), 97-106.

Suzuki, S. (2000). Leaching of several pesticides in andosol upland field under natural rain conditions. *Journal of Pesticide Science, 25*, 1–9.

Taboada, P., Barbosa, S., Castro, E., & Mosquera, V. (2006). Amyloid fibril formation and other aggregate species formed by human serum albumin association. *The Journal of Physical Chemistry B*, *110*(42), 20733-20736.

Tanford, C. (1950). Preparation and properties of serum and plasma proteins. XXIII. Hydrogen ion equilibria in native and modified human serum albumins. *Journal of the American Chemical Society*, *72*(1), 441-451.

Tayyab, S., & Qasim, M. A. (1986). A correlation between changes in conformation and molecular properties of bovine serum albumin upon succinylation. *Journal of Biochemistry*, *100*(5), 1125-1136.

Tayyab, S., Khan, N. J., Khan, M. A., & Kumar, Y. (2003). Behavior of various mammalian albumins towards bilirubin binding and photochemical properties of different bilirubin–albumin complexes. *International Journal of Biological Macromolecules*, *31*(4), 187-193.

Tomlin, C. (1997). The Pesticide Manual, British Crop Protection Council (11th ed.) Surrey, UK.

Tsiropoulos, N. G., & Lolas, P. C. (2004). Persistence of pendimethalin in cotton fields under sprinkler or drip irrigation in central Greece. *International Journal of Environmental Analytical Chemistry*, *84*(1-3), 199-205.

Tunç, S., Duman, O., Soylu, İ., & Bozoğlan, B. K. (2014). Study on the bindings of dichlorprop and diquat dibromide herbicides to human serum albumin by spectroscopic methods. *Journal of Hazardous Materials*, *273*, 36-43.

USGS National Water Quality Assessment Program: Annual use maps (1998). Retrieved from http://ca.water.usgs.gov/pnsp/use92/ index.html [Online].

Vallner, J. J. (1977). Binding of drugs by albumin and plasma protein. *Journal of Pharmaceutical Sciences*, *66*(4), 447-465.

Varshney, J. G., & Sondhia, S. (2008). Introduction to herbicides. Retrieved from http://nsdl.niscair.res.in/jspui/bitstream/123456789/559/1/Introduction%20to%20Herbicides%20-%20Formatted.pdf

Vencill, W.K. (2002). Herbicide Handbook (8th ed.) Weed Science Society of America Lawrence, KS, 493 pp.

Vivian, J. T., & Callis, P. R. (2001). Mechanisms of tryptophan fluorescence shifts in proteins. *Biophysical Journal*, *80*(5), 2093-2109.

Walker, A., & Bond, W. (1977). Persistence of the herbicide AC 92,553, N-(1-ethylpropyl)-2, 6-dinitro-3, 4-xylidine, in soils. *Pesticide Science*, *8*(4), 359-365.

Wallevik, K. (1973). Reversible denaturation of human serum albumin by pH, temperature, and guanidine hydrochloride followed by optical rotation. *Journal of Biological Chemistry*, *248*(8), 2650-2655.

Weinstock, J., & Baldwin, G. S. (1988). Nucleotide sequence of porcine liver albumin. *Nucleic Acids Research*, *16*(18), 9045-9045.

Wilcox, W. F. (1996). Influence of dinitroanaline herbicides on growth, sporulation, and infectivity of four *Phytophthora* spp. pathogenic to deciduous fruit trees. *Phytopathology*, *86*(9), 906-913.

Yamasaki, K., Maruyama, T., Kragh-Hansen, U., & Otagiri, M. (1996). Characterization of site I on human serum albumin: Concept about the structure of a drug binding site. *Biochimica et Biophysia Acta-Protein Structure and Molecular Enzymology*, *1295*(2), 147-157.

Yeggoni, D. P., Rachamallu, A., Kallubai, M., & Subramanyam, R. (2015). Cytotoxicity and comparative binding mechanism of piperine with human serum albumin and α-1-acid glycoprotein. *Journal of Biomolecular Structure and Dynamics*, *33*(6), 1336-1351.

Zhang, G., & Ma, Y. (2013). Mechanistic and conformational studies on the interaction of food dye amaranth with human serum albumin by multispectroscopic methods. *Food Chemistry*, *136*(2), 442-449.

Zhang, G., Wang, L., & Pan, J. (2012). Probing the binding of the flavonoid diosmetin to human serum albumin by multispectroscopic techniques. *Journal of Agricultural and Food Chemistry*, *60*(10), 2721-2729.

Zheng, X., Podariu, M., Matsuda, R., & Hage, D. S. (2016). Analysis of free drug fractions in human serum by ultrafast affinity extraction and two-dimensional affinity chromatography. *Analytical and Bioanalytical Chemistry*, *408*(1), 131-140.

Zimdahl, R. L. (1993). *Fundamentals of weed science*. San Diego: Academic Press.

Zulalian, J. (1990). Study of the absorption, excretion, metabolism, and residues in tissues in rats treated with carbon-14-labeled pendimethalin, PROWL herbicide. *Journal of Agricultural and Food Chemistry*, *38*(8), 1743-1754.

LIST OF PUBLICATIONS / PRESENTATIONS

1. **Lee Wei Qi**, Ida Syazwani M. Affandi, Shevin R. Feroz, Saharuddin B. Mohamad and Saad Tayyab (2016) Evaluation of pendimethalin binding to human serum albumin: Insights from spectroscopic and molecular modeling approach.
   Journal of Biochemical and Molecular Toxicology – In press
   (DOI: 10.1002/jbt.21839).

2. **Lee Wei Qi**, Nurul Iman Kameel, Saharuddin B. Mohamad and Saad Tayyab (2016) Comparison of pendimethalin binding properties of serum albumins from various mammalian species – Communicated.

3. **Lee Wei Qi**, Saharuddin B. Mohamad and Saad Tayyab (2016) Investigation of the interaction between pendimethalin and human serum albumin using spectroscopic and molecular modeling approach.
   Proceedings of the 41st Annual Conference of the Malaysian Society for Biochemistry and Molecular Biology held at Selangor, Malaysia on August 17-18, 2016. Abstract No. Poster 35, pp. 87.